INVESTIGATION OF THE USE OF SANDWICH MATERIALS IN AUTOMOTIVE BODY STRUCTURES

A THESIS SUBMITTED TO
THE GRADUATE SCHOOL OF NATURAL AND APPLIED SCIENCES
OF
MIDDLE EAST TECHNICAL UNIVERSITY

BY

DENİZ HARA

IN PARTIAL FULFILLMENT OF THE REQUIREMENTS
FOR
THE DEGREE OF MASTER OF SCIENCE
IN
MECHANICAL ENGINEERING

FEBRUARY 2012

Approval of the Thesis:

INVESTIGATION OF THE USE OF SANDWICH MATERIALS IN AUTOMOTIVE BODY STRUCTURES

Submitted by **DENİZ HARA** in partial fulfillment of the requirements for the degree of **Master of Science in Mechanical Engineering Department, Middle East Technical University** by,

Prof. Dr. Canan Özgen _____
Dean, Graduate School of **Natural and Applied Sciences**

Prof. Dr. Suha Oral _____
Head of Department, **Mechanical Engineering**

Assist. Prof. Dr. Gökhan O. Özgen _____
Supervisor, **Mechanical Engineering Dept., METU**

Examining Committee Members:

Prof. Dr. Mehmet Çalışkan _____
Mechanical Engineering Dept., METU

Assist. Prof. Dr. Gökhan O. Özgen _____
Mechanical Engineering Dept., METU

Prof. Dr. F. Suat Kadıoğlu _____
Mechanical Engineering Dept., METU

Assist. Prof. Dr. Yiğit Yazıcıoğlu _____
Mechanical Engineering Dept., METU

Assist. Prof. Dr. M. Bülent Özer _____
Mechanical Engineering Dept., TOBB ETU

Date: 07.02.2012

I hereby declare that all information in this document has been obtained and presented in accordance with academic rules and ethical conduct. I also declare that, as required by these rules and conduct. I have fully cited and referenced all material and results that are not original to this work.

Name, Last name : Deniz Hara

Signature :

ABSTRACT

INVESTIGATION OF THE USE OF SANDWICH MATERIALS IN AUTOMOTIVE BODY STRUCTURES

Hara, Deniz
M.Sc., Department of Mechanical Engineering
Supervisor : Assist. Prof. Dr. Gökhan O. Özgen

February 2012, 127 pages

The use of sandwich structures in automobile body panels is investigated in this thesis. The applications on vehicles such as trains, aeroplanes and automobiles, advantages, disadvantages and modelling of sandwich structures are discussed and studies about static, vibrational and acoustic benefits of sandwich structures by several authors are presented. The floor, luggage, firewall and rear wheel panels in sheet metal form is replaced with panel made from sandwich materials in order to reduce the weight obtained by a trial and error based optimization method by keeping the same bending stiffness performance. In addition to these, the use of sandwich structures over free layer surface damping treatments glued on floor panel to decrease the vibration levels and air-borne noise inside the cabin is investigated. It has been proven that, the same vibration performance of both flat beam and floor panel can be obtained using sandwich structures instead of free layer surface damping treatments with a less weight addition. Furthermore, the damping effect of

sandwich structures on sound transmission loss of complex shaped panels like floor panel is investigated. A 2D flat and curved panel representing the floor panel of FIAT Car model are analysed in a very large frequency range. Four different loss factors are applied on these panels and it is seen that, until it reaches damping controlled region, damping has a very little effect on TL of flat panels but has an obvious damping effect on TL of curved panels. However in that region, damping has an increasing effect on TL of both flat and curved panels.

Keywords: Sandwich Materials, Viscoelastic Materials, Vibration Damping, Sound Transmission Loss, Finite Element Method

ÖZ

OTOMOBİL GÖVDE YAPILARINDA SANDVİÇ MALZEME KULLANIMININ ARAŞTIRILMASI

Hara, Deniz
Yüksek Lisans, Makina Mühendisliği Bölümü
Tez Yöneticisi : Yrd. Doç. Dr. Gökhan O. Özgen

Şubat 2012, 127 sayfa

Bu tez çalışmasında, sandviç yapıların otomobil gövde panellerinde kullanılması incelenmiştir. Sandviç yapıların, uygulamaları, avantaj ve dezavantajları ve modellenmesi irdelenmiş olup, bu yapıların statik, titreşimsel ve akustik olarak sağladığı yararları hakkındaki başka yazarlar tarafından yapılan çalışmalar sunulmuştur. Sac halindeki taban, bagaj, arka tekerlek ve ateş duvarı panelleri, ağırlığı azaltmak amacıyla deneme yanılmaya dayanan bir optimizasyon metodu ile elde edilen sandviç malzemeden yapılan panellerle eğilme dayanımı performansı aynı tutularak değiştirilmiştir Buna ek olarak, sandviç yapıların, taban panellerin üzerine titreşim değerlerinin ve kabin için gürültünün azaltılması amacıyla yapıştırılan serbest katman yüzey sönümleme uygulamasına oranla avantajları incelenmiştir. Bunun sonucunda, serbest katman yüzey sönümleme uygulaması yapıştırılmış hem düz kiriş hem de taban panelinin aynı eğilme performansının daha

az ağırlık eklenmiş sandviç panel ile elde edilebildiği görülmüştür. Bunlara ilaveten, sönümlemenin panellerin ses iletme kaybına etkisi araştırılmıştır. İki boyutlu düz ve FIAT araba modelini temsilen bir eğimli panel çok geniş bir frekans aralığında analiz edilmişlerdir. Bu panellere dört farklı kayıp faktörü uygulanmıştır ve sönümleme kontrollü bölgeye gelene kadar, düz panellerin ses iletim kaybına çok az etki ettiği, eğimli panellerinkine ise açıkça görülen sönümleyici etkisinin olduğu görülmüştür. Bu bölgede ise sönümleme, hem düz hem de eğimli panellerde ses iletme kaybını arttırıcı bir etkisi vardır.

Anahtar Kelimeler: Sandviç Malzemeler, Viskoelastik Malzemeleri, Titreşim Sönümleme, Ses İletim Kaybı, Sonlu Elemanlar Metodu

To My Beloved Grandmother Janet Yuvarlak

ACKNOWLEDGEMENTS

I would like to express my sincere appreciation and thanks to my advisor Assist. Prof. Dr. Gökhan O. ÖZGEN for his guidance and support during my studies and research. I would like to specially thank Prof. Dr. Mehmet ÇALIŞKAN for letting me use MSC.Actran for acoustic analyses of sandwich structures. I am grateful for the considerable assistance provided by the other committee members Prof. Dr. Suat KADIOĞLU, Assist. Prof. Dr. Yiğit YAZICIOĞLU and Assist. Prof. Dr. M. Bülent ÖZER. My appreciation also goes to all of my friends and family. Last and not least, I want to express my special thanks to my parents for their support.

TABLE OF CONTENTS

LIST OF TABLES

TABLES

LIST OF FIGURES

FIGURES

LIST OF SYMBOLS

A	Total absorbtion area, cross-sectional area of beam, [m^2]
a	Length of panel, [m]
a_1	Material coefficient
B	Irradiation density, [J/m^3]
b	Width, [m]
b_1	Material coefficient
c	Speed of sound, [m/s]
c_1	Material coefficient
D	Bending stiffness, [$kg^2.m/s^2$]
D_c	Bending stiffness of core material, [$kg^2.m/s^2$]
D_f	Bending stiffness of face materials about their individual neutral axes, [$kg^2.m/s^2$]
D_o	Bending stiffness of face materials about the middle axis, [$kg^2.m/s^2$]
d	Distance between the neutral axes of the face materials, [m]
E_f	Modulus of elasticity of the face materials, [Pa]

E_c	Modulus of elasticity of the core material, [Pa]
G	Shear modulus, [Pa]
h	Thickness, [m]
I	Sound intensity, moment of inertia [kg.m^2]
K_{mn}	Denominator
L	Average sound pressure level, length of beam [Pa, m]
M	End values of m counters
M_x	Bending moment in x direction, [N.m]
M_y	Bending moment in y direction, [N.m]
m	Counter
N	End values of n counters
n	Counter
P	Sound power, [watt]
Q	Sound pressure, [Pa]
q	Load, [N]
S	Area of partition, shear stiffness, [m^2, kg^2.m/s^2]
s	Shear parameter
T	Temperature, [^{o}C]
T_A	The slope of log[(α(T)] , [^{o}C]
T_0	Peak loss factor temperature, [^{o}C]
T_x	Shear forces in x direction, [N]

T_y	Shear forces in y direction, [N]
t	Time, [s]
t_f	Thickness of face materials, [m]
t_c	Thickness of core material, [m]
w	Energy density, displacement in z direction, [J/m^3, m]
α	Coefficient
β	Coeficient
ε	Strain
ω	Natural frequency, [Hz]
ρ	Density, [kg/m^3]
ν	Poisson ratio
θ	Shear factor
σ	Bending stress, stress, [Pa]
τ	Core shear stress, [Pa]
ψ	Phase difference
η	Loss factor

LIST OF ABBREVIATIONS

2D	Two Dimensional
3D	Three Dimensional
CAD	Computer Aided Design
FE	Finite Element
FEM	Finite Element Method
FRF	Frequency Response Functions
HEX8	Hexahedral Elements with 8 Nodes
PMI	Polymethacrylimide
PS	Polystyrene
PUR	Polyurethane
PVC	Polyvinylchloride
QUAD4	Quadriteral Elements with 4 Nodes
R	Sound Reduction Index
TL	Sound Transmission Loss

CHAPTER 1

INTRODUCTION

The purpose of this thesis study is to investigate the use of sandwich structures in automobile body panels. Main motivation to replace sheet metal body panels with panels made from sandwich materials is to decrease mass of the car body thus improve motor emissions (due to reduced power needs thus smaller size motors when body weight is reduced). The objective of decreasing body panel weights is possible to achieve because body panels with sandwich structures can potentionally show the same static, vibration and acoustical performance with less weight. In this thesis, the sandwich material configurations that will help achieve the target of decreasing mass of body panels are investigated using finite element based simulations for static, acoustic and vibration behaviour.

Sandwich materials uses the simple fact that increasing the flexural rigidity of a plate or beam structure can be achieved by placing the material away from the neutral axis as much as possible. By smart distribution of a material in the cross-section of the structure increased flexural rigidity can be achieved with minimal change in weight of the structure. The concept is the same thing that makes I-beams advantageous. In sandwich structures the web of an I-beam is usually replaced by light weight and low

rigidity structural core material (foam or honeycomb pattern) while at the outer parts rigid structural materials (sheet metals or composite plates) are utilized.

One of the purposes of the use of sandwich structures in car body structures is to decrease the bending and torsional stiffness of body by replacing some body panels with sandwich structures. With the sandwich assembly, the structure gains high flexural rigidity thus a high stiffness-to-weight ratio and also a high bending strenght-to-weight ratio with a little weight additon. This will enable a reduction in weight of the car body with a static performance kept same as the sheet metal based design of the body panels.

Through the use of rigid foam cored sandwich materials, sound transmission loss characteristics of body panels may also be increased compared to sheet metal panels while keeping the weight same or less. This will enable the NVH engineer to reduce amount of acoustic barrier elements used within the passenger cabin for the desired acoustic performance. Reduced acoustic barrier elements mean reduced weight of the car body.

One of the other advantages of sandwich materials is that the vibration damping of a body panel can be increased with the use of a special configuration of sandwich materials called laminated sheet metal panels which is composed of two metal sheet panels joined with a very thin viscoelastic material core with high material damping. This configuration can replace the currently used solution for introducing vibration damping to body panels (especially floor and ceiling panels) which a thick layer of viscoleastic material bonded on sheet metal body panels (also called free layer damping treatment). In order to achieve the same damping for body panels, current free layer damping treatment approach requires larger mass addition (the viscoelastic material bonded to the anel surface) compared to the overall mass increase if the sheet metal panels were replaced by high damping laminated metal panels.

Energy saving is one of the most important issues in automotive industry and it can be achieved by reducing the weight of automobiles. With this reduction, the fuel consumption and load capacity will be increased and a less powerful and smaller sized motors will be sufficient. Furthermore, emissions of air pollutants will be reduced and high speed and accelerations can be reached with less power. When the advantages of sandwich structures are taken into consideration, sandwich structures have a good potential if they are used in automobile body panels. One of the purpose of the use of sandwich structures is to incease the bending and torsional stiffness of body by replacing some body panels with lighter sandwich structures.

As an example of potential applications of sandwich structures mentioned above, a car body model created with finite elements in Özgen's study [1] is used within this study. The sheet metal panels and panels made from sandwich materials are modelled and analyzed using this finite element model. Entire model is used in bending stiffness analyses due to the application regions of load and boundary conditions of the required bending test but only floor panel is used in vibration analysis. For two dimensional acoustical analyses, floor panel is modeled with a shape like floor panel of this finite element model.

The thesis is composed of six chapters. In the second chapter, general information about sandwich structures, general properties, applications on some vehichles including automobile, train, airplane etc., modelling and similar topics are reviewed and presented. In the third chapter, static bending analyses are performed and an optimization process is developed in order to obtain the minimum weighted polymeric foam cored sandwich panel which has the same bending stiffness as the steel panel. The forth chapter contains development of an optimization process for obtaining the panel with surface damping treatments which has the same modal damping ratio as laminated steel. It is proven that, the weight of floor panels can be

decreased by replacing the panels with damping treatments with laminated steel panels which has the less weight. The optimization is done through frequency response function analyses. In the last chapter, air-borne sound transmission of floor panel is investigated. The sound transmission losses of steel panel with and without loss factor values are analyzed and compared. It is proven that with using laminated metals at high frequencies, the amount of sound-absorbing materials attached on body panels will be eliminated.

The car body panels used in this study are floor panel, rear wheel panels, firewall panel and luggage panel. All of these panels are investigated for their static behaviour. The acoustical barriers such as mastics etc. are used commonly on the floor and firewall panels. In this thesis study, only floor panel is investigated for vibration and acoustic behaviours.

CHAPTER 2

LITERATURE REVIEW

Literature review starts with basic properties of sandwich materials. The various applications of sandwich panels and how they are modeled, manufactured and joined to other structures are mentioned in the continued sections. Finally, the studies about static, vibrational and acoustic characteristics of sandwich structures are presented.

2.1 Background

Sandwich structures are composed of a weak (low elasticity modulus) and ligh-weight core material sandwiched between two strong (high elasticity modulus) and heavy face materials (Figure 2.1). Having face material thinner or thicker than core layer is up to the designer and the purpose of use must be taken under consideration for this selection. For example, if weight is to be reduced, thin face materials should be chosen. If damping is to be increased, very thin layer of viscoelastic material may be placed between two thick face materials as in the case of laminated steel. [2]

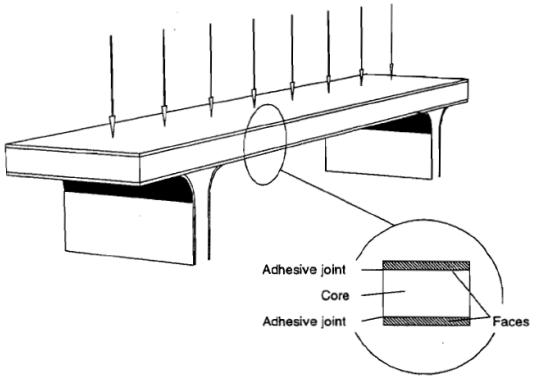

Figure 2.1 *Schematic of a structural sandwich panel*

According to Zenkert [2], the properties of primary interest for the face materials are high stiffness giving high flexural regidity, high tensile and compressive strength, impact resistance, surface finish, wear resistance and environmental resistance such as chemical, UV, heat etc. The face materials can be divided into two as metallic and non-metallic materials. Metallic materials contains steel, stainless steel, aluminium and titanium alloys. The most important non-metallic materials are the fibre composites. The reasons of their importance are that the manufacturing of sandwich composites is easier than of metal face sandwich structures and the anositropic behaviour of fibre composites allows us to place them in one direction to carry the load in that particular direction, and a different amount in another direction. The examples of fibre composites are glass fibres, aramid fibres, carbon fibres, matrices, wood and the fibre composites created using different materials combinations and manufacturing techniques. The material properties of these material types can be found in [2].

According to Zenkert [2], the properties of primary interest for the core materials are density, shear modulus, shear strength, stiffness perpendicular to the faces and thermal and acoustical insulation. The types of core materials are balsa wood, honeycomb cores, corrugated cores, metallic foams, homogenic elastomers and cellular foams. These types are shown in Figure 2.2.

Sandwich structures with cellular foamed cores do not have the same high bending stiffness and strenght-to-weight ratios as honeycomb sandwich structures. They on the other hand have other advantages such as cheapness and manufacturing easily. In addition to these, cellular foams offer high thermal insulation, acoustical damping and the water penetration is a little problem. The most used cellular foams are Polyurethane (PUR), Polystyrene (PS), Polyvinylchloride (PVC) and Polymethacrylimide (PMI), Polyurethane foam is the cheapest than all of the others and it not only produced by finite size blocks but also can be manufactured in a continuous process. Polystyrene foam has better mechanical and thermal insulation than Polyurethane foam and can be used in load-carrying structures. Polyvinylchloride foam has better mechanical properties than those of both Polyurethane and Polystyrene but it is more expensive. But Polyvinylchloride foam has a drawback which is poor resistance to heat (they can not be manufactured by autoclave). The best mechanical properties are contained in Polymethacrylimide cores but it is very expensive. [2]

In sandwich materials with honeycomb cores, aluminium, impregnated glass and aramid fibre mats are the most used materials to construct the core.

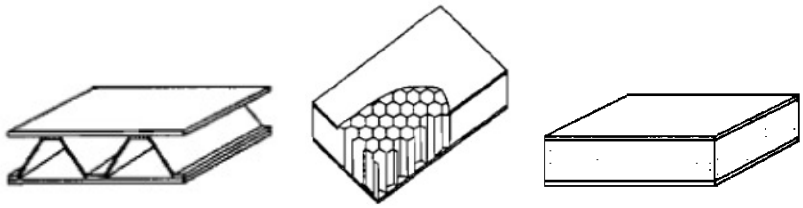

Figure 2.2 *The core materials types ((a) corrugated, (b) honeybomb (c) cellular or balsa)*

In most of the foam cored and honeycomb cored sandwich structures, bending loading are carried only by the face layers while the core resists transverse shear

loads (similar to the middle part of an I-beam) providing the faces to remain in place. However, a partition of the bending loads are also carried by the core layers in corrugated core construction. [3]

Due to their high bending stiffness-to-weight ratio, sandwich structures results in lower lateral deformations, higher buckling resistance and higher natural frequencies than do sheet metals. Therefore, at the same loading and boundary conditions, sandwich structure of similar static, strength and buckling performance can be obtained with lower overall weight.

Integration of vibration damping into a panel can be achieved by laminated metals. With laminated metals, noise and vibration characteristics can be improved without adding much weight and cost (reduced vibration levels can reduce structure borne noise). This allows for the reduction or elimination of sound absorbing materials and mastics used in automobile body panels for controlling cabin noise. [4]

2.2 Applications of Sandwich Structures

The concept of using two seperated faces is thought to have been first discussed by Duleau, in 1820, and later by Fairbairn. But it was not applied commercially until 1930. During World War I, sandwich panel concept was first used before utilization in small planes in World War II. The first mass production of sandwich laminates (with balsa core) was for Mosquito aircraft produced in England shown in Figure 2.3. [2]. After that day, the researches and applications of sandwich structures in industry are increased day after day. The applications are in a very wide area such as aeroplanes, trains, automobiles, fast ferries, ships, buildings and roofs etc.

Figure 2.3 *RAF Mosquito [5]*

Some other examples of transportation vehicles that contains sandwich structures are given in Figure 2.4, 2.5, 2.6, and 2.7. The utilization of sandwich structures in truck containers provides high thermal insulation and loading capacity. Also Danish IC3 train, Swedish SES SMYGE (surface-effect ship) and Airbus also uses sandwich structures in some parts.

Figure 2.4 *Sandwich container of truck [2]*

Figure 2.5 *Parts of the Danish IC3 train including flooring, interior and exterior panels are made of sandwich structures [2]*

Figure 2.6 *SES SMYGE [2]*

Figure 2.7 *Airbus Window Panel (PH 831) [6]*

There are lots of companies manufacturing different types of sandwich structures and the number is growing. One of these companies is Hylite. Aixam Microcar uses sandwich floor panels in Aixam 300 and Aixam 400 models. By this way, total weight is reduced by half with 1 m^2 panel. Also, Audi used these sandwich structures in A2 models in floor panels. The weight of floor panel is reduced from 500-600 kg to 350 kg [7].

Metawell GmbH. manufactures honeycomb cored sandwich structures. Volkswagen uses these structures in California model in cupboards, kitchen cabinets, folding tables, bed plates and roof storages. These structures are also used as crashbox of Apollo and rear bench seat of Audi A2. The weight of rear brench seat is reduced from 5.6 kg to 1.5 kg [8].

Laminated steel type sandwich structures named the Bondal Steel that ThyssenKrupp Steel AG manufactures are used as dash panels and oil sumps in automotive industry [9]. The same type sandwich structures named the Dynalam that Roush manufactures are used as engine covers, transmission covers and body panels in automotive industry [10]. Quiet Steel. a type of also laminated steel, are used in 2004 Ford F-150 Triton V8 as oil pan, in 2001 Ford Explorer Sport Trac., Cadillac CTS, 2003 Crysler Town, Country and Voyager and Dodge Caravan as cowl panel, in 2003 Lincoln Navigator as oil pan and dash panel and in 2003 Cadillac as dashboard. [12, 13, 14].

2.3 Manufacturing of Sandwich Structures

Pros and cons of manufacturing process or manufacturing time of sandwich structures are not included in the scope of this thesis. However, how honeycomb and foam cored sandwich structures produced and assembled to other structures are briefly discussed in this chapter.

The honeycombs are manufactured by corrugating process. In the corrugating process, pre-corrugated meral sheets are stacked into blocks and bonded together. After the adhesive between the sheets are cured, blocks can be cut from the stack. The process is shown in Figure 2.8. [2]

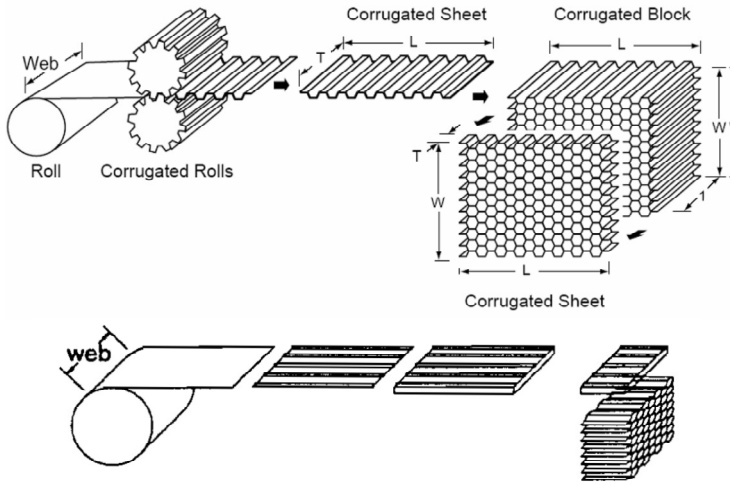

Figure 2.8 *Schematic of the manufacturing of honeycomb cores (corrugating and expansion process)* [2], [14]

When variation of thickness of honeycomb sandwich structures is desired, presses can be used to form the structure as shown in Figure 2.9. This process is called 'crushed-core-process'. [6]

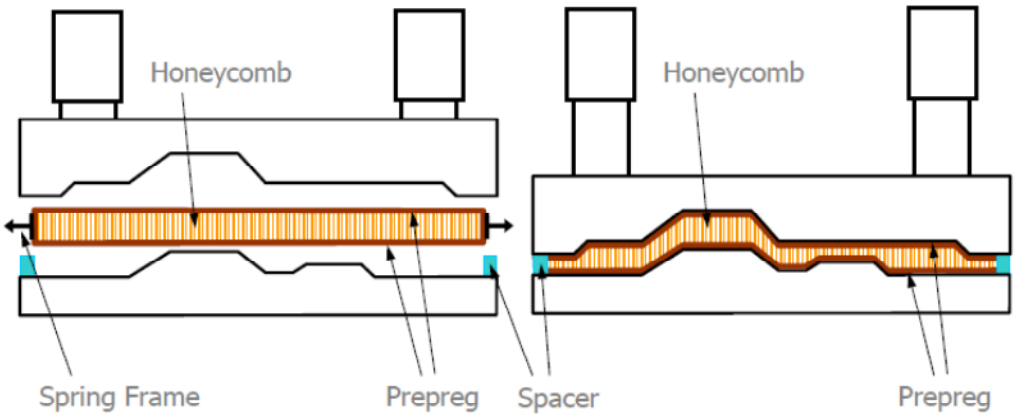

Figure 2.9 *Open and closed press for forming honeycomb structure [6]*

Cellular foam sandwich material can be manufactured with double-band rolls shown in Figure 2.10. Foam is poured on lower face material and adhered by self pressure and heat is applied to upper and lower face materials. This process goes on continiously and panels can be cut in desired dimensions.

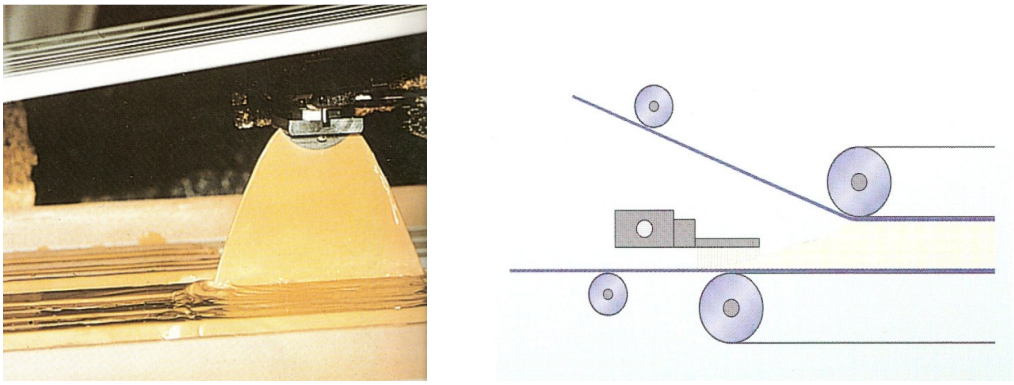

Figure 2.10 *Schematic of the manufacturing of foam cores[6]*

Laminated metals are shipped to stamping plants in a continuous coil or steel sheets. Then, the parts are stamped and shipped for assembly. They do not require a joining process to other structures since it can be welded to chassis as they are simple plates because the core is very thin as minimum 0.001 inch. The weld type commonly used to attach is squeeze-type resistance spor welding (STRSW) but MIG weld can also be used if there is a difficulity of access at every attachment points but weld comtamination from the core may come up. Also using winshield urethane adhesive is another method to attach laminated metals on chassis.

But some other methods are required for foam of honeycomb cored sandwich structures. One of these methods is using of end closures. With this method a free end of sandwich structure is protected from humidity and other environmental explosure. The types of end closures differ by the structure joint where the sandwich panel is to be joint. End closures are manufactured in the same process with panel

(pre-fabricated) or attached to the panel at the end of the process (post-fabricated) as seen in Figure 2.11 and 2.12. [15]

Figure 2.11 *Schematic of some types of pre-fabricated end-closures [15]*

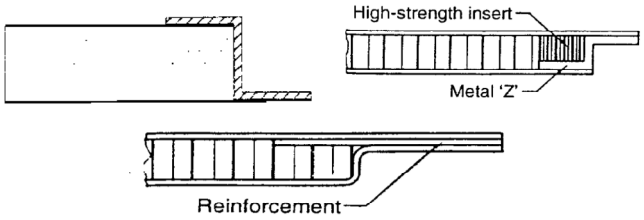

Figure 2.12 *Schematic of some types of post-fabricated end-closures [15], [16]*

Flat sandwich structures are mostly bonded in heated platen presses. Honeycomb sandwich structures can also be bonded and joined to other structures are shown in Figure 2.13.

Figure 2.13 *Schematic of some types of pre-fabricated end-closures [16]*

Sandwich panels with curved surfaces which prohibit press bonding are usually made by curing in an autoclave or vacuum bag setup in an oven. [16]

2.4 Modeling of Sandwich Structures

For two dimensional analyses performed by MSC.Nastran, first and second order triangular and quadrangular shell elements, shown in Figure 2.14 and 2.15, can be used to characterize each layer of sandwich structure.

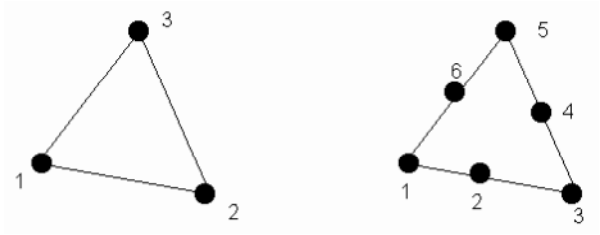

Figure 2.14 *Topology of triangular elements (3 and 6 nodes) [17]*

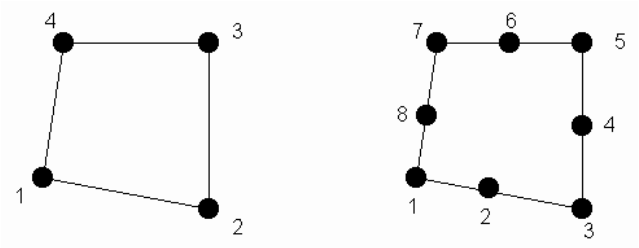

Figure 2.15 *Topology of quadrangular elements (4 and 8 nodes) [17]*

Three dimensional static and vibration analyses can be performed by using both pentahedral and hexahedral solid elements, shown in Figure 2.16 and 2.17. The sandwich can be modelled in three ways. First of these is the modelling of all layers as shell elements. Secondly, face materials are modeled with shell elements and core material by solid elements (offset shell/solid model which is showin in Figure 2.18). And finally, all layers can be modeled by solid elements.

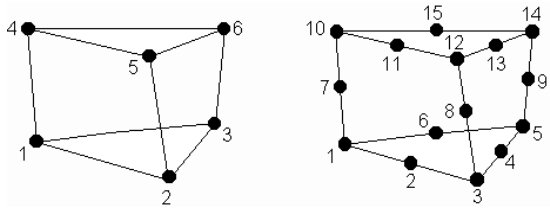

Figure 2.16 *Topology of pentahedral elements (6 and 15 nodes) [17]*

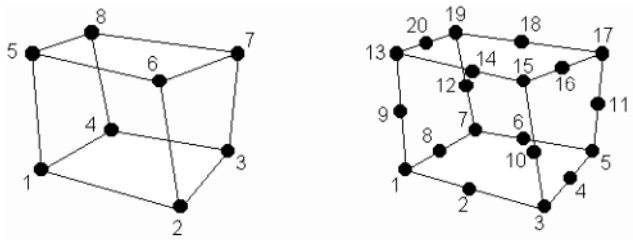

Figure 2.17 *Topology of hexahedral elements (8 and 20 nodes) [17]*

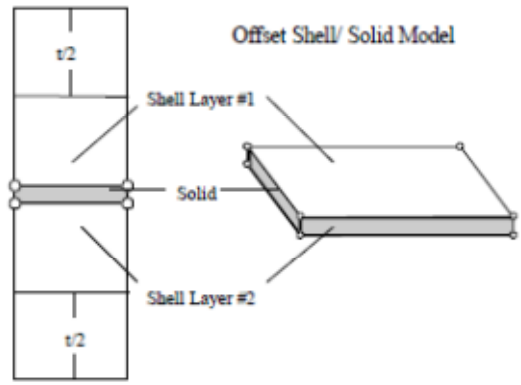

Figure 2.18 *Offset shell/solid model [4]*

For acoustical analyses MSC.Actran uses only solid-shell elements even if the panel to be analyzed is very thin. In this program, two dimensional acoustical analyses must be handled with only quadrangular elements. Both pentahedral or hexahedral elements can be used in three dimensional acoustical analyses. The properties of

these solid elements are to be chosen as shell. The orientation of panel is adjusted by the program itself by adding a simple code into the input file. [17]

Some authors like Manet [18], Mignery [4], Hazard et al. [21] and Balmet et al. [19] have studied the finite element modeling of sandwich structures.

Manet [18] has investigated the dependency of element types such as 8-node quadrilateral elements, multi-layered 8-node quadrilateral shell elements and multi-layered 20-node cubic elements to the displacements and stresses of a simply supported sandwich beam subjected to a uniform pressure. Also, the influence of mesh refinement has also been investigated. A local method called Reissner Method is presented. The displacement values with all the models is shown to have good agreement. The author also implies that the fine meshed models with 8-node quadrilateral elements are the most suitable for planar problems and multi-layered 8-node quadrilateral shell elements with sandwich option is a good way of computing sandwich materials. In addition to this, local Reissner method gives excellent results for interlaminar stress calculation and can be used for the design of new sandwich materials. This study showed us, both shell and solid elements can be used in static bending analyses.

In their study, Balmet et al. [19] have modelled constrained viscoelastic layer with 8-node hexahedral elements and the face materials with 4-node quadrilateral elements. The frequency response functions analyses of sandwich structures with different core thickness (minimum 0.1 mm) and materials are compared as the temperature changes.

Migner [4] has modeled the laminated steel panels in her study. The element type of steel layers are offset shell and solid elements for viscoelastic core material. The details of this study will be considered in Chapter 2.6.

Hazard et al. [21] has developed a partition of unity finite element method for the research of passive damping of structural vibrations by the use of viscoelastic layers. The method is based on the use of an interface element which couples the lower and upper layers without additional degrees of freedom. This method has been applied to the Midlin plate elements and these elements allows the vibration simulations with increased accuracy and lower cost than FEM. The method used in this study can be used in vibrational analyses in order to improve this thesis.

2.5 Static Deformation Analysis of Sandwich Structures

Wennhage [22] has studied about the weight optimization of sandwich materials. In this study a method to to minimize the mass per unit area of a sandwich panel, taking into account structural and acoustic requirements separately and together is presented. The formulas for maximum deformation and stresses are also used in this thesis study. In the author's other study [23], an optimization method of some body parts of railway vehicle with and without acoustic constraints. As a result of this study, the acoustic requirements produces a heavier design than when the optimization is performed with mechanical constraints only.

2.6 Vibration Characteristics Analysis of Sandwich Structures

The structural vibration of automobile body panels can be decreased by passive vibration or damping control methods such as a special case of sandwich structure

called laminated panels and surface damping treatments. They are glued on the most vibrating regions of the body panels at the resonances of panels. As an example, free layer surface damping treatments glued on flor panel of FIAT Tipo body are shown in Figure 2.19, 2.20 and 2.21. Damping treatments increase the weight of panel too much.

Mignery et al. [4] has introduced a finite element preprocessor called DAMP that eases the design process of the layers of laminated steels. This preprocessor utilizes both MSC.Patran and MSC.Nastran parameters in the mesh generation process and so, it can be used in optimization studies for structural vibration and acoustical analyses. It is also told that, although the thickness of laminated steels are higher than steel alone, it is lighter than the acoustic barriers, sound absorbing materials or mastics with the same vibration performance. At the end of this study, it is shown that the natural frequencies of the equivalent stiffness laminated design are close to the original steel design and the frequency response curve is considerably damped.

This study has provided guidance to identify layer thicknesses of lamimated steel panel used in this thesis. Also, finite element preprocessor DAMP can be used as a future study in order to improve this thesis.

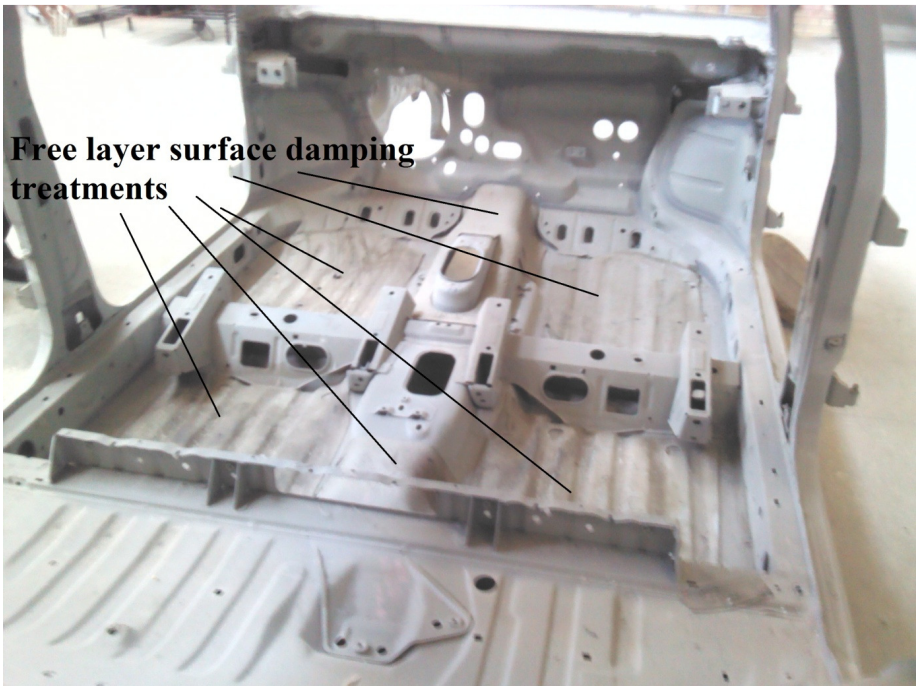

Figure 2.19 *Floor panel with additions of free layer surface damping treatments*

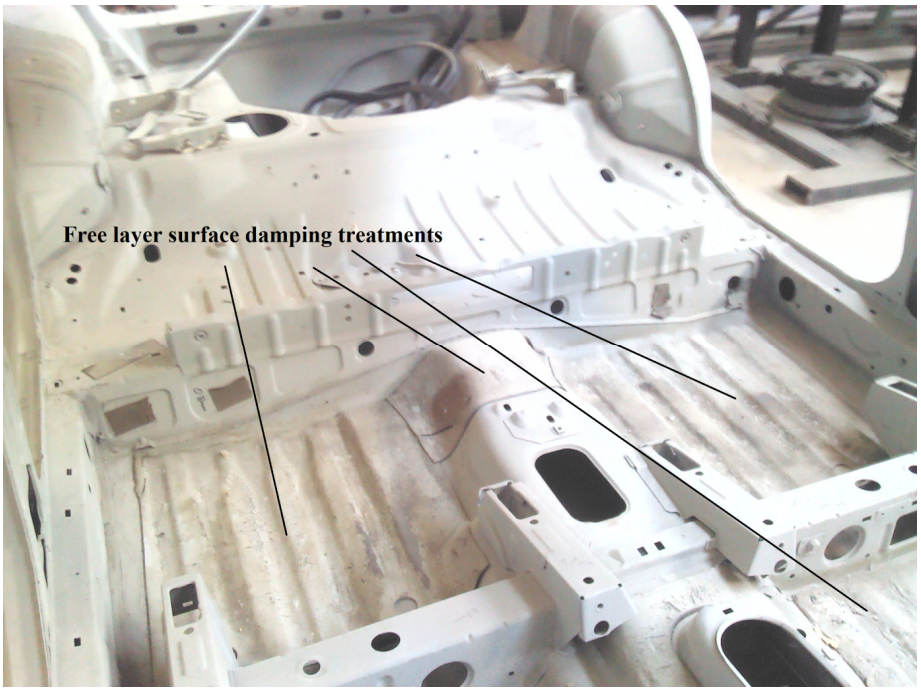

Figure 2.20 *Floor panel with additions of free layer surface damping treatments*

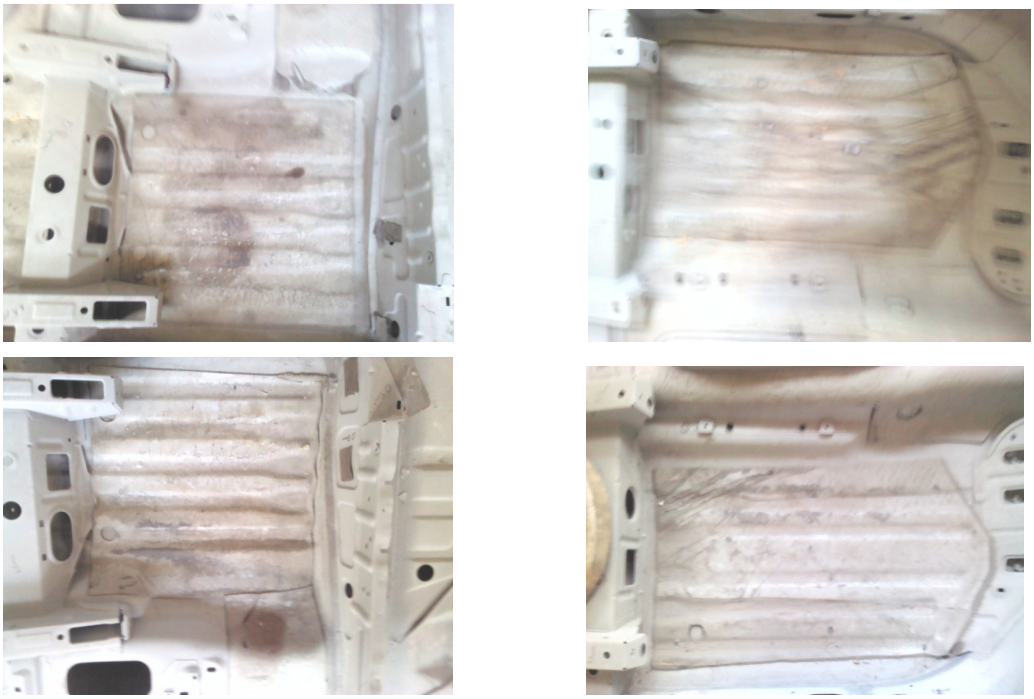

Figure 2.21 *Photographic image of surface damping treatments placed under seats*

Viscoelastic materials are used widely for vibration damping of automobile body panels in order to increase modal loss factor of the panel which is attached on it. These materials are attached on panels as core materials of sandwich structures (constrained layer surface damping treatments) or glued on solid surfaces as free layer surface damping treatments as in Oberst Beam and Van Oort Beam [43]. Several types of viscoelastic materials and also elastic materials can be stacked on the vibrating surface as multiple constrained layer-pairs. The effective damping treatment can be done by adding a viscoelastic material in locations where the greatest possible cyclic displacement occurs (partial coverage) as the structure vibrates in the modes of interest to dissipate as much vibrational energy.

According to Jones [43], viscoelastic materials with high loss factor should be used for vibration damping thus the materials are at transition region and at the temperature close to the peak loss factor temperature T_0. Also, low density materials

should be selected in order to have less weight addition. Materials with low elasticity modulus should be used as a core material of sandwich structures because modal strain energy created by shear forces is highly dissipated by these materials due to their strength to shear stresses. In addition to this, materials with high modulus of elasticity should be used as free layer surface damping treatments because of their strength to tensile stresses. [43]

There are lots of viscoelastic materials used for vibration damping. LD-400 damping tiles, Antivibe DS (formerly Aquaplas-F70 damping sheets), Paracril BJ, Viton-B, Styrene Butadine Rubber (SBR) and Butyl Rubber should be used as free layer damping treatment because of their high elasticity modulus. 3M-467 viscoelastic adhesive, 3M ISD-110 viscoelastic adhesive and Soundcoat N5 must be used as core material of a sandwich structure because of their low elasticity modulus and very high loss factor. [43]

Farage et al. [20] have studied about the numerical modelling of viscoelastic materials. They have made an assessment of a time-domain formulation which is called Golla-Hughes method (GHM). The comparison of experimental and numerical calculation of acceleration with respect to time is made and they have shown a good agreement. The method used in this study can be used as future study to improve this thesis.

Wang [24] has proposed a method that uses a equivalent modulus of elasticity, Poisson's ratio, thickness and loss factor that characterizes the panel with surface damping treatment. This method shows its validity by two numerical examples as beaded and curved panel such as real car floor panel. This method can be also used as future study to improve this thesis.

2.7 Sound Transmission Loss Characteristics and Analysis of Sandwich Structures

The driving comfort requires less noise inside the cabin. The noise in an automobile is created by engine, road, exhaust pipe, air flow (aerodynamic noise), brakes and tizzes. A large proportion of sound is generated by the vibration of solid structures. The noise is transmitted to the cabin through windows, doors, dash, roof (headliner) and floor panel.

There are two types of sound which are structure-borne and air-borne sound. The mechanical energy involved is transmitted from remote mechanical or acoustical resources by means of audio-frequency vibrational waves propagating in connected structures. This phenomena is classified as 'structure-borne sound' and it is shown in Figure 2.22.

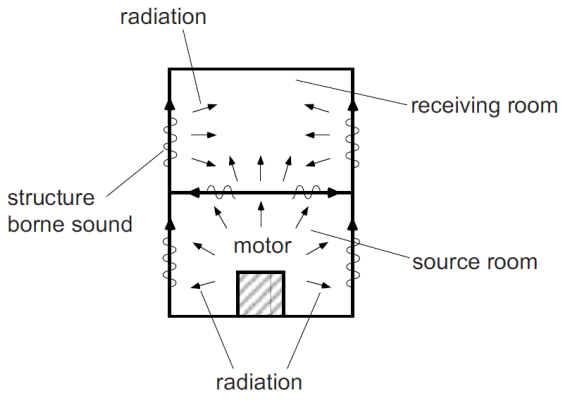

Figure 2.22 *Structure-borne sound [25]*

The term air-borne sound is used to describe sound waves which are being carried by the atmosphere. The transmission of sound through air is caused by a sound source,

rather than two objects impacting on each other. The air-borne sound transmission occurs by the sound waves that arrives to the partition between two air cavities makes it vibrated and then vibration is also transmitted to the other air cavity. (Figure 2.23)

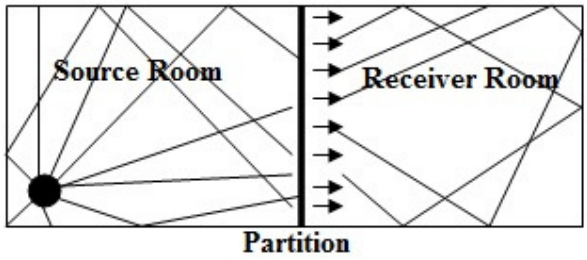

Figure 2.23 *Air-borne sound*

One of the sound sources in automobiles is the engine. The engine is attached to the chassis with engine mounts. These engine mounts act as vibration isolators and with these isolators the vibration, caused by the imbalance of rotating motor parts, at high frequencies are highly reduced. But at low frequencies, the vibrations transmitted to the body panels cause structure-borne sound which will have to be suppressed to prevent transmission into the cabin cavity. Furthermore, air-borne sound transmission through the firewall panel. shown in Figure 2.24, is also occured by the vibration of motor parts. Thus the motor is a source of both air-borne and structure-borne sound. As another example, exhaust pipe is a source of both air-borne and structure-borne sound because the exhaust flow is a supersonic flow at the free end of pipe and this flow causes air-borne sound. This flow also causes vibrations in the exhaust assembly which is connected to the body panels and transmitted vibrations may contribute to the structure-borne in the passenger cabin. The noise coming from road-tire interaction is also a source of both air-borne and structure-borne sound. The air-borne sound is transmitted through wheel panels that placed on the top of the wheels. The structure-borne sound is caused by vibraitons transmitted to the body panels through suspension components.

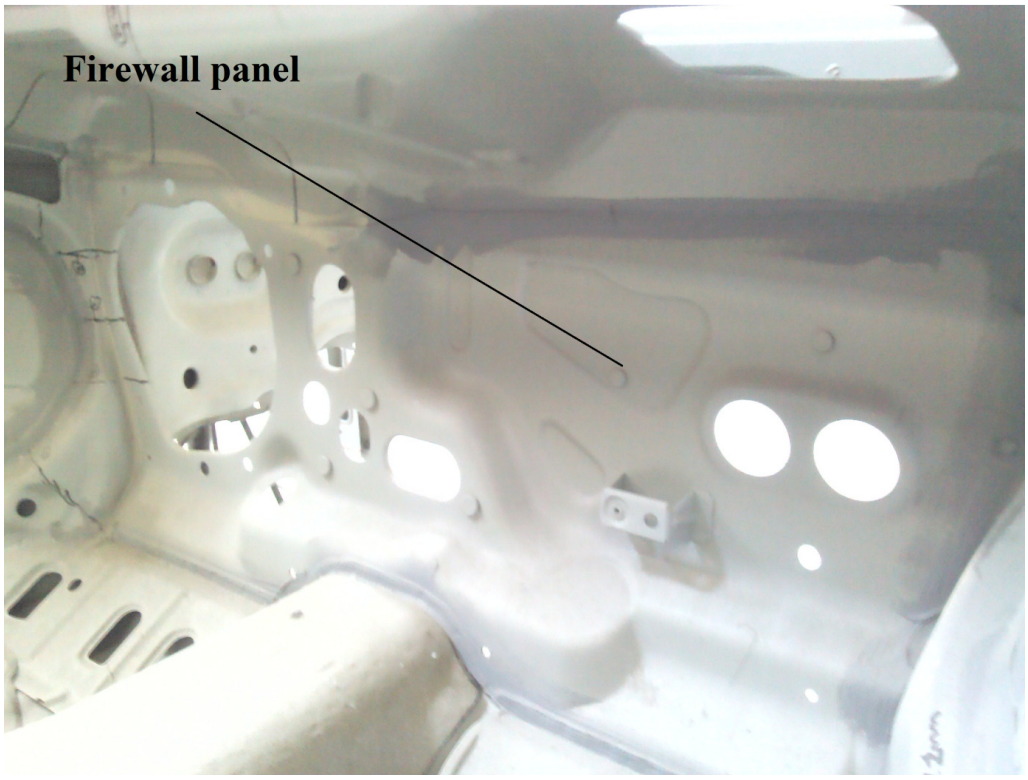

Figure 2.24 *Photographic image of firewall panel*

The air-borne sound coming from road can be decreased by passive vibration or damping control methods such as a special case of sandwich structure called laminated panels and acoustic barrier layers which are commonly materials of rubber glued to a layer of chip foam or a fibrous matting [44]. In the automotive industry, reduction or elimination of damping treatments due to their heaviness are investigated. Laminated steel panels have a better acoustical performance than sheet metal panels with a very little weight addition and still lighter than sheet steel panels with damping treatments. Thus, using laminated steel panels instead of utilization of damping treatments is a better way of improving acoustical performance without adding too much weight.

Fully elimination of surface damping treatments in the entire body can not be possible because they are also used for structure-borne sound transmission reduction transmitted through wheel panels, engine etc.

Air-borne noise transmission performance of a panel is characterized by sound transmission loss. The sound transmission loss of a panel is a measure of the ability to stop incoming acoustic power from being transmitted through itself.

Kuttruff [26] has identified the sound intensity (I) as the energy passing per second through an imaginary window of unit area perpendicular to the direction in which the wave travels. The sound intensity is defined in this book by the relationship,

$$I = \frac{P}{S} \tag{2.1}$$

where P is sound power and S is area of partition. According to Kuttruff [26], sound transmission loss (TL) or sound reduction index (R) through a partition between two adjacent rooms is characterised by the ratio of sound intensity of impinging and tranmitted wave.

$$TL = 10log\left(\frac{I_i}{I_t}\right) \text{ dB} \tag{2.2}$$

The sound intensity of impringing wave is stated in this book as $I_i = P_i/S$ and the sound intensity of transmitted wave as $I_t = P_t/S$. Thus,

$$TL = 10log\left(\frac{P_i}{P_t}\right) \text{ dB} \tag{2.3}$$

The incident power is $P_i = B.S$ where B is irradiation density and defined in Kuttruff's book [26] as,

$$B = \frac{c}{4}w \tag{2.4}$$

where c is speed of sound. Energy density (w=4P/cA) is the energy of a sound wave per unit volume. The relationship between sound intensity and sound energy density is $I = c.w$. Therefore $P_i = \frac{c}{4}S.w_i$ and $P_t = \frac{c}{4}A.w_t$ where A is is the total absorption area of the receiving room in Sabins. Sabin is the unit of sound absorption. One square meter of 100% absorbing material has a value of one metric Sabin.

Thus sound transmission loss is expressed in [26] by,

$$TL = 10log_{10}\left(\frac{w_i}{w_t}\right) + 10log_{10}\left(\frac{S}{A}\right) \tag{2.5}$$

Sound transmission loss is also defined in Kuttruff's book [26] as,

$$TL = L_i - L_t + 10log_{10}\left(\frac{S}{A}\right) \text{ dB} \tag{2.6}$$

where L_i and L_t's are average sound pressure levels of source and receiving rooms. The term $10log_{10}\left(\frac{S}{A}\right)$ is frequency independent term and only increases whole sound transmission loss values. Therefore in calculations within this thesis study, this term will be neglected.

The transmission coefficient, τ, is defined in [27] as the ratio of transmitted to incident sound energy. Thus, sound transmission loss can also be expressed by,

$$TL = 10log(1/\tau) \tag{2.7}$$

The ideal range of transmission coefficient is between 0 and 1. $\tau = 1$ implies that all incident energy is transmitted. This case can be expressed as the tranmission of

sound through an open window where the sound energy has no obstruction to its path. In the same way, $\tau = 0$ implies that sound is not tranmitted like sound isolation.

Bies et al. has described [28] how sound transmission loss of panels changes with respect to frequency (Figure 2.25) The sound transmssion loss is controlled by the panel's stiffness at low frequencies. At the first resonance of panel, the transmission loss is minimum, meaning that sound transmission is maximum. Broad frequency range occurs at frequencies above the first resonance and in this region transmission loss is controlled by the surface density of the panel. In this frequency range, tranmission loss increases with frequency at the rate of 6 dB per octave. At high frequencies, at the region of critical frequency, coincidence occurs. The sound transmission loss again rises at very high frequencies and this region is called damping controlled region. The rise in this region is at the rate of 9 dB per octave.

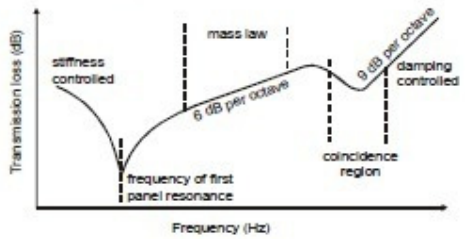

Figure 2.25 *The characteristics of sound transmission loss [28]*

The standard of estimating the sound transmission loss is ISO-140-3 [29]. This part of standard specifies a laboratory method of measuring the airborne sound insulation of building elements such as walls, floors, doors, windows etc. This standard suggests an estimation prosudure called 'two rooms method'. In this method, a specimen in consideration is placed between two rooms that have air in them. A spherical unit power sound source (acoustic load) is placed at the corner of one of the air cavities in order to generate a sound field. According to the standard, volumes and corresponding dimensions of the two test rooms should not be exactly the same. A difference in room volumes and/or in the linear dimensions of at least 10% is recommended.

Sound transmission loss can be calculated by MSC.Actran software program by simulating the test described in ISO 140-3 [29]. For this analysis, a finite element model must be prepared in MSC.Patran, HyperMesh or a similar program. Within this model, air cavities and panel between them must be created with finite elements, that are compatible with MSC.Actran (commonly HEX and QUAD), and the nodes of adjacent elements of panel and air cavities must be common to get a correct result. A sphere type (point element) sound source with unit power is placed at the far corner of source air cavity. Several elements in inner sections of both air cavities are seperated from the elements in outer sections and all the regions (inner source air cavity, outer source air cavity, inner receiver air cavity, outer receiver air cavity and panel) set to be a separate material. At the end of calculation, PLT file, that MSC.Actran gives as an output, shows mean squre pressure values of all materials separately for each frequency values in Hz previously defined in DAT file. Sound transmission loss in each frequency is calculated in Excel program by following equation:

$$TL = 10\log\left(\frac{Q_{MS_i}}{Q_{MS_t}}\right) \tag{2.8}$$

Narrow band sound transmission loss can be plotted by setting y-axis to be TL value, and x-axis to be frequency in Hz. But plotting of narrow band sound transmission loss is impractical and time consuming. In order to see the results comfortably, the whole frequency range is divided into frequency bands. Instruments to analyze noise is called bandwidth filters. Each band covers a specific range of frequencies. The bandwidth is characterized by lower and upper bound and center frequencies of bandwidths and determined by the difference of f_u and f_l ($\Delta f = f_u - f_l$) [25]. The bandwidth is proportional to the center frequency of the filter. With increasing center frequency the bandwidth also increases. The most commonly used representatives of filters with constant relative bandwidth are the octave, third-octave and tenth-octave band filters. The center frequencies are determined by a general formula,

$$f_c = 2^{1/n} \tag{2.9}$$

Where n is integers as counters starting from zero. Upper and lower frequencies are determined with the below formulas,

$$f_u = f_c . 2^{1/2m} \tag{2.10}$$

$$f_l = f_c / 2^{1/2m} \tag{2.11}$$

where, m is representing band type. For example 1 represents octave band, 3 represents third-octave band and 10 represents tenth-octave band. The lower and upper limits and center frequencies of all types of octave bands used in this thesis are given in tables in Appendix A, B and C. In addition to these, the limiting frequencies are also standardized in the international regulations EN 60651 and 60652.

The advantage of high octave band measurements is that they have finer resolution of the spectrum than the octave band because of having more data points in the same frequency range.

Octave band transmission loss and third-octave band transmission loss can be calculated using narrow band transmission loss. Beranek [30] has written that The National Bureau of Standards and the Riverbank Labarotories at Geneva. generally measure at frequencies of 125, 250, 500, 1000, 2000 and 4000 Hz. The average transmission loss is determined by calculating the arithmetic average of the transmission losses existing in the band. But it must be taken into account that, averaging must be handled in linear scale. Firstly transmission loss values in logarithmic scale must be converted into linear scale, then the averaging is done and

the this value must be converted into logarithmic scale again at last. When plotting octave band (or 1/3, 1/10 octave band etc.) transmission loss, this average transmission loss value is plotted at the center frequency of the band.

Also, ISO 140-3 standard [29] has formulized this averaging method as below:

$$L = 10log\frac{1}{n}\sum_{i=1}^{n} 10^{L_i/10} \text{ dB} \tag{2.12}$$

Acoustic wavelength is the ratio of speed of sound over frequency. The sound pressure varies harmonically [26] and shown in Figure 2.26.

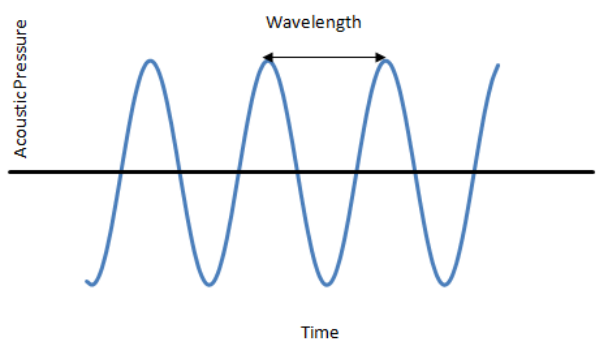

Figure 2.26 *The wavelength [26]*

The sound pressure varies harmonically has 5 important points where the pressure is minimum, maximum and zero. Therefore the finite element model of air cavities prepared for estimating sound transmission loss of a panel between them must have at least 5 nodes and 4 elements binded with that nodes in a wavelegth so as to get good results. The upper reliable frequency limit of analysis is determined by taking this element size restriction into consideration.

The lower frequency limit depends on the room size. The wave must proceed at least two wavelength size to get a good diffuse field in acoustic rooms. Therefore the minimum edge of room dimensions must be larger then two times of wavelenght in the frequency. The lower reliable frequency limit of analysis is determined by taking this room size restriction into consideration. [29]

In literature, there are lots of studies about sound transmission loss characteristics of panels with different estimation methods. One of the authors studied sound transmission loss of panel with 'two-room method' is Papadopoulos [31]. The author [31] has investigated the relationship between the acoustic modes and the air cavity geometry. The room (air cavity) walls have been introduced some geometric modifications and an optimization prosedure based on finite element analysis is develeoped. In his next study [32], this prosedure is extended to arbitrarily shaped rooms. A model that has two reverberation rooms meeting certain sound field criteria is designed. Also, optimization of this model is investigated. Using this model, numerical prediction of sound transmission loss is performed [33] with a procedure that is in compliance with the ISO standards and recommendations for acoustical measurements. Simply supported and clamped single-layered panels such as steel, glass and aluminium with different thicknesses are modelled and the calculated sound transmission loss is compared with the published experimental results. In this thesis study, these finite element model and analysis conditions will be recreated in MSC.Patran and the analysis results will be compared with these calculated results in order to verify the calculation process using MSC.Actran.

Xin et al. [34] have investigated the air-borne sound insulation of a rectangular double-panel which is clamped on an infinite acoustic rigid baffle. The analyses are performed analytically and experimentally, and these analyses are compared with that of a simply supported one. The experimental measurements have good agreement with the analytical results in both boundary conditions. The comparison between the sound transmission loss plots of simply supported and clamped ones

shows that, the natural frequencies of a clamped double-panel partition are higher than the simply supported one except for the plate-cavity-plate resonance frequency. Also, the sound transmission loss values show noticeable discrepancies for the two cases at the low frequencies and the discrepancies depend on the incident elevation angles at the higher frequencies.

Lee et al. [35] have used a modified transfer matrix method to evaluate the normal incidence sound transmission loss of multilayer solid materials. Firstly, the original transfer matrix method was measured via a standing wave tube method. The modification of transfer matrices of solid layers is performed in accord with data from the vibration of thin plates and the mass law effect. The method is validated with the experiments on several kinds of materials. This modified transfer matrix method can also be used by the authors who wants to improve this thesis study.

There are also studies about the applications of sound transmission loss analyses in automotive industry.

Fredö C. R [36] had also studied about the minimization of sound transmission of a cab floor. The author has developed an optimization process to enable the noise transmission peaks to be shifted into acceptable frequency ranges, and the noise transmission is reduced for most of the common RPM ranges. The weight of the floor is also reduced.

Bregant et al. [37] have modelled a 3D cavity representing the earth-moving machine cab by means of finite element structural mesh. After the cab vibration load experimental acquisition, the cab inner vibro-acoustic field is evaluated using a BEM coupled analysis. An optimization code is developed to carry out the the vibro-acoustic field optimization by modifiying the structural parameters. This prosedure can be applied in order to improve the vibro-acoustic behaviour.

Zuo et al. [38] have performed an vibro-acoustic experiment to test a prototype of fuel cell car. They identified the characterictics and sources of interior noise through analyzing the test data. They obtained that, the assembly unit of traction motor of the vehicle, the hydrogen-pump and fan of the fuel cell system are the main sources of interior noise. They also investigated the noise difference of driver's and passenger's ears. The driver always hears more noise that the passenger and it is said that the difference of two noise decreases as the vehicle's speed increases. The traction motor becomes the dominant noise type, also as the vehicle's speed increase.

Also Liu et. al., [39] have studied about the prediction of sound inside vehicles. Finite and boundary element models are created and adopted to perform vibro-acoustic analysis. These models have good agreement with the experimental measurements.

'Two room method' suggested by ISO-140-3 standard will be used in this thesis study to estimate the the sound transmission loss characteristics of different sandwich panel and structure configurations. The laboratory method will be simulated by generating a finite element model in MSC.Patran and performing the finite element based vibro-acoustic harmonic response analyses in MSC.Actran.

CHAPTER 3

USE OF SANDWICH MATERIALS FOR REDUCING THE WEIGHT OF CAR BODY-IN-WHITE PANELS CONSIDERING STATIC STIFFNESS CHARACTERISTICS

3.1 Introduction

Within the scope of this thesis, the applications on a passenger car body-in-white model will be investigated. For this purpose, the finite element model of FIAT Car body model that Özgen [1] has used in his study will be used. The floor panel, firewall panel, rear wheel panels and luggage panel of this body model will be designed with sandwich materials. These panels are chosen due to their load carrying conditions. Floor panel is chosen as the load-carrying panel and others are the examples of non-load-carrying panels. In this design study, the curvatures and shapes of panels will not be changed but its sandwich configurations such as thicknesses and materials of both face and core layers will be determined.

In this chapter, it is aimed to obtain a minimum weighted sandwich panel for these panels having the same static performance as steel panel. This performance is maximum displacement in the panels observed in the bending stiffness analysis of car body-in-white under test loads. For this purpose, while determining the sandwich

material configurations for these panels, the sandwich material parameters that give maximum displacement close to the maximum displacement given by sheet metal panels will be determined.

Static behavior of a car body structure is usually characterized by stiffness values of the structure. The bending and torsional stiffness measures are used in the automobile body analysis. When a new model automobile is to be designed, the bending stiffness of the body is one of the most important issues.

Bending stiffness of an automobile body may be determined by applying 6432 N vertical load on mid floor area of the body and clamping the regions where suspensions are situated as seen in Figure 3.1 [1]. With this load/boundary conditions, the floor panel becomes the load carrying panel. That's why, one of the body panels to be designed in this study for weight minimization is selected as the floor panel.

Figure 3.1 *Load/boundary conditions of FIAT car body-in-white [1]*

In order to find sandwich material parameter that will reduce the mass of the selected FIAT car body-in-white panels, an optimization process is developed for this thesis study. Since theoretical formulas of maximum displacement of both sheet metal and sandwich panels with complex shape under distributed load are not known, to obtain

preliminary values for sandwich material paramteres first analytical deflection and static stress-strain formulas for flat sandwich and homogenious panels are used in this in optimization process. These formulations are used along with the optimization functions available in MATLAB. The formulas, introduced by Zenkert [2], Young [40], Plantema [41] and Wennhage [22], are verified by estimating the maximum displacement of a randomly chosen sandwich panel configuration under two different boundary conditions with Matlab codes and MSC.Nastran analyzes. After that, optimizations of both clamped and simply supported flat sandwich panels are performed with Matlab codes, and the maximum displacement of resulting optimum sandwich panel is then verified whether it is the value that is set to be constraint.

Afterwards, the sandwich panel configurations that Matlab codes resulted are set to be an initial guess of the optimum configuration. Then, core material thicknesses of these initial guesses are increased until the maximum displacement of panel reaches the value of steel panel. The configuration that fits this value is claimed to be optimum panel configuration. The optimization results are validated by performing MSC.Nastran analyses.

To investigate the maximum displacement of automobile floor panel. FIAT car body-in-white CAD model used in reference [1] is used. This model is shown in Figure 3.2. In this study, load/boundary conditions and the panel thicknesses are also used as in that study. The maximum displacement of FIAT car's floor panel is determined through MSC.Nastran analysis and this value is set to be a constraint of the optimization process. Two different constraint conditions are applied for design of simply supported sandwich panel in order to see how the optimization parameters change.

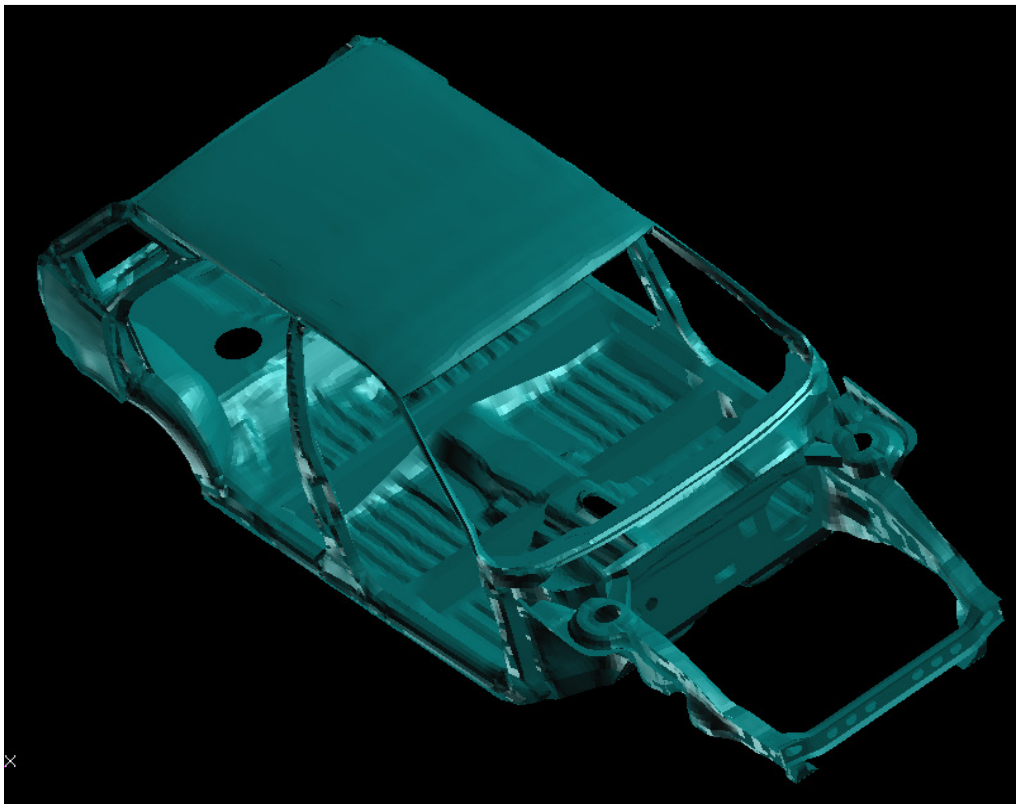

Figure 3.2 *FIAT car body-in-white CAD model*

Finally, the optimization of other body panels are performed with a similar method. In this method, the face layer thicknesses are chosen as not to be thicker than the half of original panel thickness. The core layer thickness is increased from zero milimeter until the maximum displacement of sandwich panel reaches the value of steel panel. The configuration that fits this value is said to be optimum panel configuration. This design procedure is described in below flowchart.

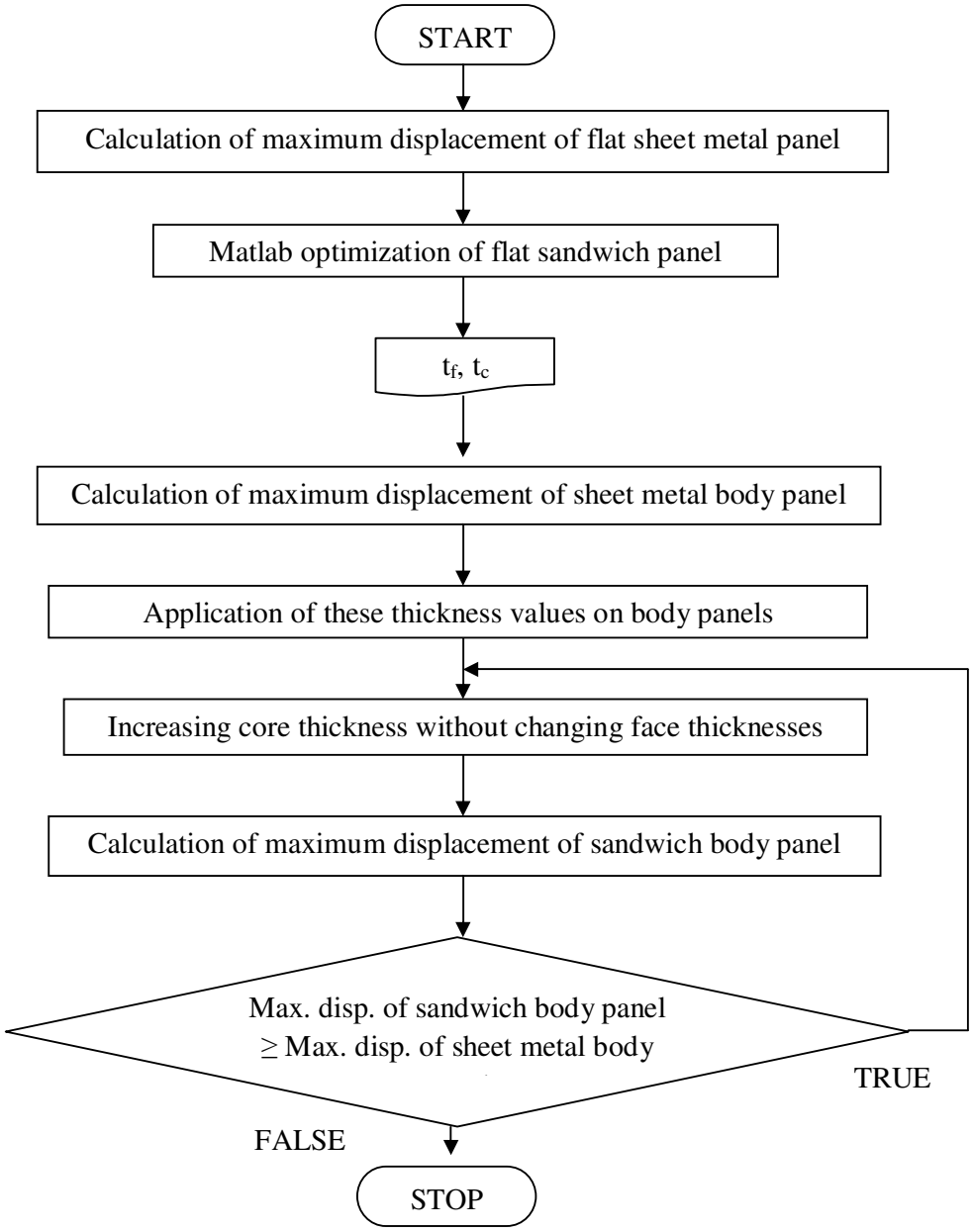

Figure 3.3 *Flowchart of Design Procedure*

3.2. Deflection of Sandwich Panels under Distributed Loading

Displacement and stress formulas of sandwich panels under transversely applied distributed loading necessary for optimization process are discussed in this section. Maximum deflection of randomly chosen sandwich configuration is calculated with

Matlab using these formulas and these formulas are validated by MSC.Nastran analyses.

The length and width of flat panel are chosen as 1.87 m and 1.49 m as measured from the FIAT car's CAD model used. This length is selected by measuring the distance between firewall and luggage panels and, selected width is the width of body-in-white. 6432 N distributed load at transverse (-z) direction is applied on this panel. Displacement boundary conditions are clamped and simply supported and investigated separately.

The orientation of panel on the coordinate system is shown in Figure 3.4. The long edge, lies in x axis, is denoted as a and the short edge lies in y axis, is denoted as b. In this case a is 1.87 m and b is 1.49 m.

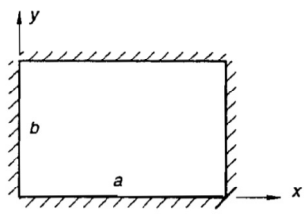

Figure 3.4 *The orientation of coordinate system for a rectangular clamped flat plate [2]*

3.2.1 Clamped Sandwich Panels

The displacement formulas of a rectangular clamped sandwich panel under distributed load introduced by Plantema [41] and Zenkert [2] are given in this section. They have both given formulations for maximum displacement and it occurs at the middle point. The displacements formulas for other points calculated with the

help of maximum displacement formulas are also given. The displacement formula introduced by Plantema [41] is,

$$w_{\max} = \frac{qa^2b^2}{\pi^4 D}\{[3(\frac{b^2}{a^2}+\frac{a^2}{b^2})+2]^{-1}+\frac{4}{3s}(1+\frac{b^2}{a^2})^{-1}\} \qquad (0.7 < b/a < 1.4) \qquad (3.1)$$

where D is the bending stiffness of sandwich panel. q is the pressure and s is the shear paramater. The bending stiffness D is composed of bending stiffness of core material (D_c), two times bending stiffness of face materials about their individual neutral axis (D_f) and bending stiffness of face materials about the middle axis (D_0). Total bending stiffness of sandwich panel having equal thicknesses of face materials is derived as,

$$D = 2D_f + D_0 + D_c = \frac{E_f t_f^3}{6} + \frac{E_f t_f d^2}{2} + \frac{E_c t_c^3}{12} \qquad (3.2)$$

If face materials with unequal thickness are used, distance between the neutral axes of face materials is $d = t_c + t_1/2 + t_2/2$ and the bending stiffness is $D = E_1 t_1 E_2 t_2 d^2/(E_1 t_1 + E_2 t_2)$. Subindex 1 indicates upper face material, subindex 2 indicates lower face material and subindice c indicates core material properties as shpwn in Figure 3.5.

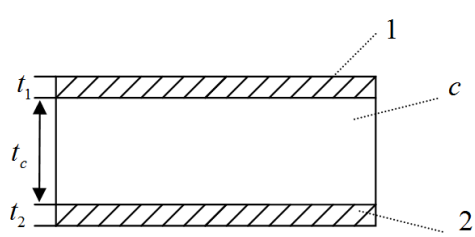

Figure 3.5 *Sandwich panel with unequal face thicknesses*

The pressure q is the ratio of total force over total area and the shear parameter s is defined as,

$$s = \frac{b^2 S}{\pi^2 D} \tag{3.3}$$

where the shear stiffness S is defined as,

$$S = \frac{G_c d^2}{t_c} \tag{3.4}$$

When the maximum displacement for other points on the panel is wanted to be calculated, Equation (3.5) can be used.

$$w = w_{max} sin^2 \frac{\pi x}{a} sin^2 \frac{\pi y}{b} \tag{3.5}$$

An approximate solution of Zenkert [2] for maximum displacement of clamped sandwich panels with thin faces under distributed loading is,

$$\overline{w} = \frac{qb^4(1-\vartheta^2)}{\pi^4 D\left[3\left(\frac{b}{a}\right)^4 + 2\left(\frac{b}{a}\right)^2 + 3\right]} + \frac{4qb^2}{3\pi^2 S\left[\left(\frac{b}{a}\right)^2 + 1\right]} \tag{3.6}$$

Also, when the displacement for other points on the panel is to be calculated with Zenkert's [2] approach, Equation (3.7) can be used.

$$w = (W_b + W_s)\sin^2\frac{\pi x}{a}\sin^2\frac{\pi y}{b} = \overline{w}\sin^2\frac{\pi x}{a}\sin^2\frac{\pi y}{b} \tag{3.7}$$

3.2.2 Simply Supported Sandwich Panels

The simply supported boundary condition for a rectangular flat panel can be applied by setting displacement and moment about the x axis to be zero at x=0 and x=a and displacement and moment about the y axis must be zero at y=0 and y=b.

The displacement formulas of a rectangular simply supported sandwich panel under distributed load introduced by Zenkert [2] and Military Handbook 23A [42] are given. In the optimization study, in addition to displacement formulas, stress definitions will also be necessary for constraints of optimization process. The stress definitions given by Wennhage [22] and Military Handbook 23A [42] are also given in this section.

Zenkert [2] has introduced the displacement formulas for simply supported isotropic sandwich structures with weak core material under distributed loading in two different conditions as thick and thin face materials. Weak core approximation is defined as the condition given in Equation (3.8).

$$\frac{D_c}{D_0} < 0.01 \quad \text{if} \quad \frac{6E_f t_f d^2}{E_c {t_c}^3} > 100 \tag{3.8}$$

Thin face approximation is desribed in Equation (3.9). The conditions that are not complying with this condition are defined as thick face approximation.

$$\frac{2D_f}{D_0} < 0.01 \quad \text{if} \quad 3\left(\frac{d}{t_f}\right)^2 > 100 \ \text{ or } \ \frac{d}{t_f} > 5.77 \tag{3.9}$$

The exact displacement field of a sandwich panel with thick faces can be written as,

$$w = \sum_{n=1.3.5\ldots}^{\infty} \sum_{m=1.3.5\ldots}^{\infty} \frac{16q}{mn\pi^2 K_{mn}} \left[1 + \frac{D}{S(1-\vartheta^2)}\left(\left[\frac{m\pi}{a}\right]^2 + \left[\frac{n\pi}{b}\right]^2\right)\right] sin\frac{m\pi x}{a} sin\frac{n\pi y}{b} \tag{3.10}$$

where the denominator K_{mn} is defined as,

$$K_{mn} = \frac{2D_f D_0}{S(1-\vartheta^2)^2}\left[\left(\frac{m\pi}{a}\right)^2 + \left(\frac{n\pi}{b}\right)^2\right]^3 + \frac{2D_f + D_0}{1-\vartheta^2}\left[\left(\frac{m\pi}{a}\right)^2 + \left(\frac{n\pi}{b}\right)^2\right]^2 \tag{3.11}$$

Although this formula is derived for sandwich panels with thick faces, it can also be used for sandwich panels with thin faces. The formula for sandwich panel with thin faces is given as,

$$w = \frac{16qb^4(1-\vartheta^2)}{\pi^6 D} \sum_{n=1,3,5\ldots}^{\infty} \sum_{m=1,3,5\ldots}^{\infty} \frac{1+\pi^2\theta\left[\left(\frac{mb}{a}\right)^2 + n^2\right]}{mn\left[\left(\frac{mb}{a}\right)^2 + n^2\right]^2} sin\frac{m\pi x}{a} sin\frac{n\pi y}{b} \tag{3.12}$$

where the shear factor $\theta = D/b^2 S(1-\vartheta^2)$. The maximum diplacement occurs at x=a/2 and y=b/2.

In Military Handbook 23A [42], the maximum displacement formula has been derived in a different way. A theoretical coefficient K_3, dependent upon the aspect

ratio a/b, is found out from the chart given in Appendix F in order to derive these formulations. Firstly the parameters λ_f and V are needed to be calculated as,

$$V = \frac{\pi^2 D}{(b^2 S)} = \frac{\pi^2 E t_f t_c}{2\lambda_f b^2 G_c} \tag{3.13}$$

$$\lambda_f = 1 - \vartheta^2 \tag{3.14}$$

Where b is denoting the total thickness of sandwich structure. Maximum displacement of the sandwich panel is calculated as,

$$\delta = K_3 \frac{2qb^4}{h^2 E_f t_f} \tag{3.15}$$

where h is sum of face and core thicknesses. In the optimization study, in addition to displacement formulas stress definitions will be necessary for constraints of optimization process. Under a distributed load, face materials resist tensile and compressive stresses while core material resists shear stresses. Maximum stress definitions of face materials in both x and y directions have been introduced in Wennhage's study [22] as in (3.13) and (3.14) respectively.

$$\sigma_{fx} = \frac{M_x}{t_f(t_f + t_c)} \tag{3.16}$$

$$\sigma_{fy} = \frac{M_y}{t_f(t_f + t_c)} \tag{3.17}$$

where bending moments M_x and M_y are calculated as,

$$M_x = \frac{16q}{\pi^2}\sum_{m=1,3,5\ldots}^{M}\sum_{n=1,3,5\ldots}^{N}\frac{\left(\frac{m\pi}{a}\right)^2+\vartheta\left(\frac{n\pi}{b}\right)^2}{mn\left[\left(\frac{m\pi}{a}\right)^2+\left(\frac{n\pi}{b}\right)^2\right]^2}\sin\frac{m\pi x}{a}\sin\frac{n\pi y}{b} \tag{3.18}$$

$$M_y = \frac{16q}{\pi^2}\sum_{m=1,3,5\ldots}^{M}\sum_{n=1,3,5\ldots}^{N}\frac{\left(\frac{n\pi}{a}\right)^2+\vartheta\left(\frac{m\pi}{b}\right)^2}{mn\left[\left(\frac{m\pi}{a}\right)^2+\left(\frac{n\pi}{b}\right)^2\right]^2}\sin\frac{m\pi x}{a}\sin\frac{n\pi y}{b} \tag{3.19}$$

Where m and n are counters and M and N are the end values of counters. The more accurate moment values can be obtained by selecting M and N as large as possible.

Wennhage [22] has written the shear forces formulas as,

$$T_x = \frac{16q}{\pi^2}\sum_{m=1.3.5\ldots.}^{M}\sum_{n=1.3.5\ldots}^{N}\frac{\cos\frac{m\pi x}{a}\sin\frac{n\pi y}{b}}{mn\left[\left(\frac{m\pi}{a}\right)^2+\left(\frac{n\pi}{b}\right)^2\right]}\frac{m\pi}{a} \tag{3.20}$$

$$T_y = \frac{16q}{\pi^2}\sum_{m=1.3.5\ldots.}^{M}\sum_{n=1.3.5\ldots}^{N}\frac{\sin\frac{m\pi x}{a}\cos\frac{n\pi y}{b}}{mn\left[\left(\frac{m\pi}{a}\right)^2+\left(\frac{n\pi}{b}\right)^2\right]}\frac{n\pi}{b} \tag{3.21}$$

Core shear stress is given by the following expressions, with x=0, y = b/2 for T_x and x = a/2, y = 0 for T_y,

$$\tau_{cx} = \frac{T_x}{(t_f+t_c)} \tag{3.22}$$

$$\tau_{cy} = \frac{T_y}{(t_f + t_c)} \tag{3.23}$$

Also in Military Handbook 23A [42], the maximum face bending stress and xore shear stress formulas have been derived in a different way. Theoretical coefficients K_1 and K_2 dependent upon the aspect ratio a/b, are found out from charts given in Appendix D and E in order to derive these formulations. According to the book, maximum face bending stress is calculated by the formula,

$$\sigma_f = K_2 \frac{qb^2}{ht_f} \tag{3.24}$$

And maximum core shear stress is calculated as,

$$\tau_c = K_3 \frac{qb}{h} \tag{3.25}$$

Safety factor of face materials needed for constraint definitions of optimization process can be calculated by dividing yield stress of face material by maximum face bending stress. By the same way, safety factor of core material can be calculated by dividing shear stress of core material by maximum core shear stress.

3.2.3 Verification of Theoretical Formulas

In this section, a random sandwich structure configuration is chosen in order to verify the theoretical formulas given in above section. A bending analysis in

MSC.Nastran program is prepared and the result is compared with the result of Matlab calculation using the above formulas.

Steel is used for the face material of chosen sandwich panel. The material properties are given in Table 3.1.

Table 3.1 *Properties of steel*

Property	***Value***
Modulus of elasticity	206 GPa
Poisson ratio	0.3
Density	7800 kg/m^3

Polyurethane foam is selected for the core material due to its cheapness and easyness of manufacturing. The Polyurethane foam with 40 kg/m^3 density shown in Zenkert's book [2] is chosen as core material. The properties of PUR are shown in Table 3.2.

Table 3.2 *Properties of PUR foam used in this study*

Property	***Value***
Modulus of elasticity	12 MPa
Poisson ratio	0.499
Density	40 kg/m^3
Shear modulus	4 MPa
Maximum allowable core stress	0.25 MPa

Thicknesses of face and core materials are chosen as 0.25 mm and 8.5 mm respectively. The distributed of load 2308 Pa applied on this panel is calculated by dividing total force (6432 N) by total surface area.

3.2.3.1 Clamped Sandwich Panels

The maximum displacement of the sandwich panel configuration whose dimensions and materials properties are given above under distributed load is calculated with a Matlab code according to the formulation that Zenkert [2] has proposed for the clamped sandwich structures given in 3.2.1. section. The maximum displacement is resulted as 21.6 mm.

The maximum displacement of the clamped sandwich panel configuration under distributed load is analyzed with MSC.Nastran program. Face materials are modelled with offset shell elements and core materials are modelled with solid elements. The boundary conditions are applied on all the nodes at the edges that are attached to all layers of the structure. The maximum displacement is resulted 23.3 mm as shown in Figure 3.6.

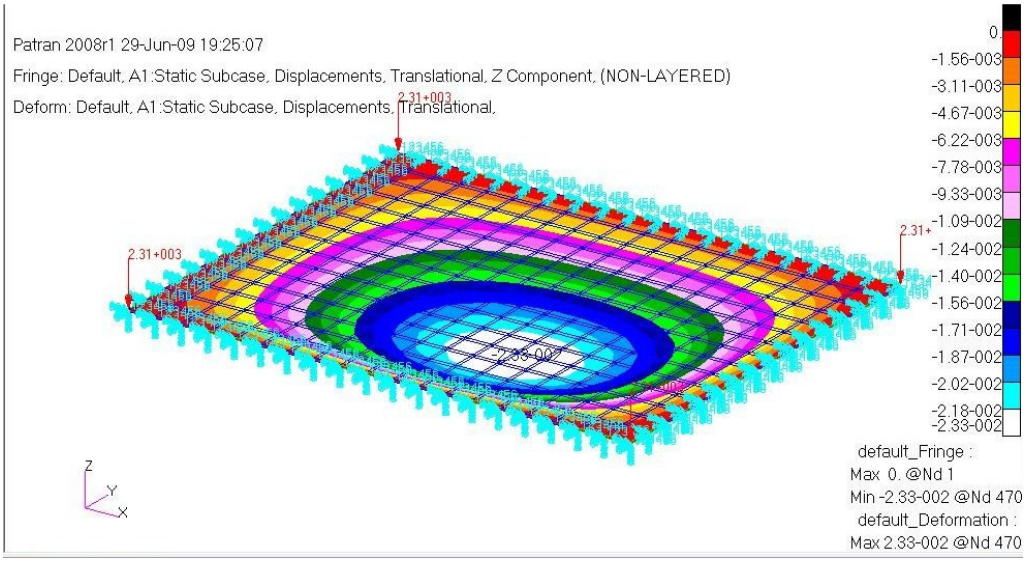

Figure 3.6 *Displacement result of randomly chosen clamped sandwich panel analyzed with MSC.Nastran*

The results of Matlab calculation and MSC.Nastran analysis are close to each other. The error can be decreased by using a finer mesh. According to the results, the formulation that Zenkert D. has proposed can be used.

3.2.3.2 Simply Supported Sandwich Panels

The maximum displacement of the simply supported sandwich panel configuration whose dimensions and materials properties are given above under distributed load is calculated with the Matlab according to the formulation that Zenkert [2] has written for simply supported, isotropic sandwich structures with both thick and thin faces and weak core material under distributed loading in 3.2.2 section. The same panel and loading condition as in clamped one are also chosen and the maximum displacement resulted as 44.6 mm.

The maximum displacement of the sandwich panel configuration whose dimensions and materials properties are given above under distributed load is analyzed with MSC.Nastran program. Face materials are modelled with offset shell elements and core materials are modelled with solid elements. The boundary conditions a of simply supporting boundary conditions for a flat plate is given in Figure 3.7. The boundary conditions are applied to all the node that are attached to all layers of the structure. The maximum displacement is 46.6 mm and shown in Figure 3.8.

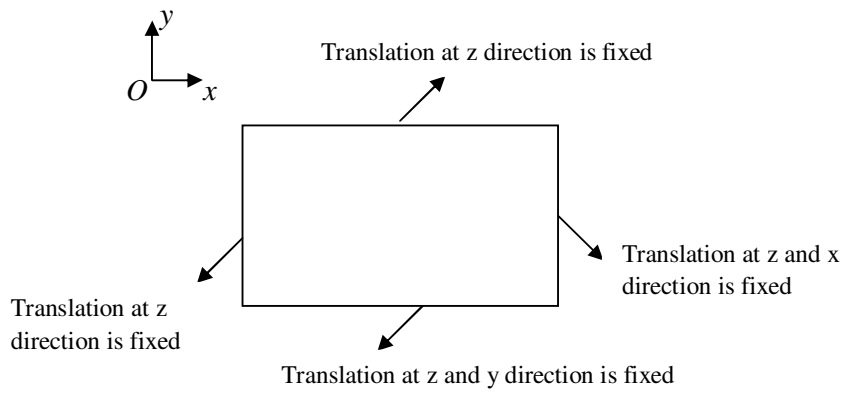

Figure 3.7 *Boundary conditions of simply supporting boundary conditions for a flat plate*

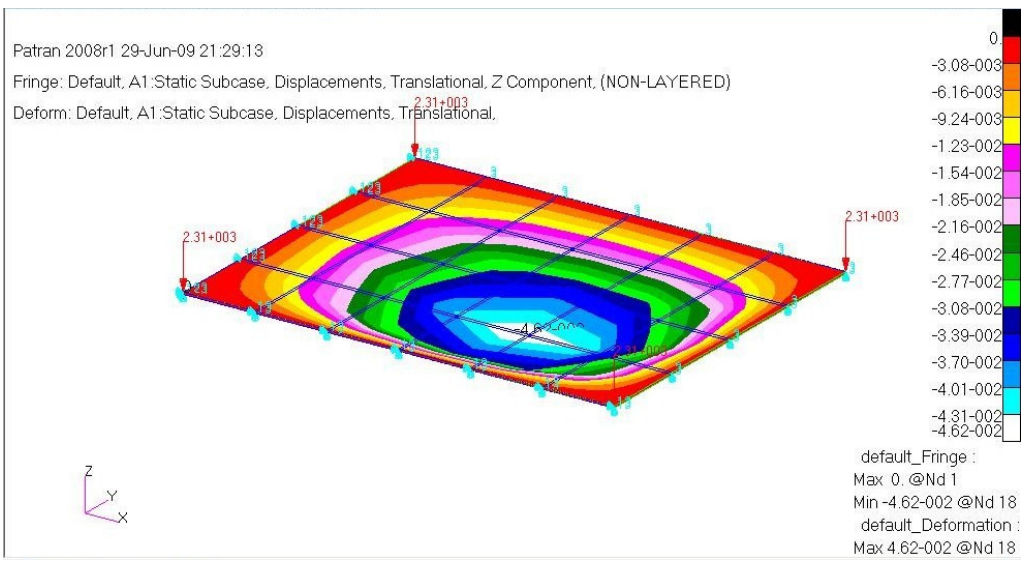

Figure 3.8 *Displacement result of randomly chosen simply supported sandwich panel analyzed with MSC.Nastran*

The results of Matlab calculation and MSC.Nastran analysis are close to each other. The error can be decreased by using a finer mesh. According to the results. the formulation that Zenkert [2] has proposed can be used.

3.3 Deflection of Flat Sheet Metal Panels under Distributed Loading

Displacement formulas of flat rectangular sheet metal panels under transversely applied distributed load introduced by several authors are given in this section. Maximum deformation of steel flat panel with 1 mm thickness is calculated with Matlab using these formulas separately and these formulas are validated by MSC.Nastran analyses.

The length and width of flat panel are chosen as 1.87 m and 1.49 m as used in above sections. Also 6432 N distributed load at -z direction is applied on this panel. Displacement boundary conditions are investigated separately.

In the previous sections displacement formulas for both clamped and simply supported sandwich panels were written by several authors. Displacement calculations for sheet metal flat panels can be derived by selecting the same material for face and core materials in the derivations that Plantema [41] and Zenkert [2] have derived for sandwich structures.

Young [40] has prepared tables in order to calculate the maximum displacement of both clamped and simply supported rectangular flat plates for a sheet metal having 0.3 Poisson ratio. Within this table, the terms of derivation can be found from the width-to-lenght ratio (α).

The maximum displacement of the panel can be calculated by,

$$\delta_{max} = -\frac{\alpha q b^4}{E t^3} \tag{3.26}$$

where the coefficient α dependent upon a/b is given in Tables 3.3 and 3.4 for clamped and simply supported flat panels.

Table 3.3 *The coefficient α for clamped sheet metal panel with υ=0.3 under distributed loading [40]*

a/b	1	1.2	1.4	1.6	1.8	2	∞
α	0.0138	0.188	0.0226	0.0251	0.0267	0.0277	0.0284

Table 3.4 *The coefficient α for simply supported sheet metal panel with υ=0.3 under distributed loading [40]*

a/b	1	1.2	1.4	1.6	1.8	2	3	4	5	∞
α	0.0444	00616	0.077	0.0906	0.1017	0.111	0.1335	0.14	0.1417	0.1421

3.3.1 Verification of Theoretical Formulas

In this section, steel flat panel with 1 mm thickness is chosen in order to verify the theoretical formulas given in above section. Other dimensions, load/boundary conditions and material properties of steel are the same as the verification of theoretical formulas of sandwich panels. A bending analysis in MSC.Nastran program is performed and the result is compared with the one with Matlab calculations.

3.3.1.1 Clamped Flat Sheet Metal Panels

The maximum displacement results of clamped steel flat panel under distributed load are calculated with theoretical formulas which are given in Table 3.5 and MSC.Nastran analysis shown in Figure 3.9. Formulas of Plantema [41] and Zenkert [2] for clamped sandwich structures are considered as for sheet metal panels with selecting the same material for both face and core layers. In the FE model, the

boundary conditions are applied as the same for clamped sandwich structures. The results are close to each other. Thus, formulas are acceptable.

Table 3.5 *Comparison of calculations with formulas and MSC.Nastran analysis*

Calculation Method	Maximum displacement
Plantema [41]	1.24 m
Zenkert [2]	1.13 m
Young [40]	1.10 m
MSC.Nastran	1.11 m

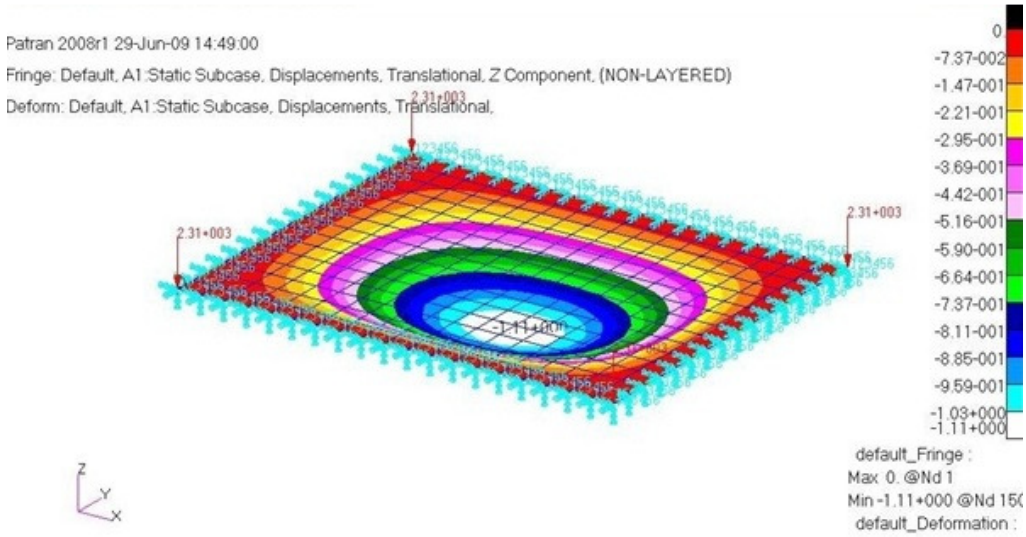

Figure 3.9 *Displacement result of clamped 1 mm steel sheet metal flat panel analyzed with MSC.Nastran*

3.3.1.2 Simply Supported Flat Sheet Metal Panels

For the verification of formulas for simply supported flat sheet metal panels, total load of 23.08 Pa is used instead of 2308 Pa since the displacement under 2308 Pa is greater than the panel's lenght. Application of boundary conditions are the same as simply supported sandwich panels. Zenkert's [2] formula for simply supported

sandwich structures are considered as for sheet metal panels with selecting the same material for both face and core layers. The results of calculations and MSC.Nastran analysis, illustrated in Figure 3.10, have shown a good agreement with each other as shown in Table 3.6. Thus, this value can be used for maximum displacement constraint.

Table 3.6 *Comparison of results*

Calculation Method	***Max displacement***
Zenkert D. [2]	38.1 mm
Young W. C. [40]	36.3 mm
MSC.Nastran analysis	36.5 mm

In the optimization study, maximum stress of steel sheet metal panel will be necessary in order to consider for optimization constraints. The stresses are also checked within this analysis and the maximum stress is resulted as 20.4 MPa as shown in Figure 3.11. Safety factor is calculated as 9.11 by dividing the yield stress (186 MPa) by maximum stress.

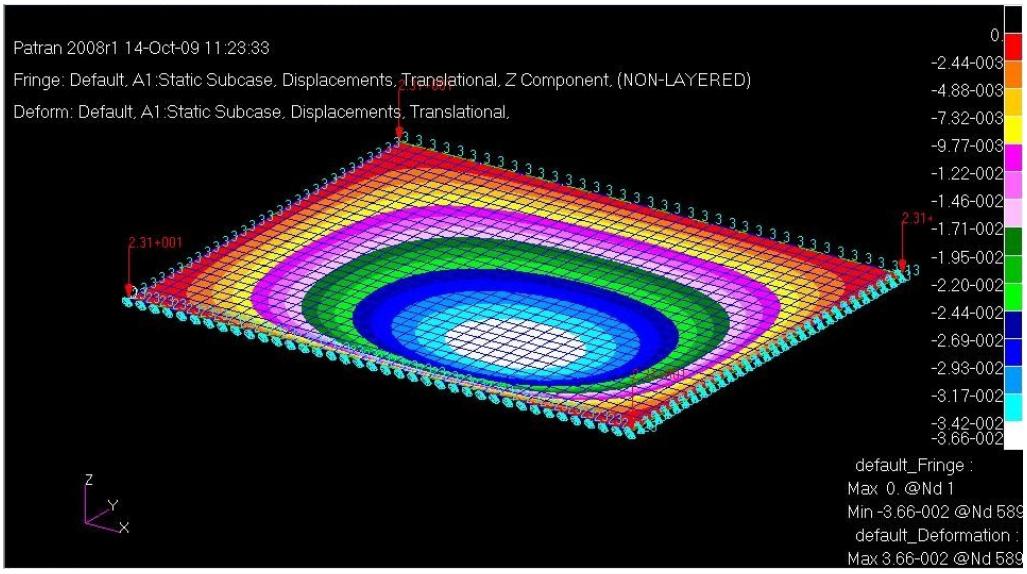

Figure 3.10 *Displacement result of simply supported 1 mm steel sheet metal flat panel analyzed with MSC.Nastran*

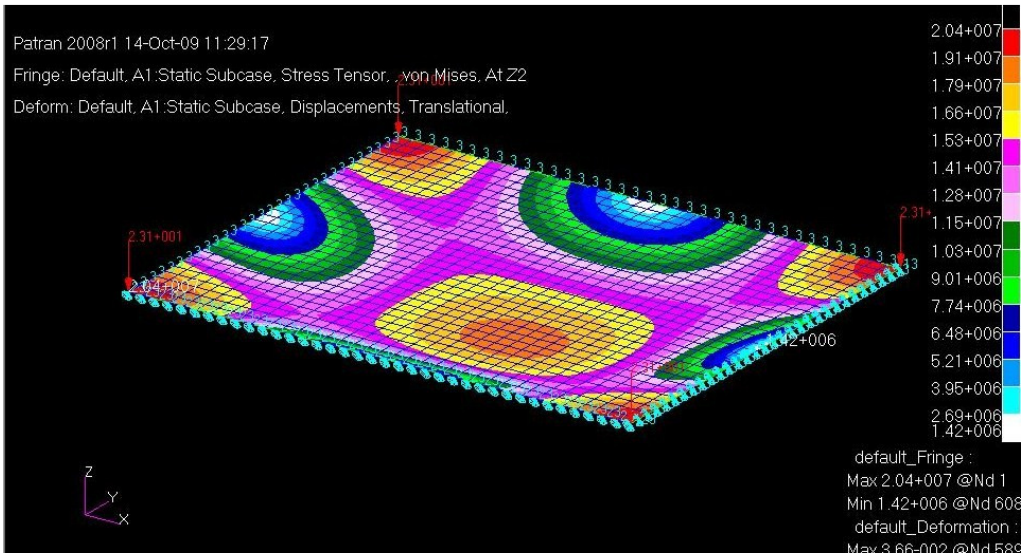

Figure 3.11 Stress result of simply supported 1 mm steel sheet metal flat panel analyzed with MSC.Nastran

3.4 Optimization of Sandwich Structures Used in Automobile Floor Panel

In this section, minimum weighted sandwich panel for automobile floor panel having the bending stiffness as steel panel is obtained. The optimum flat sandwich panel is found and then this optimum panel configuration is applied on floor panel. The core thickness is increased until the maximum displacement reaches the value of steel panel.

Optimization of flat sandwich panel is handled in Matlab. The function ‘fmincon’, which is used to find minimum of constrained nonlinear multivariable function, is used as optimization function in Matlab. The inputs of this function are objective function, initial guesses of desing parameters, equality and inequality constraints which are defined as matrices, upper and lower bounds, constraint function and optimization settings respectively. The outputs of this function are values of design parameters, value of minimized objective function, ‘exitflag’ which results the

optimization is done correctly or not and ‘output’ which gives an information about optimization results.

FIAT Car model that is used in Özgen’s [1] study is also used as a car model in this study. For the flat panel optimization, the length and width are chosen as 1.87 m and 1.49 m as they are used in previous sections. The same 6432 N distributed load at -z direction as also in previous sections is applied on the floor panel. The load/boundary conditions are shown in Figure 3.12. The displacements of nodes with orange color are set to be zero and and the force with yellor color is applied on the nodes under the seats. These nodes are shown in Figure 3.13.

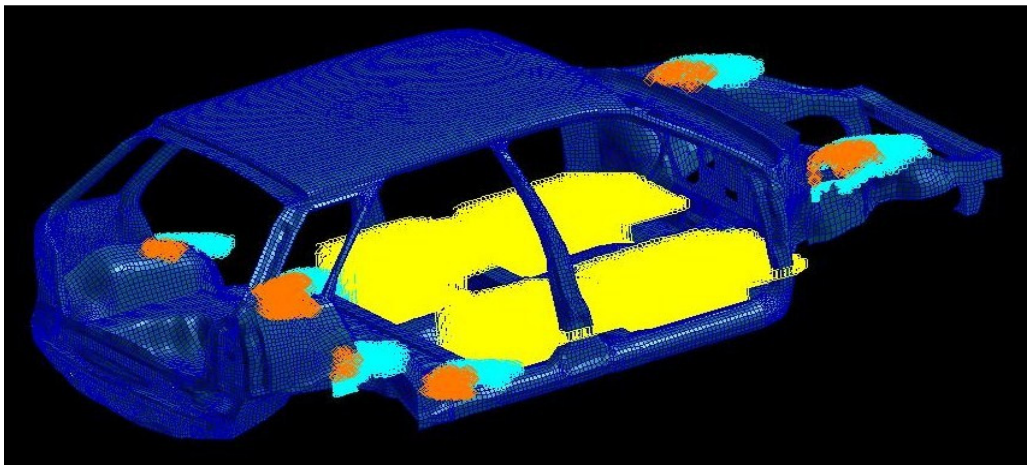

Figure 3.12 *Load/Boundary conditions of FIAT car model*

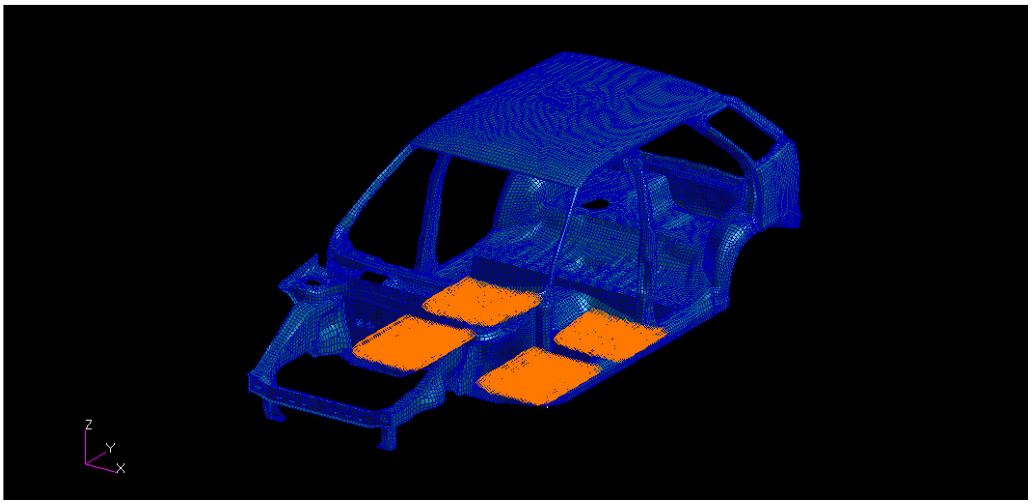

Figure 3.13 *Application region of loading*

Steel is chosen for face materials and Polyurethane foam for core material. The reason for these selections are that, steel is the mostly used material in automotive bodies and Polyurethane is the cheapest polymeric foam. This foam will be economically efficient for the mass production of bodies.

The objective function to be minimized is defined as the ratio of the sandwich panel weight to steel panel weight which is currently used.

$$f = \frac{W_{sandwich}}{W_{plate}} = \frac{2\rho_f t_f + \rho_c t_c}{\rho_{plate} t_{plate}} \tag{3.26}$$

This optimization study divided into two as with clamped and simply supported boundary conditions. The application of these conditions are desribed in subsections in details. Since floor panel is a part of body, no boundary conditions are applied on the nodes on the edges of floor panel.

3.4.1 Clamped Sandwich Panels

The optimization of clamped sandwich panels are handled with contraint inequalities. As constraints, face thicknesses must be equal and have at least 0.1 mm thickness each and total thickness of sandwich panel must not exceed 10 mm.

The maximum displacement formula used for optimization constraint definition is chosen as the formula that Plantema [41] has introduced for clamped sandwich structures.

The steel sheet metal floor panel with 1 mm thickness is analyzedwith MSC.Nastran under the distributed load of 6432 N (2.6104 N load on each nodes). The maximum displacement results as 2.37 mm and this analysis is shown in Figure 3.14.

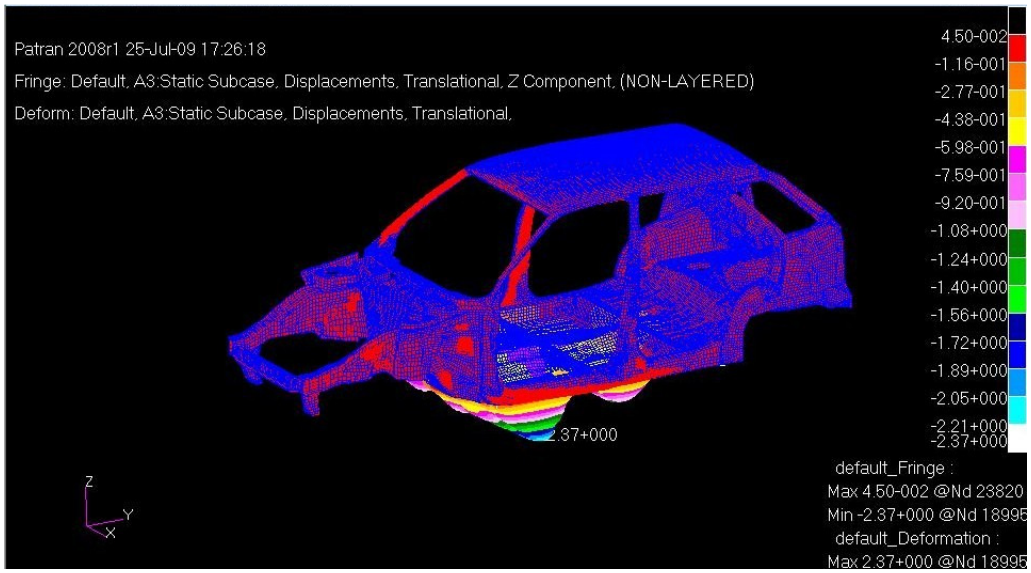

Figure 3.14 *Displacement result of 1 mm steel sheet metal floor panel analyzed under load of 6432 N with MSC.Nastran*

The optimization code has given the results as 0.1 mm face materials thickness and 1.3 mm core material thickness. With this configuration, the objective function is 0.2069 and this means the weight is reduced by approximately %80 by replacing the steel panel with sandwich structure. A clamped sandwich panel with these thicknesses of layers is modelled and analyzed with MSC.Nastran program in order to verify the optimum configuration. Both face and core materials are modelled with shell elements. The analysis gives the maximum displacement of 1.17 m as shown in Figure 3.15. As a constraint, it was asked to be 1.11 m and it is acceptable.

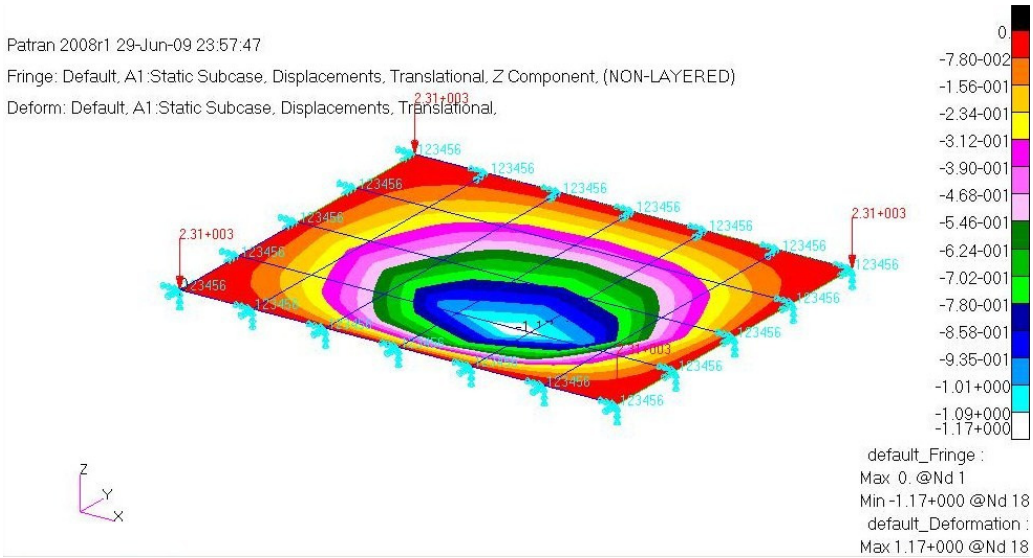

Figure 3.15 *Displacement result of the optimum sandwich clamped flat panel analyzed with MSC.Nastran*

But the analysis with this configuration applied on the floor panel of FIAT car model has given the maximum displacement result as 12.3 mm as shown in Figure 3.16. Therefore in order to find the optimum configuration the thickness of core material is increased until the the maximum displacement reaches the value that analysis with steel panel has given (Figure 3.17).

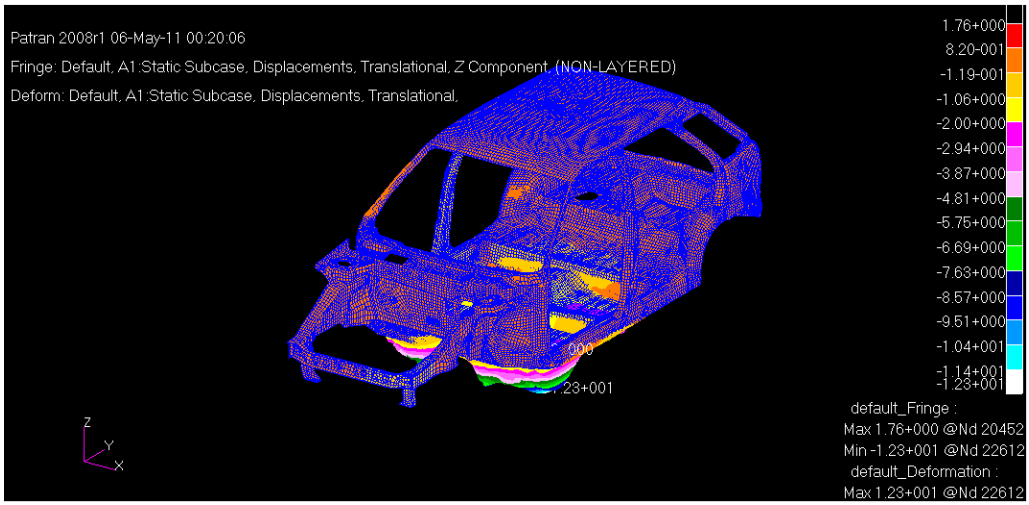

Figure 3.16 *Displacement result of the optimum clamped flat sandwich structure applied on the floor panel analyzed with MSC.Nastran*

The thickness of the core layer of this optimum sandwich flat panel configuration is increased until the maximum displacement is reached the value of steel sheet metal floor panel. The optimum configuration consists of 0.1 mm face material and 15.5 mm core material. With this configuration the objective function is 0.28 and this means the weight is reduced by %72 by replacing the steel panel with sandwich structure.

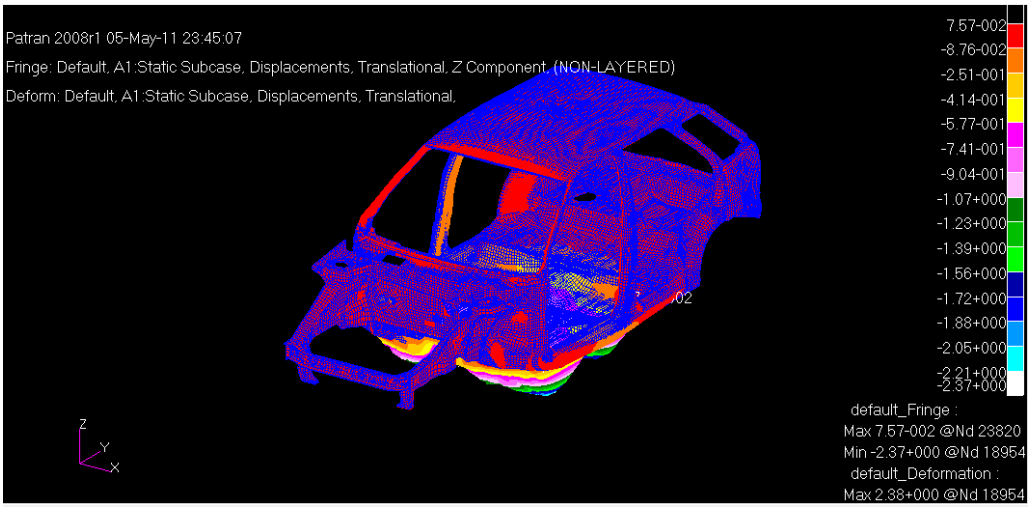

Figure 3.17 *Displacement result of the optimum sandwich floor panel analyzed with MSC.Nastran*

3.4.2 Simply Supported Sandwich Panels

As clamped sandwich panel, simply supported sandwich panel is also optimized with equality and inequelity constraints. This optimization study is divided into two by different constraint types.

As first type constraints face thicknesses must be equal and have at least 0.2 mm thickness each and total thickness of sandwich panel must not exceed 10 mm. Steel flat plate with 1 mm thickness has the maximum displacement of 36.6 mm under 23.08 Pa distributed load. Therefore this value is chosen as displacement constraint. As stress considerations, steel flat plate with 1 mm thickness has the safety factor of 9.11. Therefore, the safety factor for face layers and core layer at both x and y directions must be at least this value. As the second type, only the thickness limitations are changed in order to see how the optimization results depends on the thickness limitations. For this type, face thicknesses must also be equal and have at

least 0.1 mm thickness each and total thickness of sandwich panel must not exceed 20 mm.

The maximum displacement and safety factors formulas used for optimization constraint definition are chosen as the formula that Zenkert [2] has introduced for simply supported sandwich structures with thin faces.

The optimization gave the results for first type constraints as the face material thickness as 0.2 mm and core material thickness as 0.725 mm. By this configuration, the objective function is 0.4027 meaning the weight is reduced by 59.63%. In addition to these, this configuration has the maximum displacement of 0.0366 m. Safety factors for face materials at x and y directions are 13.35 and 10.10 respectively, whereas the safety factors for core material at x and y directions are 19.24 and 17.51 respectively. These calculations are performed with Zenkert D.'s formulas for thin faced simply supported sandwich structures and verified by the approach given in Military Handbook MIL-HDBK-23A [42] (safety factor for face and core material are 10.33 and 17.70 respectively) and MSC. Nastran analysis shown Figure 3.18. The displacement values are close to each other and it is acceptable.

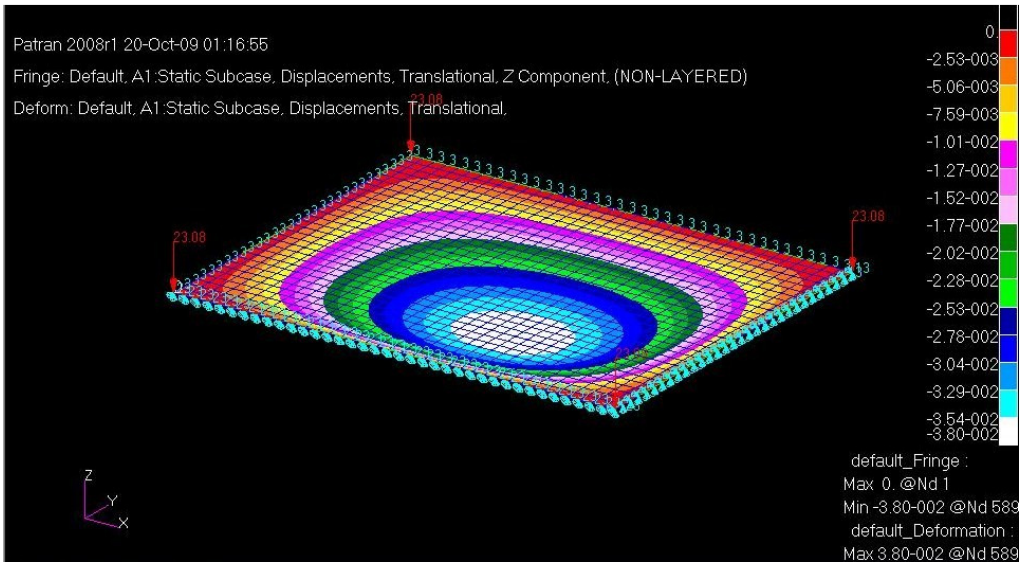

Figure 3.18 *Displacement result of the optimum simply supported sandwich flat panel analyzed with MSC.Nastran (constraint type 1)*

The sandwich structure configration is applied on the floor panel of FIAT car model. Under the same loading conditions the analysis has given 0.11 mm maximum displacement as shown in Figure 3.19.

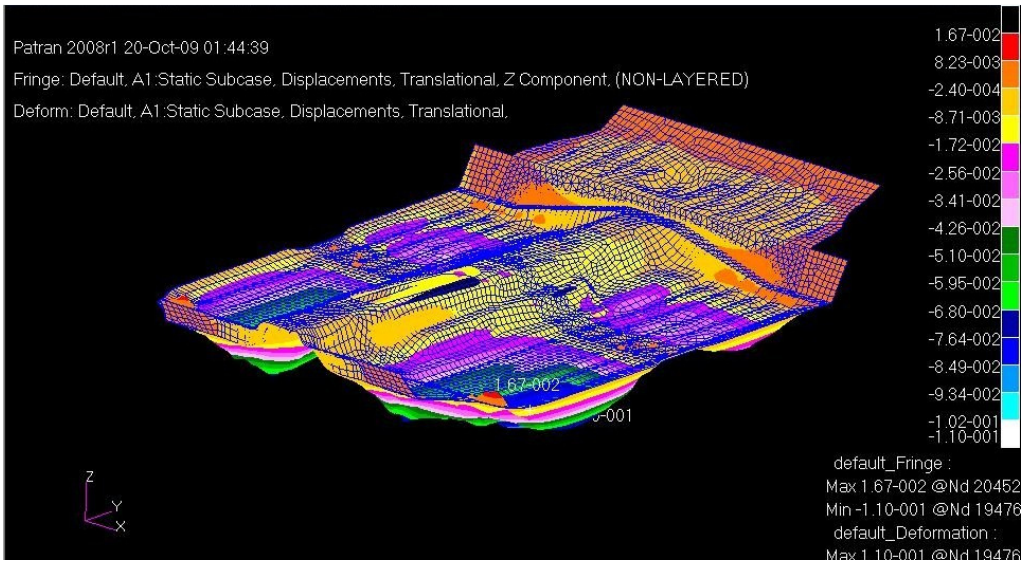

Figure 3.19 *Displacement result of the optimum simply supported flat sandwich structure applied on the floor panel analyzed with MSC.Nastran (constraint type 1)*

Steel sheet metal floor panel is analyzed in MSC.Nastran under the distributed load of 64.32 N. 0.026104 N load is applied on each nodes where driver and passengers steps on and maximum displacement resulted as 0.0237 mm as shown in Figure 3.20.

The core material thickness is increased until the same maximum displacement of steel sheet metal panel is reached. 11 mm core material thickness is obtained and with this configuration the maximum displacement is 0.024 mm as shown in Figure 3.21 and the weight is reduced by 54.36%.

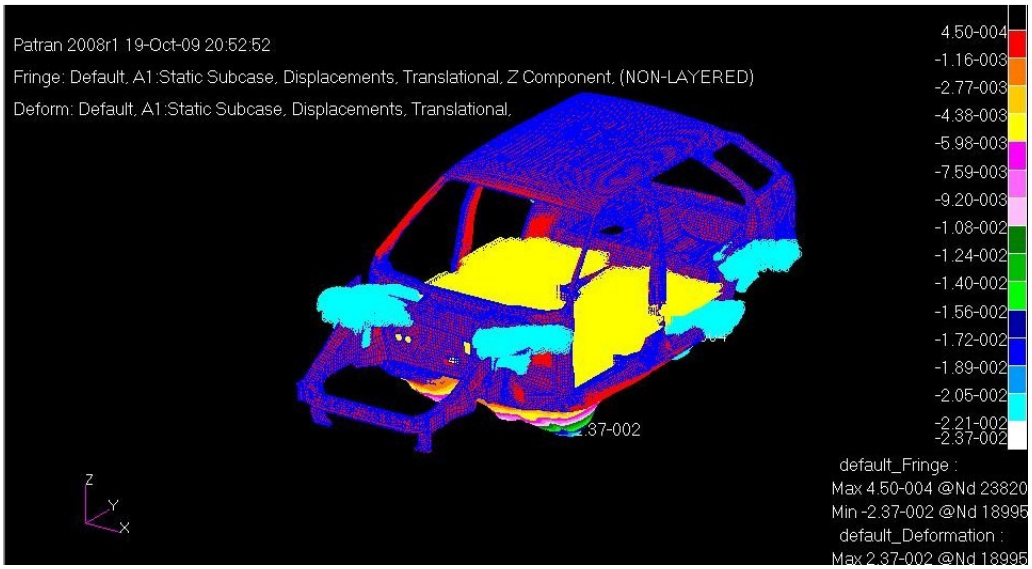

Figure 3.20 *Displacement result of 1 mm steel sheet metal floor panel analyzed under load of 64.32 N with MSC.Nastran (constraint type 1)*

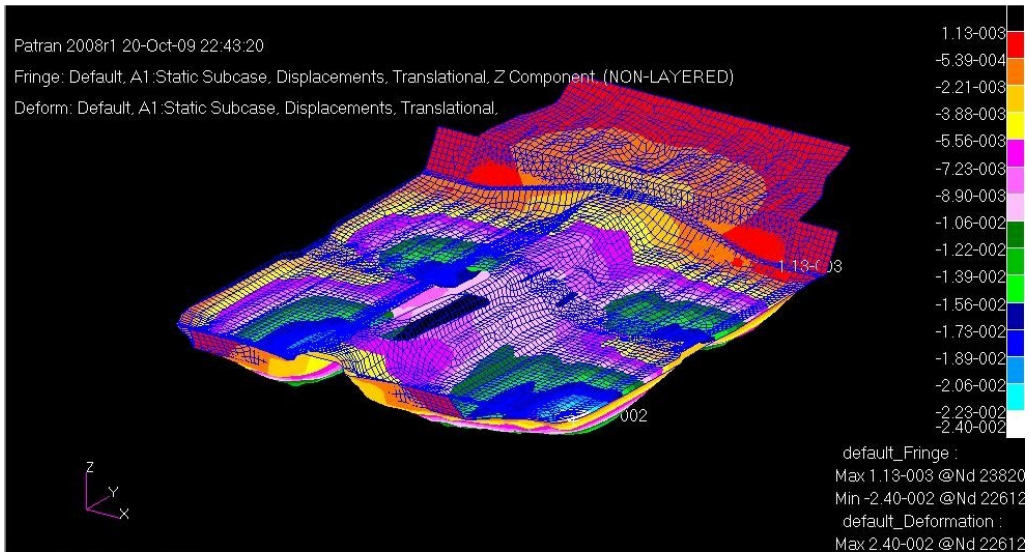

Figure 3.21 *Displacement result of the optimum sandwich floor panel analyzed with MSC.Nastran (constraint type 1)*

The optimization for second type constraints gave the results as the face material thickness as 0.1626 mm and core material thickness as 0.8628 mm. By this

configuration. the objective function is 0.3296 meaning the weight is reduced by 67.04%. In addition to these, this configuration has the maximum displacement of 0.0366 m. Safety factors for face materials at x and y directions are 12.04 and 9.11 respectively, whereas the safety factors for core material at x and y directions are 21.33 and 19.42 respectively. These calculations are performed with Zenkert D.'s formulas for thin faced simply supported sandwich structures and verified by the approach given in Military Handbook MIL-HDBK-23A [42] (safety factor for face and core material are 9.31 and 19.61 respectively) and MSC. Nastran analysis shown Figure 3.22. The displacement values are close to each other and it is acceptable.

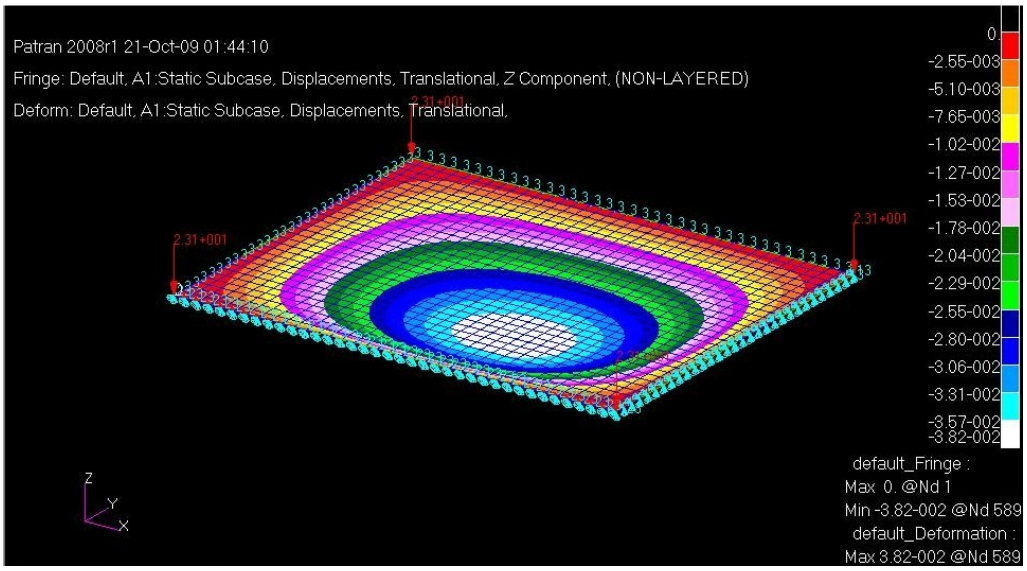

Figure 3.22 *Displacement result of the optimum simply supported sandwich flat panel analyzed with MSC.Nastran (constraint type 2)*

The sandwich structure configration is applied on the floor panel of FIAT car model. Under the same loading conditions the analysis has given 0.11 mm maximum displacement as shown in Figure 3.23.

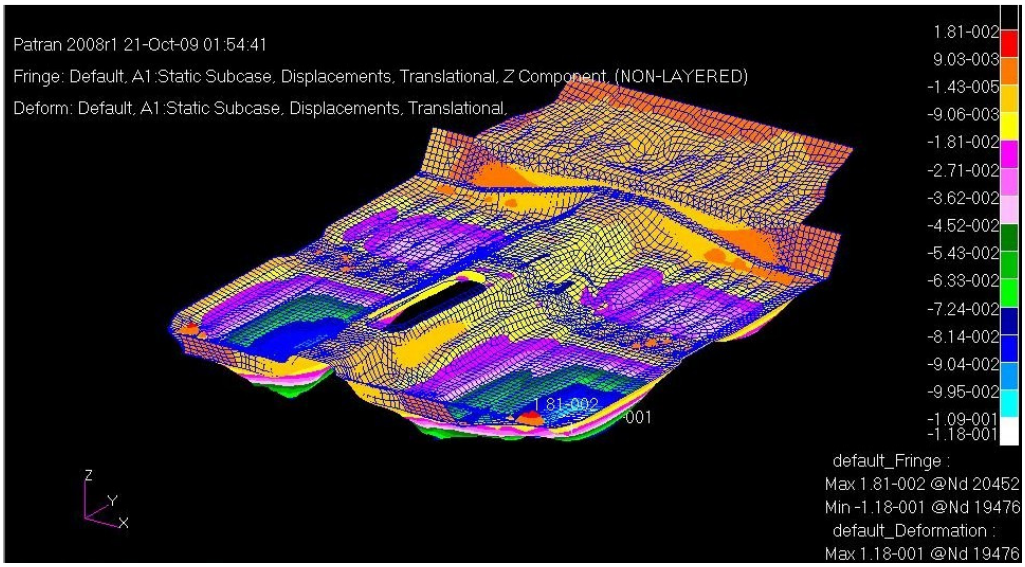

Figure 3.23 *Displacement result of the optimum simply supported flat sandwich structure applied on the floor panel analyzed with MSC.Nastran (constraint type 2)*

The core material thickness is increased until the same maximum displacement of steel sheet metal panel is reached. 12.5 mm core material thickness is obtained and with this configuration the maximum displacement is 0.0235 mm as shown in Figure 3.24 and the weight is reduced by 61.07%.

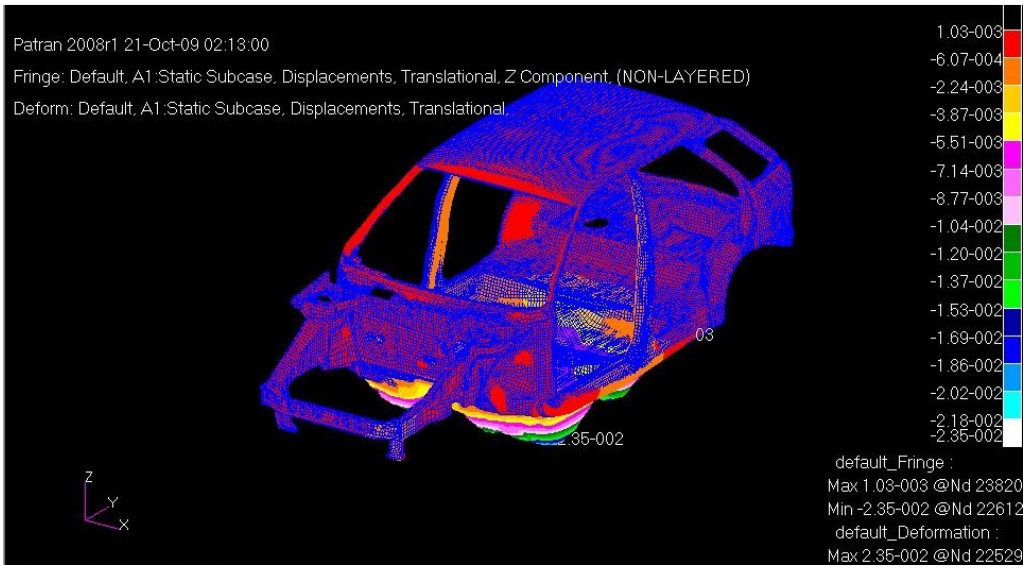

Figure 3.24 *Displacement result of the optimum sandwich floor panel analyzed with MSC.Nastran (constraint type 2)*

3.5 Optimization of Sandwich Structures Used in Other Automobile Body Panels

The luggage, firewall and rear wheel panels are also optimized within this study. The above optimization process could not be applied for these body parts due to their complex geometry. In this process, the thickness of face materials are chosen as thinner than the half of original panel thickness and core thicknesses are increased from zero until maximum displacement reaches the value of the one for steel panels. Optimization of every part is handled individually.

The same materials for both face and core layers are the same as before. The distributed load of 23.08 Pa is applied on the floor panel. The maximum deformation for luggage panel is investigated in z direction because the panel lies on xy plane. However, because of firewall panel's lying on yz plane and rear wheel panel's

complex shape, the maximum displacement is investigated not only one direction but in magnitudes. The results are shown in Table 3.7.

Table 3.7 *The results of optimizations of other body panelss*

Sandwich Panel Optimizaton	Luggage (1 mm thickness)	Firewall (1.8 mm thickness)	Rear Wheel (0.7 mm thickness)
Face and core thicknesses	t_f=0.2 mm t_c=10 mm	t_f=0.4 mm t_c=9 mm	t_f=0.2 mm t_c=1.5 mm
Weight reduction	54.87%	52.42%	49.04%
Max displacement	9.05×10^{-5} mm (z direction)	3.84×10^{-3} mm (magnitude)	9.43×10^{-4} mm (magnitude)
Max displacement without using sandwich panel	9×10^{-5} mm (z direction)	3.86×10^{-3} mm (magnitude)	9.33×10^{-4} mm (magnitude)

The analyses steel panel and sandwich panel of luggage panel are shown in Figures 3.25 and 3.26.

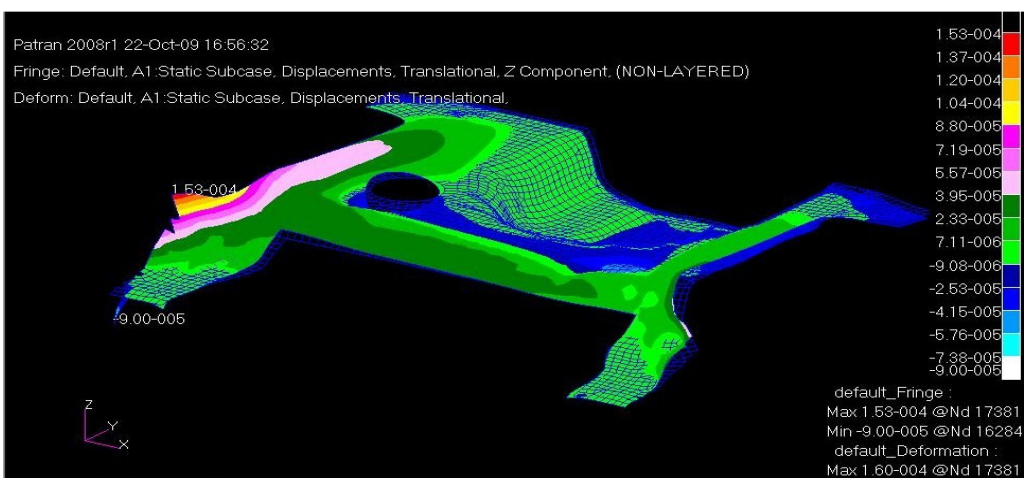

Figure 3.25 *Steel Luggage Panel*

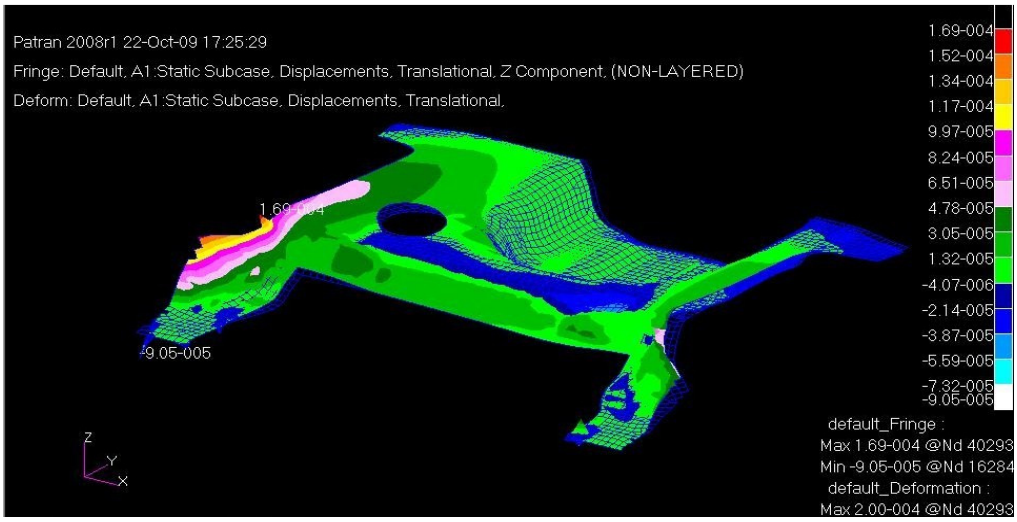

Figure 3.26 *Sandwich Luggage Panel*

The analyses steel panel and sandwich panel of firewall panel are shown in Figure 3.27 and 3.28.

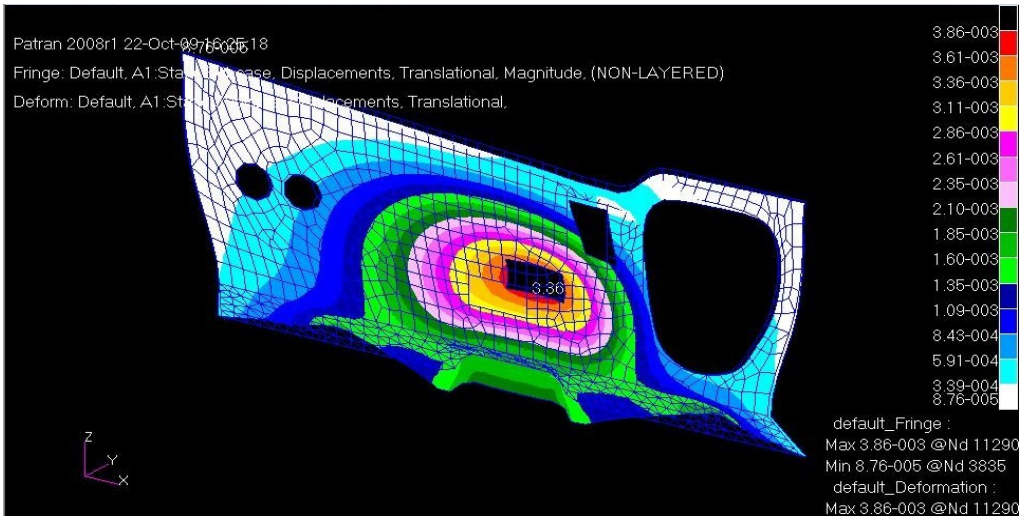

Figure 3.27 *Steel Firewall Panel*

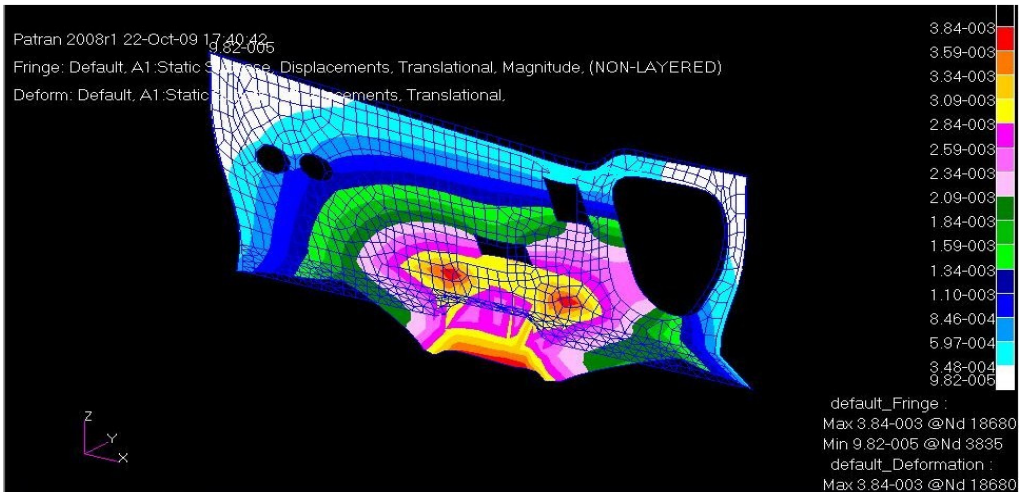

Figure 3.28 *Sandwich Firewall Panel*

The analyses steel panel and sandwich panel of rear wheel panel are shown in Figure 3.29 and 3.30.

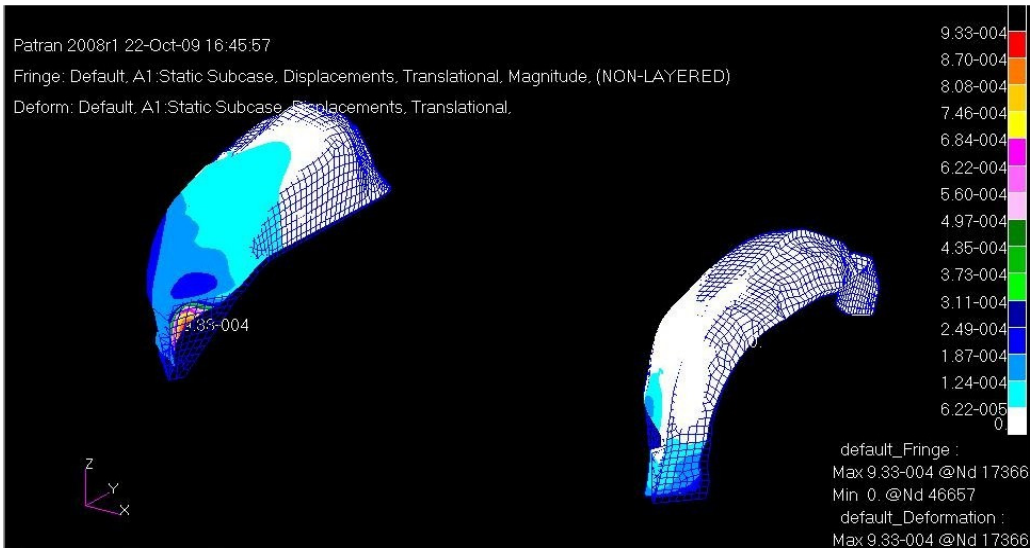

Figure 3.29 *Steel Rear Wheel Panel*

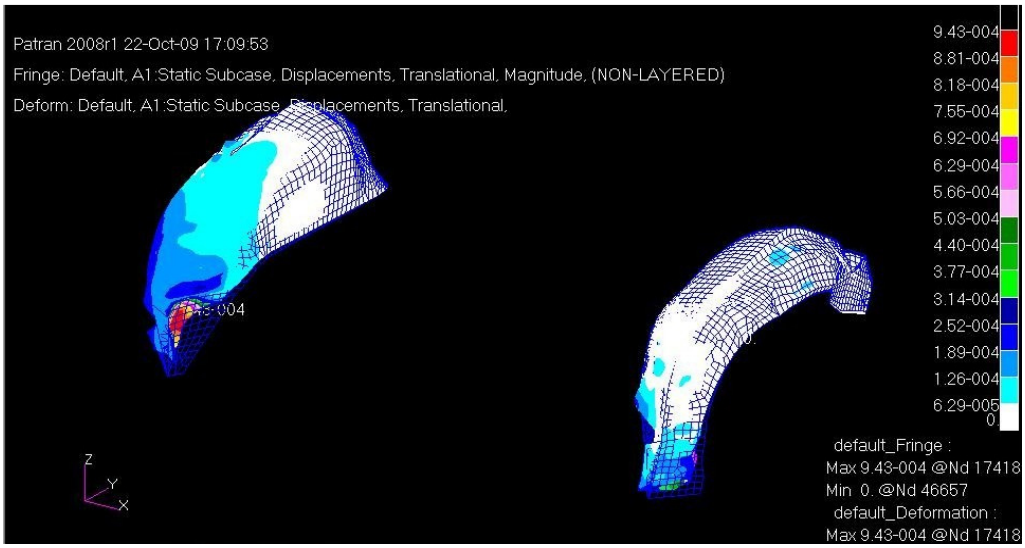

Figure 3.30 *Sandwich Rear Wheel Panel*

CHAPTER 4

USE OF SANDWICH MATERIALS FOR REDUCING THE WEIGHT OF CAR BODY-IN-WHITE PANELS CONSIDERING VIBRATION DAMPING PERFORMANCE

4.1 Introduction

Noise level inside the automobile cabin is a critical parameter for driving comfort. The vibration characteristics of floor car body panels affect the noise inside. There may be noise contribution at the structural resonance frequencies of car body panels of the passenger cabin and this noise can be reduced with passive vibration control techniques such as adding a viscoelastic layer on the panel as free-layer surface damping treatments or adding a very thin viscoelastic layer between two steel plates as sandwich material. The first alternative is widely used in automotive industry and the second one will be investigated in this study. With these techniques, amplitudes of the structural vibration responses at resonance frequencies of the cabin body panels can be reduced and thus the driving comfort may be improved due to less vibration and noise contribution from structure-borne noise coming from body panels.

The purpose of this study, is to investigate the difference between the amounts of viscoelastic material addition for sandwich material and free layer surface damping treatment applications. The investigation is done using the same viscoelastic material for both of these methods. Since there is no data to design a free layer surface damping treatment thickness, a laminated steel, a special type of sandwich structure, with a specific thickness and materials for face and core layers is chosen. Free layer surface damping treatment with the same material as the core layer of laminated steel is added on steel sheet metal panel with the initial thickness guess of the thickness of laminated steel's core layer. The thickness is incrementally increased until the same damping performance (i.e modal loss factors for panel frequency response functions) is as laminated steel configuration is achieved. Then, total weights of both panel with free layer surface damping treatment and laminated steel is compared in order to show that laminated steels may have the same damping performance as panels with free layer surface damping treatments with a lesser weight addition to panels.

The floor panel is chosen as the case study for this part of this theses and the floor panel of the FIAT car model used in Özgen's [1] study utilized for this purpose. It is reshaped by closing the gaps for shift gear box on it. The reason of this is that, this panel has also been used in acoustical analyses in the next chapter thus, no sound energy should pass through the gap. The vibrational analyses are performed only for the floor panel itself independent of remaining body panels. In this study, surface damping treatments is applied as fully coverage because FIAT car floor panel has damping treatments almost everywhere as shown in Figure 2.20 and 2.21.

The design process is first applied on beams since theoretical formulas for estimating the loss factor at each mode and frequency response function plots are known. Frequency response function of a simply supported steel single layered beam and sandwich structure, whose dimensions are randomly chosen, are plotted by MSC.Actran. Then, the free layer surface damping treatment thickness is obtained by adding the same viscoelastic material with the same thickness as the core of

sandwich structure on the beam. The process continues by increasing the thickness of damping treatment until the loss factor of the structure reaches that of sandwich material for the first few modes except the first (fundamental) one. A thickness is obtained for each modes and the free layer surface damping treatment thickness is accepted to be their average. Loss factors and frequency response functions (FRF) are estimated with MSC.Actran along with theoretical formulas and have shown a good agreement. Finite element analyses are made with MSC.Actran due to its features of defining the viscoelastic material properties. After process is verified, the same process is applied on floor panel of FIAT car model.

Before the investigation, viscoelastic materials will be discussed. In this section, definition, general properties and the effects of temperature and frequency on the behaviour of these materials will be described. Then, the analytical solutions to modal loss factor and frequency response function calculations of any point at a simply suppported beam are given.

4.2 Behaviour of Viscoelastic Materials

Viscoelastic materials are rubber-like polymers having damping characteristics and stiffness strongly vary with frequency and temperature. When a harmonically varying stress is applied to a viscoelastic materal, the resulting strain is also harmonic, of the same frequency but with a phase of time lag relative to the applied stress [43]. How stress and strain changes with respect to time is shown in Figure 4.1.

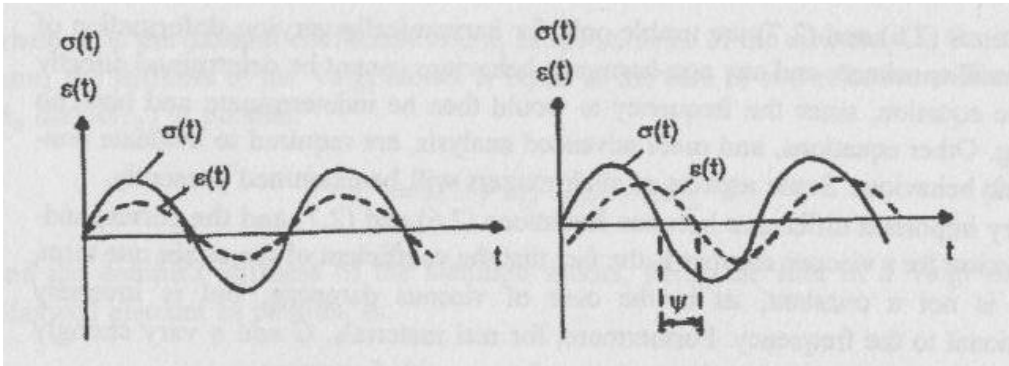

Figure 4.1 *Harmonic excitation and response for elastic and viscoelastic solid [43]*

The relationship between stress and strain for elastic and viscoelastic solids are given in Equations (4.1) and (4.2).

$$\sigma = E\varepsilon \text{ for elastic solids} \tag{4.1}$$

$$\sigma = E(1 + i\eta)\varepsilon \text{ for viscoelastic solids} \tag{4.2}$$

where η is loss factor. It can also be expressed as the ratio of imaginary part of the complex modulus of elasticity over real part. This complex modulus of elasticity and loss factor are much affected by temperature and frequency. The effect of temperature is shown in Figure 4.2.

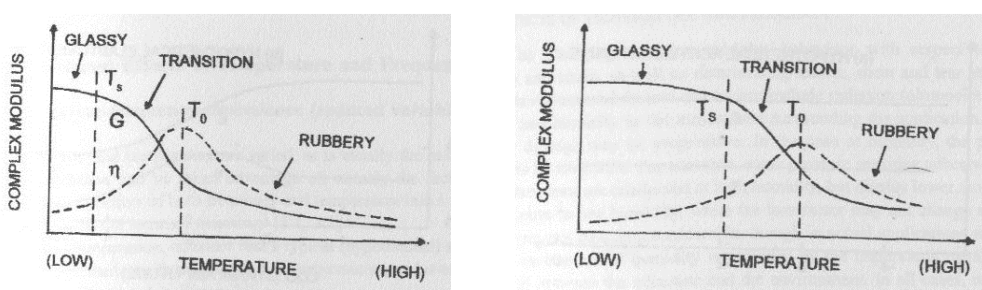

Figure 4.2 *The effect of temperature on elastic and viscoelastic solid [43]*

The characteristics of complex modulus and loss factor is divided into three as *glassy*, *transition* and *rubbery*. The modulus is very high and loss factor is very low at the glassy region. This region ends at the softening temperature and softening temperature of elastic solid is higher than viscoelastic solid.

As the temperature increases after the glassy region. modulus starts to fall rapidly. Loss factor starts to rise significantly until it reaches its maximum value at the temperature called *peak loss factor temperature* T_0. At the rubbery region both modulus and loss factor fall.

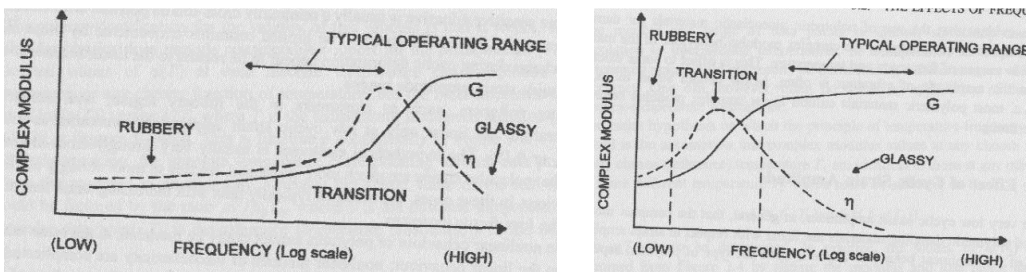

Figure 4.3 *The effect of frequency on elastic and viscoelastic solid [43]*

The effect of frequency is opposite of that of temperature. Loss factor is maximum at the transition region whereas modulus is maximum at the glassy region.

Jones [43] has introduced a general formula for the estimation of modulus of elasticity and loss factor of viscoelastic materials.

$$E^* = \frac{a_1 + b_1(if\alpha(T))^\beta}{1 + c_1(if\alpha(T))^\beta} \tag{4.3}$$

$$\log(\alpha(T)) = T_A\left(\frac{1}{T+273} - \frac{1}{T0+273}\right) \tag{4.4}$$

where a_1, b_1, c_1 and β are material coefficients. T is the current temperature. T_0 is the peak loss factor temperature. T_A is the slope of the line representing the plot of log[α(T)] versus 1/T.

4.3 Vibration Damping of Beams

In this study, vibration damping of beams are investigated by two methods as fully covered free layer damping treatment and laminated steel beam. The best methods to understand the effects of vibration damping are calculating loss factors and FRF plotting. According to Jones [43], the loss factor of a beam with free layer surface damping treatment is calculated by Oberst's equation:

$$\frac{(EI)^*}{E_1 I_1} = 1 + e^* h^3 + 3(1+h)^3 \frac{e^* h}{1+e^* h} \tag{4.5}$$

where $e^* = E_2^* / E_1$ and $h = H_2 / H_1$. Subindex 1 represents the base beam and subindex 2 represents the added viscoelastic layer. For a sandwich beam with a viscoelastic core layer, Equation (4.6) is used [43].

$$(EI)^* = \frac{E_1 {H_1}^3}{12} + \frac{{E_2}^* {H_2}^3}{12} + \frac{E_3 {H_3}^3}{12} - \frac{{E_2}^* {H_2}^2}{12}\left(\frac{H_{31}-D}{1+g^*}\right) + E_1 H_1 D^2 + {E_2}^* H_2 (H_{21} - D)^2 + E_3 H_3 (H_{31} - D)^2 - \left(0.5 {E_2}^* H_2 (H_{21} - D) + E_3 H_3 (H_{31} - D)\right)\left(\frac{H_{31}-D}{1+g^*}\right) \tag{4.6}$$

where the various parameters are:

$$D = \frac{E_2{}^* H_2(H_{21} - 0.5H_{31}) + g^*(E_2{}^* H_2 H_{21} + E_3 H_3 H_{31})}{E_1 H_1 + 0.5E_2 H_2 + g^*(E_1 H_1 + E_2 H_2 + E_3 H_3)} \tag{4.7}$$

$$H_{21} = 0.5(H_1 + H_2) \tag{4.8}$$

$$H_{31} = H_2 + 0.5(H_1 + H_3) \tag{4.9}$$

$$g^* = \frac{G_2{}^* \lambda^2}{E_3 H_2 H_3 \pi^2} \tag{4.10}$$

$$\lambda_n = \frac{\pi L}{\beta_n} \tag{4.11}$$

where subindex 1 and 3 stand for lower and upper face layers, and subindex 2 stands for core layer again. Some iterations are needed since both sides of the above equations depends on the same frequency. Initial guess of natural frequency is calculated as if no damping treatment is added as if it is a single layer beam. The natural frequencies of a beam is calculated by the formula [45],

$$\omega_n = \frac{1}{2\pi}\left(\frac{\beta_n}{L}\right)^2 \sqrt{\frac{EI}{\rho A}} \text{ [Hz]} \tag{4.12}$$

where L is length of beam, n is the mode number, I is the moment of inertia ($I=b.H^3/12$, b is width and H is thickness), A is cross-sectional area (A=b.H), ρ is

density, E is modulus of elasticity and β is coefficient which depends on the boundary condition of the beam as shown in Table 4.1 [45].

Table 4.1 *Determination of β*

Boundary Condition	**β**
Simply supported - Simply supported	n.π
Clamped - Free	(2n-1).π/2
Clamped - Simply supported	(4n+1).π/4
Clamped - Clamped	(2n-1).π/2

$(EI)^*$ is calculated with the natural frequency calculated with Equation (4.12) for the first iteration. Then the natural frequency is again calculated with Equation (4.13) for free layer surface damping treatment and Equation (4.14) for sandwich structure. [45]

$$\omega_n = \frac{1}{2\pi}\left(\frac{\beta_n}{L}\right)^2 \sqrt{\frac{Re[(EI)^*]}{\rho(\rho_1 H_1 + \rho_2 H_2)}} \text{ [Hz]} \tag{4.13}$$

$$\omega_n = \frac{1}{2\pi}\left(\frac{\beta_n}{L}\right)^2 \sqrt{\frac{Re[(EI)^*]}{\rho(\rho_1 H_1 + \rho_2 H_2 + \rho_3 H_3)}} \text{ [Hz]} \tag{4.14}$$

After the iterations coverge to a stable $(EI)^*$, the modal loss factor is calculated for each mode from:

$$\eta_n = Im[(EI)^*]/Re[(EI)^*] \tag{4.15}$$

The other method is to plot the displecement FRF's. The frequency response function plot of any point at x meter offset from the edge of a simply supported beam with a viscoelastic material addition with length of L is calculated from [45]:

$$H_q(\omega) = \frac{1}{E_1 I_1}\left[\frac{\frac{\sin\left(\frac{n.\pi}{L}x\right)}{\frac{L}{2}}}{\frac{(EI)^*}{E_1 I_1}\left(\frac{n.\pi}{L}\right)^4 - \frac{b(\rho_1 H_1 + \rho_2 H_2)}{E_1 I_1}\omega^2}\right] sin\left(\frac{n\pi}{L}x\right) \tag{4.16}$$

The modal loss factors can be determined also through FRF plots by half power point method.

4.4 Verification of Design Process By An Application of Vibration Damping of Beams

The aim of this study is to find a thickness of a free layer surface damping treatment applied on steel beam whose average modal loss factor is the same as sandwich structure. The chosen laminated steel panel has 0.1 mm thick 3M-467 viscoelastic adhesive bonded between two steel sheets with 0.5 mm thickness each. The reason of this core material selection is that 3M-467 viscoelastic adhesive has a potential of having very high loss factor and low elasticity modulus by setting frequency and temperature at transition region and thus suitable for the utilization as a core material. Theoretical details of core and free layer surface damping treatment material selection were mentioned at literature review.

The properties of steel were given in the above chapter (Table 3.1) and the material coefficients of 3M-467 viscoelastic adhesive for calculation of complex shear

modulus instead of elasticity modulus are given in Table 4.2. From this table, elastic modulus can be obtained by E = 2.G.(1+ν) and generally ν is 0.499 [43].

Table 4.2 *Material coefficients of 3M-467 viscoelastic adhesive for calculation of complex shear modulus*

Coefficient	Value
a1	0.0425 MPa
b1	0.214 MPa
c1	0.00125
TA	5278 K
T0	23.9 °C
β	0.505

First of all, the dimensions of the steel beam to be investigated has 1 mm thickness and 1 m length. The orientation in the coordinate system is shown in Figure 4.4.

Figure 4.4 *Orientation of the beam in the coordinate system*

The boundary condition of this beam is selected as simply supported and these conditions are applied as fixing the translation at x and y direction of one edge and y direction of the other. With an arbitrary selection, a unit harmonic force is applied at

+z direction on the quarter of length as seen with purple triangle in Figure 4.4. The driving point frequency response functions (H_q) are calculated also at this point.

The first ten modes, shown in Table 4.3 are considered in this study. The calculations are handled in order to investigate the first six or seven modes, therefore the frequency range is 0-120 Hz with the increment of 0.1 Hz. FRF plot of steel beam is shown in Figure 4.5.

Table 4.3 *Natural frequencies of first ten modes of a simply supported steel beam*

Mode	**1**	**2**	**3**	**4**	**5**	**6**	**7**	**8**	**9**	**10**
Freq. [Hz]	2.4	9.4	21.2	37.6	58.8	84.7	115.3	150.6	190.6	235.3

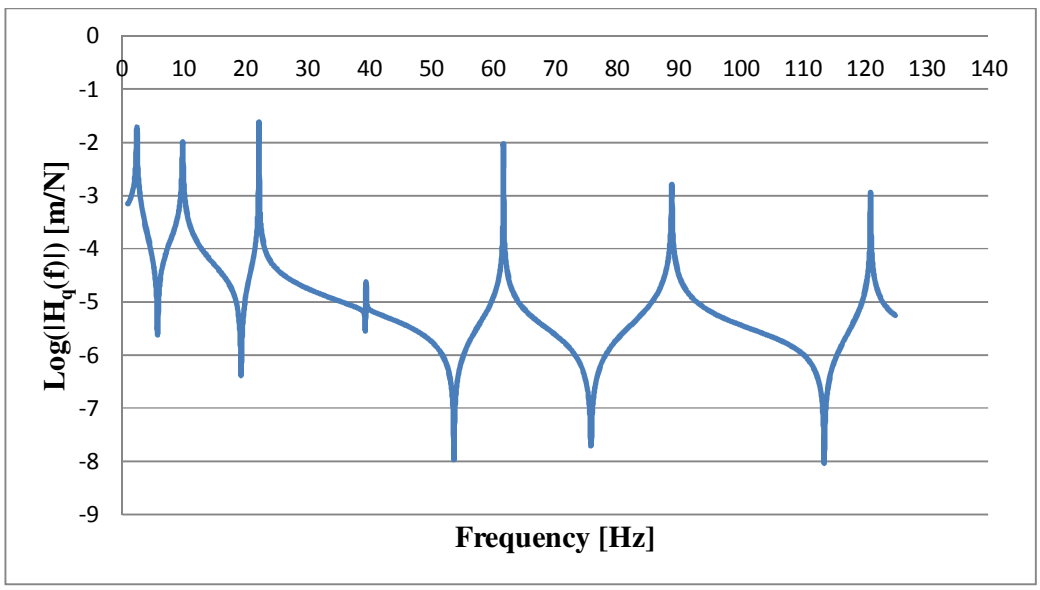

Figure 4.5 *FRF plot of simply supported steel beam*

The design process starts with choosing an appropriate sandwich structure configuration. A sandwich structure are composed of with steel face layers of 0.5

mm and 3M-467 viscoelastic adhesive core layer with 0.1 mm. The material properties of 3M-467 viscoelastic adhesive are determined at the temperature of 100°C because of its low loss factor values thus the modes can easily been seen. Density and Poisson's ratio are given in Table 4.4. In order to get correct results, the frequencies to be inputs of MSC.Actran, must be selected mostly around the natural modes of the structure. Real and imaginary part of its elasticity modulus and loss factors are shown in Table 4.5.

Table 4.4 *Poisson ratio and density of 3M-467 viscoelastic adhesive*

Property	Value
υ	0.499
ρ	1080 kg/m^3

Table 4.5 *Modulus of elasticity and loss factors of 3M-467 viscoelastic adhesive*

Frequency [Hz]	Elasticity Modulus (Real Part) [Pa]	Elasticity Modulus (Imaginary Part) [Pa]	Loss Factor
1	134050	6736.2	0.0503
7	145130	17996	0.1240
15	153450	26443	0.1723
25	161110	34224	0.2124
40	170140	43390	0.2550
70	184090	57558	0.3127
100	195270	68914	0.3529
150	210690	84569	0.4014

Frequency response functions of the sandwich beam are plotted with MSC.Actran and theoretical formulas given in Equation 4.16. The plots with these methods are shown and compared in Figure 4.6. Also the loss factors determined with both of these methods are compared in Table 4.6. As seen, both results have shown a good agreement.

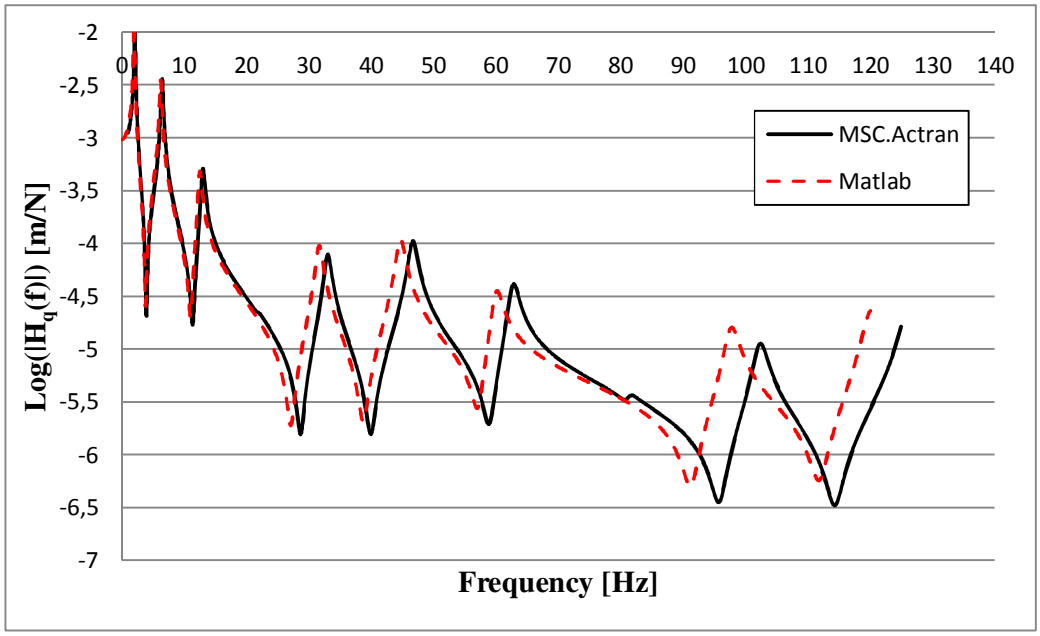

Figure 4.6 *FRF's of the sandwich beam determined via MSC.Actran and theoretical formulas*

Table 4.6 *Loss factors of the sandwich beam determined via MSC.Actran and theoretical formulas*

Method	**Modes [Hz]**						
	1	**2**	**3**	**4**	**5**	**6**	**7**
Matlab	0.0250	0.0430	0.0427	0.0382	0.0335	0.0295	0.0262
MSC.Actran	0.0250	0.0420	0.0450	0.0330	0.0280	0.0255	0.0200

In order to find a free layer surface damping treatment thickness, the initial guess of viscoelastic material (the same material of the core layer of sandwich structure at the same temperature) addition is chosen to be the core layer thickness of the sandwich structure. The modal loss factors of beam with free layer surface damping treatment are increasing with the mode number in an order but in sandwich structure they are not. Therefore, the initial guess of thickness is increased until the average modal loss factor of 2nd, 3rd, 4th, 5th, 6th and 7th modes satisfies the same average loss factor of the sandwich structure. And with this design criteria, free layer surface damping

treatment is obtained as 41.5 mm. The modal loss factors of beams with free layer surface damping treatment with these thickness values are given in Table 4.7. Frequency response functions of the beam with 41.5 mm free layer surface damping treatment are plotted with MSC.Actran and theoretical formulas. The plots with these methods are shown and compared in Figure 4.7. Also the loss factors determined with both of these methods are compared in Table 4.8. As seen, both results have shown a good agreement.

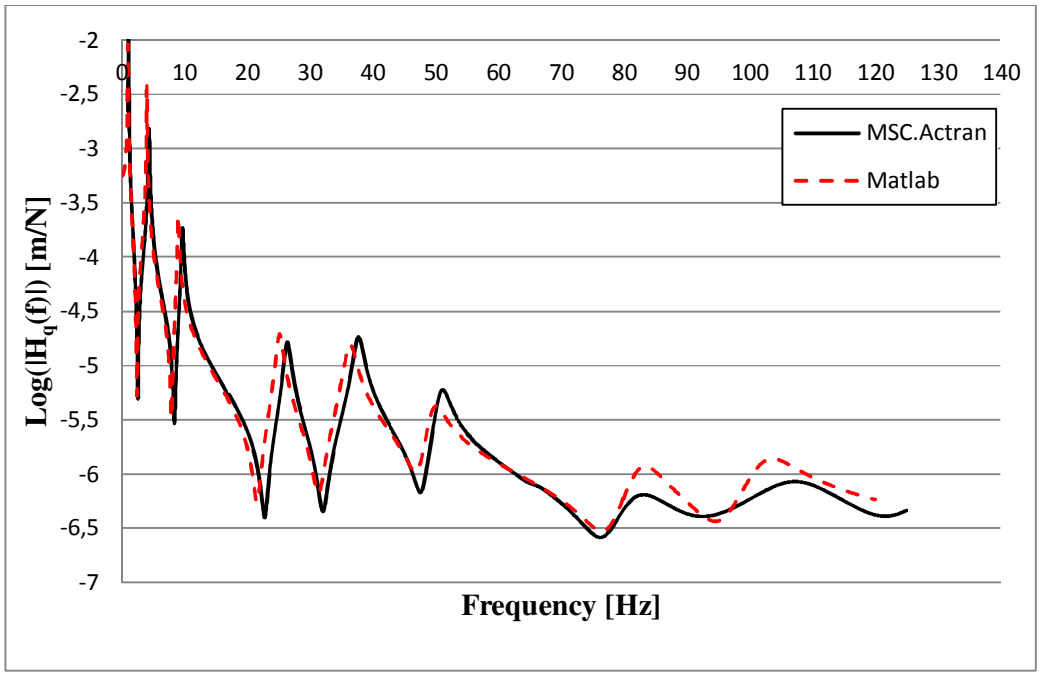

Figure 4.7 *FRF's of the beam with free layer surface damping treatment determined via MSC.Actran and theoretical formulas*

Table 4.7 *Loss factors of the beams with free layer surface damping treatment determined via MSC.Actran and theoretical formulas*

Method	**Modes [Hz]**						
	1	**2**	**3**	**4**	**5**	**6**	**7**
Matlab	0.0079	0.0154	0.0238	0.0317	0.0394	0.0471	0.0547
MSC.Actran	0.0077	0.0160	0.0240	0.0320	0.0390	0.0465	0.0560

The comparison of FRF plots of steel beam, sandwich beam and beam with free layer surface damping treatment is shown in Figure 4.8.

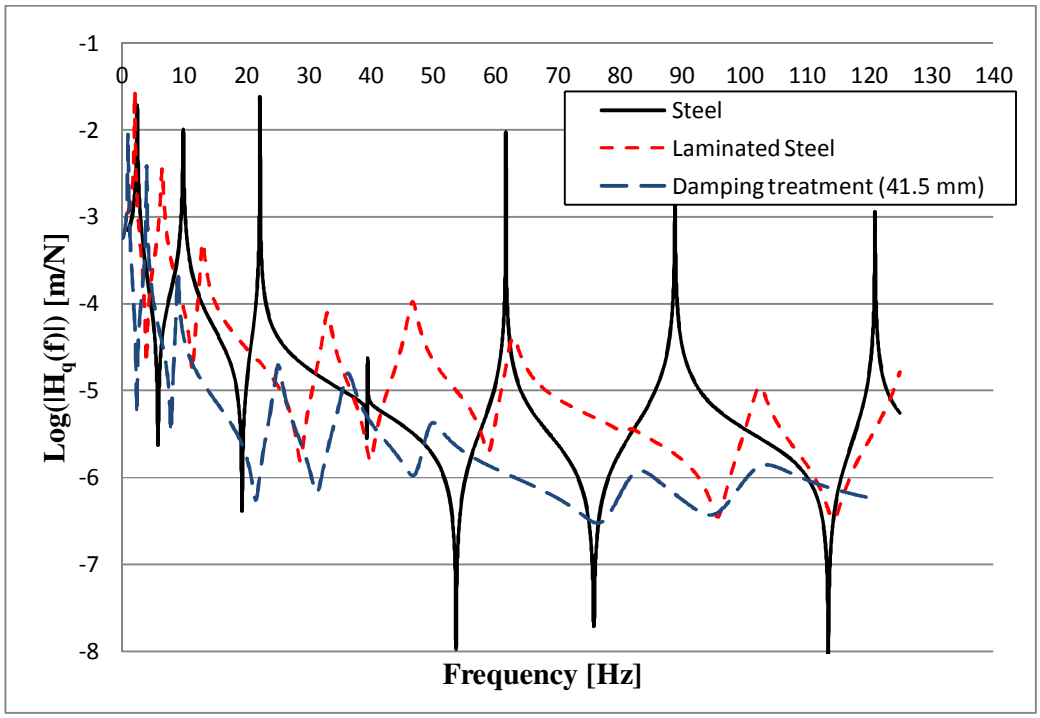

Figure 4.8 *Comparison of FRF plots of beams*

As seen, the same average modal loss factor of first few modes of sandwich structure with a 0.1 mm viscoelastic material addition is obtained by adding the same material on the top of beam as free layer surface damping treatment with 41.5 mm thickness. By this way, the weight is reduced by %85 with using a sandwich structure instead of free layer surface damping treatment.

4.5 Vibration Damping of Floor Panel of FIAT Car

The purpose of this study is to find a thickness of a free layer surface damping treatment applied on steel sheet metal panel whose first modal loss factor is the same as sandwich structure. The chosen laminated steel panel has 0.1 mm thick 3M-467 viscoelastic adhesive bonded between two steel sheets with 0.5 mm thickness each as in the previous study.

The mesh of floor panel of FIAT Tipo is created by HEX8 solid-shell elements with 0.05 m global edge length. The panel is clamped from its all edges and a unit harmonic force is applied at +z direction from the point (Point A) where the driver steps on. The FRF plots of this point are considered as driving point FRF and will be shown as H_A.

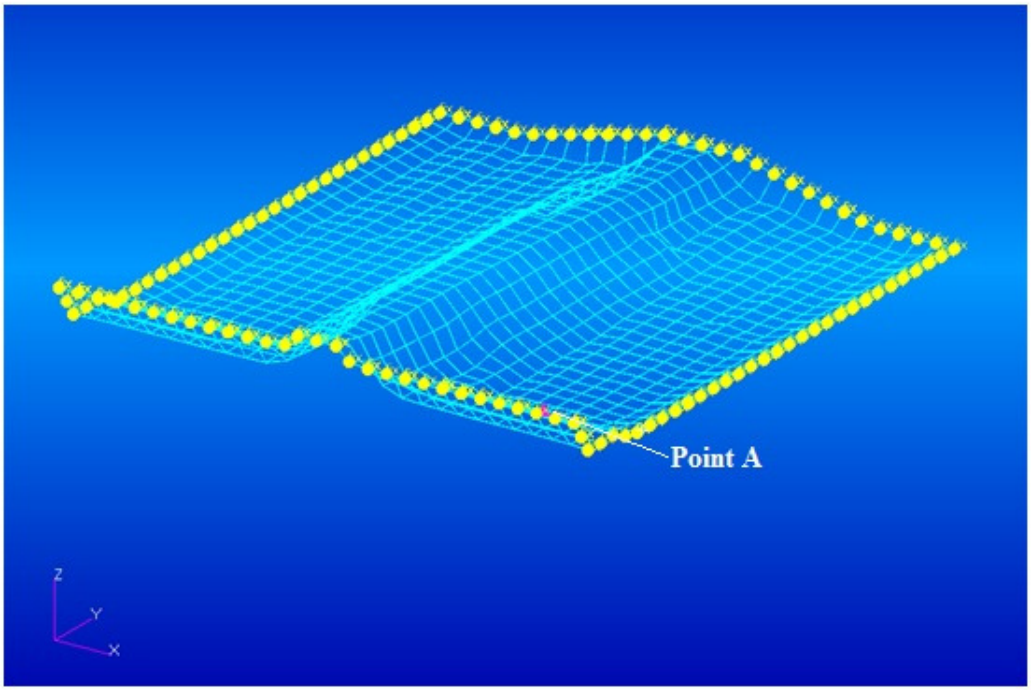

Figure 4.9 *The floor panel and load/boundary conditions of FIAT Car*

The normal mode analysis by MSC.Actran has resulted the natural frequencies as 55.25 Hz. 56.70 Hz. 74.23 Hz. 76.85 Hz. 112.94 Hz. 113.62 Hz. 119.14 Hz. 121.39 Hz. 138.17 Hz and 141.53 Hz. FRF plot of steel floor panel in the frequency range of 1-200 Hz, where the first ten modes occur, is given in Figure 4.10. As seen, the normal mode analyses and frequency response function analyses are also consistent.

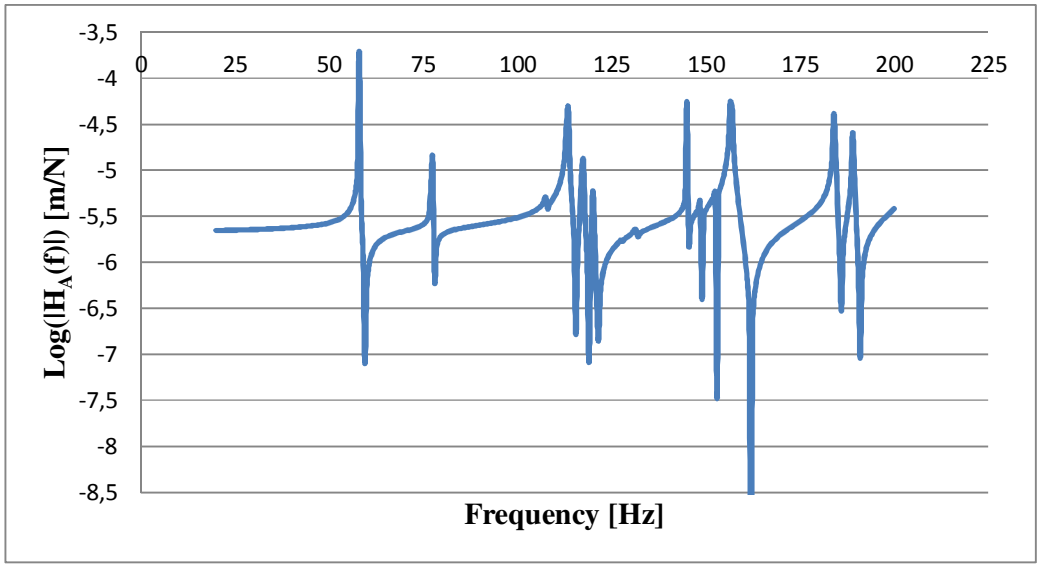

Figure 4.10 *FRF of steel floor panel*

For the estimation of FRF of the sandwich panel, the modulus of elasticity values are taken at 100°C and again from the frequencies close to natural frequencies. The modulus of elasticity is shown in Table 4.9.

Table 4.8 *Modulus of elasticity and loss factors of 3M-467 viscoelastic adhesive*

Frequency [Hz]	Elasticity Modulus (Real Part) [Pa]	Elasticity Modulus (Imaginary Part) [Pa]	Loss Factor
20	157520	30577	0.1941
50	175236	48565.8	0.2771
75	186100	59598.2	0.3202
100	195270	68914	0.3529
125	203370	77132	0.3792
150	210690	84569	0.4014
175	217440	91413	0.4204
200	223710	97787	0.4371

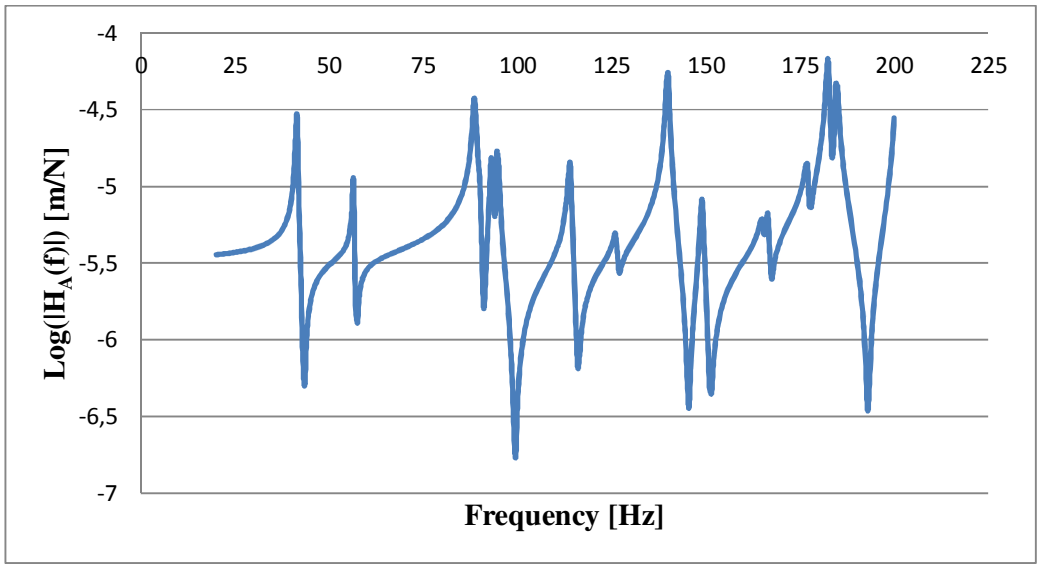

Figure 4.11 *FRF of sandwich floor panel*

In order to find a free layer surface damping treatment thickness, the initial guess of viscoelastic material (the same material of the core layer of sandwich structure at the same temperature) addition is chosen to be the core layer thickness of the sandwich structure. The modal loss factors of beam with free layer surface damping treatment are increasing with the mode number in an order but in sandwich structure they are

not. Therefore, the initial guess of thickness is increased until the average modal loss factor of 2nd, 3rd, 4th, 5th and 6th modes satisfies the same average loss factor of the sandwich structure. And with this design criteria, free layer surface damping treatment is obtained as 18 mm. Frequency response functions of the floor panel with sheet metal, sandwich structure and 18 mm free layer surface damping treatment are plotted in Figure 4.12.

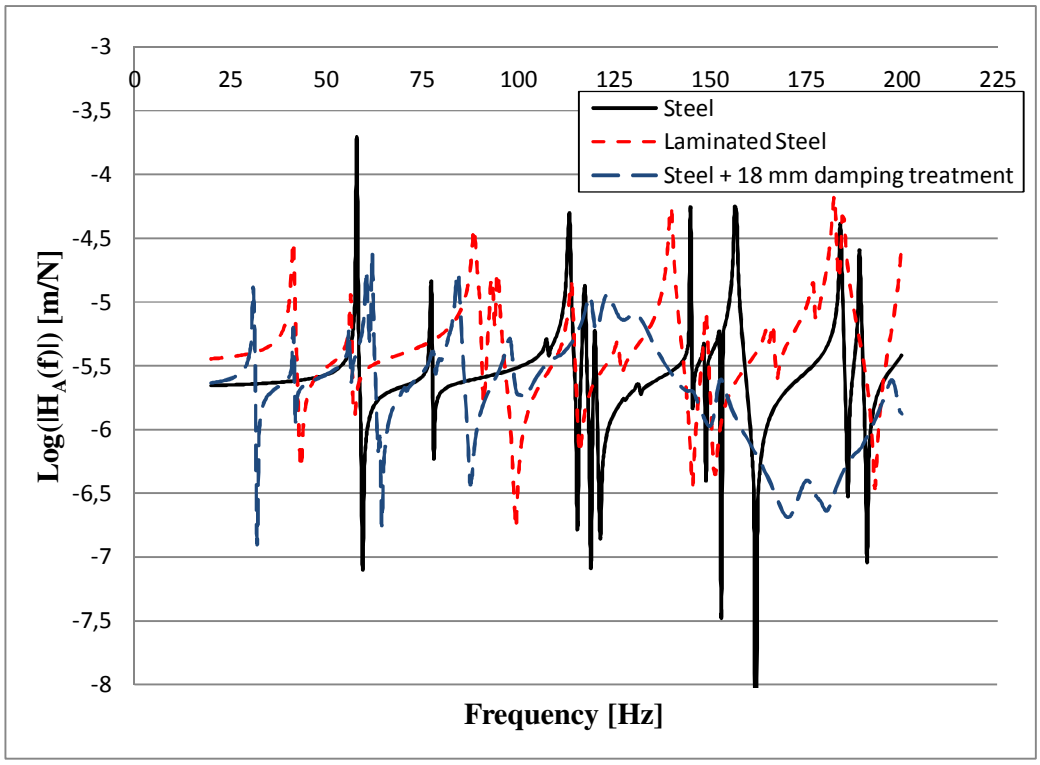

Figure 4.12 *Comparison of FRF plots of floor panel*

Table 4.9 *Comparison of loss factors of sandwich structure and damping treatments*

Method	**Modes**					
	1	**2**	**3**	**4**	**5**	**6**
Sandwich	0.011	0.009	0.010	0.010	0.025	0.039
18 mm damping treatment	0.01	0.0096	0.011	0.0012	0.0255	0.0037

As seen, the same average modal loss factor of first few modes of sandwich structure with a 0.1 mm viscoelastic material addition is obtained by adding the same material on the top of steel panel as free layer surface damping treatment with 18 mm thickness. By this way, the weight is reduced by %68 with using a sandwich structure instead of free layer surface damping treatment.

CHAPTER 5

USE OF SANDWICH MATERIALS FOR REDUCING THE WEIGHT OF CAR BODY-IN-WHITE PANELS CONSIDERING SOUND TRANSMISSION LOSS CHARACTERISTICS

5.1 Introduction

As vibration, noise inside the automobile cabin is a critical factor for driving comfort. For a comfortable drive, the noise levels must be very low inside the cabin. As discussed in previous chapters, both structure-borne and air-borne sound contributes to the noise inside the cabin. The air-borne sound transmission occurs by the sound waves that arrives to the body panels makes them vibrated and then vibration is also transmitted to the air cavity inside cabin. Therefore the damping of panels is critical for air-borne sound transmission. The purpose of this study is to investigate the effects of damping characteristics on sound transmission loss of panels in a wide frequency range. The increase of damping has a potential of incrementally reduce the transmitted air-borne sound. It was seen in the previous chapter that, the utilization of laminated steel, which is a special type of sandwich panel with thin viscoelastic core layer with high damping, is one of the methods to

increase damping. Hence, by using laminated steels, the amount (or thickness) of acoustic barriers added on body panels and the total weight can be reduced without changing the sound transmission loss performance.

Firstly a curved panel is created and natural mode analyses are performed with MSC.Nastran and MSC.Actran and compared in order to verify the calculations of MSC.Actran. By performing analyses with MSC.Nastran, it is seen that the natural frequency results are consistent with various mesh sizes (verified with both solid and shell elements) but the results of MSC.Actran calculations are not consistent with MSC.Nastran's. But this problem is not encountered for flat panels. Instead of modelling laminated steel, the same damping effect of laminated steel is created by adding a damping property (loss factor) to a sheet metal panel. This investigation is done through comparison of sound transmission losses of flat and curved sheet metal panels with different loss factors such as 0, 0.1, 0.2 and 0.4.

Estimation of sound transmission loss is accomplished by using two room method as suggested in ISO-140-3 standard [29] with two dimensional analyses. The estimation procedure with MSC.Actran software program is verified by the study of Papadopoulos [33]. The panels with same size, material and boundary conditions are modelled and analyzed with two and three dimensional analyses.

5.2 Verification of Sound Transmission Loss Estimation with MSC.Actran

Papadopoulos [33] has analyzed sound transmission loss of 4.8 mm thick simply supported steel flat plate by two room method. The dimensions of plate and rooms are given in Figure 5.1.

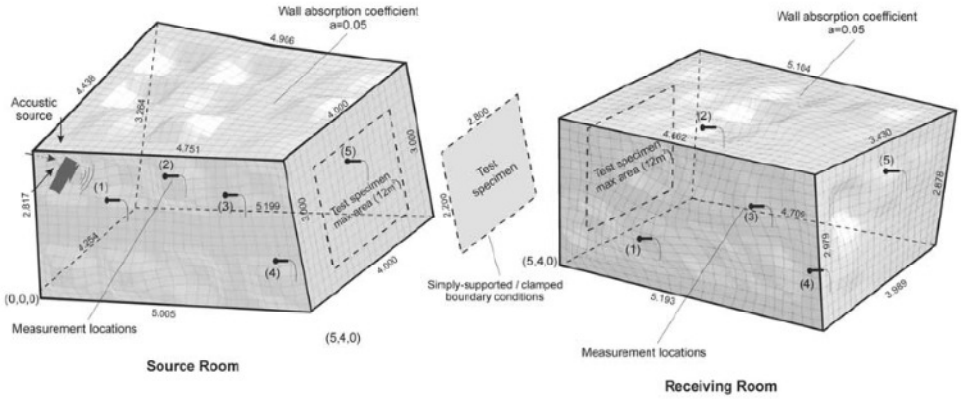

Figure 5.1 *The 3D FE model which Papadopoulos [33] has prepared*

HEX20 type of elements with characteristic lenght of 0.1 m are used to create air cavities in order to provide at least 5 nodes within one wavelenght in the frequency range 0-704 Hz. The air density is chosen to be $\rho = 1.2$ kg/m^3, acoustic bulk modulus $K_f = 1.4 \times 10^5$ H/m^2 and speed of sound c = 341.5 m/s. Isotropic and linear QUAD8 type of elements are used to create the structural part in order to provide at least 8 nodes within one wavelenght. The modulus of elasticity of steel is E = 196 GPa. material density $\rho = 7700$ kg/m^3 and Poisson ratio $\nu = 0.31$. The model contains totally 80000 nodes and 20000 elements.

A unit sound source is placed at the corner of one of the rooms called source room. The analysis is made with the frequency range of 0-704 Hz and is set to be at least 30 frequency values at each octave band. The sound transmission loss [dB] v.s. frequency [Hz] plots of this analysis is shown in Figure 5.2.

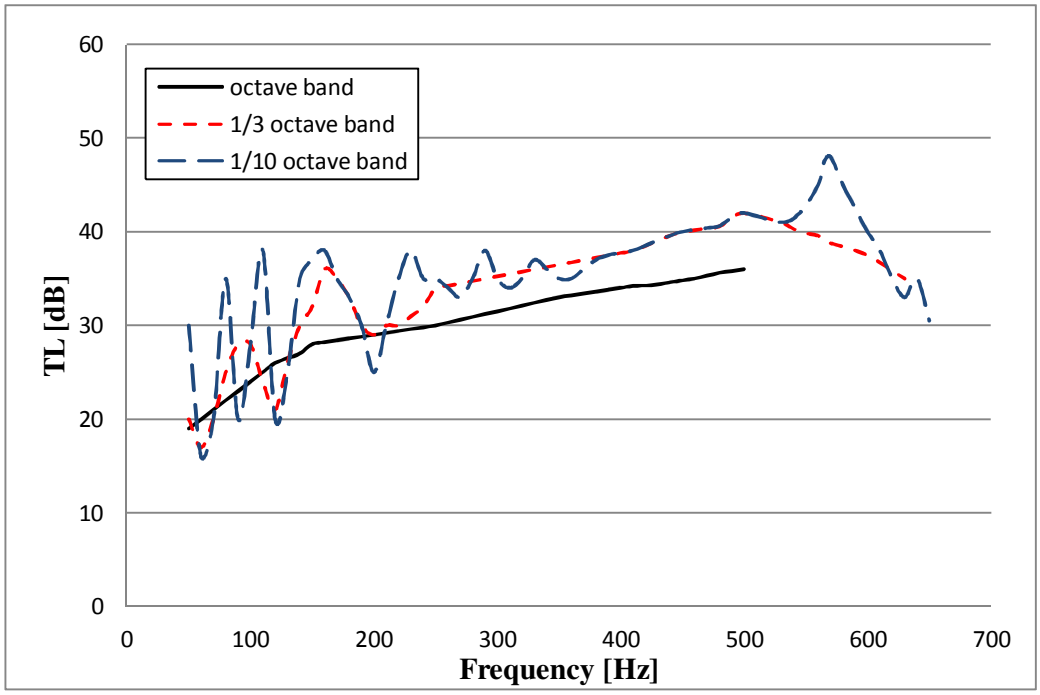

Figure 5.2 *The sound transmission loss of steel panel of Papadopoulos's [33]study*

The panels with same size, material and boundary conditions are analyzed two and three dimensionally in order to verify the estimation process with MSC.Actran. The frequency range of these analyses are 44-740 Hz (containing four octave bands) and each octave band has at least 50 frequency value.

The dimensions of source and receiving rooms for two dimensional model are approximately 9 m x 7.3 m and 8.55 m x 8.5 m respectively. In the 3D model, the dimensions in x, y and z directions of source and receiver rooms are chosen as 4.4 m x 3 m x 5 m and 3.9 m x 2.7 m x 5.2 m. Air cavities and steel panel is meshed with HEX8 elements for 3D model and QUAD4 for 2D model with the same characteristic lenght of 0.1 m.

For two dimensional model, simply supported boundary condition is applied as fixing the translational degree of freedom at the normal direction of the panel. The conditions are applied on the corner nodes of both sides which are attached to source air cavities. The other degrees of freedom, including rotational ones, are set to be free. And for three dimensional model, according to the MSC.Actran manual [17], simply supported boundary condition is applied as in Figure 5.3. The translational degree of freedom at the normal direction of the panel is fixed and the other degrees of freedom, including rotational ones, are set to be free. The conditions are applied on the corner nodes of surface that are neighboring the source room.

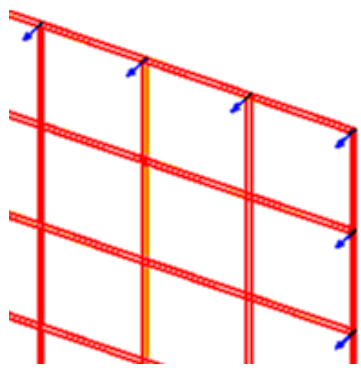

Figure 5.3 *The boundary conditions of simply supported panel for 3D [17]*

The air propeties are default values that MSC.Actran manual has proposed [17] and given in Table 5.1. The properties of steel are the same as in the study of Papadopoulos [33].

Table 5.1 *Properties of air*

Property	Value
c	340 m/s
ρ_f	1.225 kg/m^3
c_p	1004.5 J/(K.m^3)
c_v	717.5 J/(K.m^3)

The sound transmission loss is determined with the instructions denoted in literature survey. The two dimensional finite element model is shown in Figure 5.4 whereas the three dimensional model is in Figure 5.5.

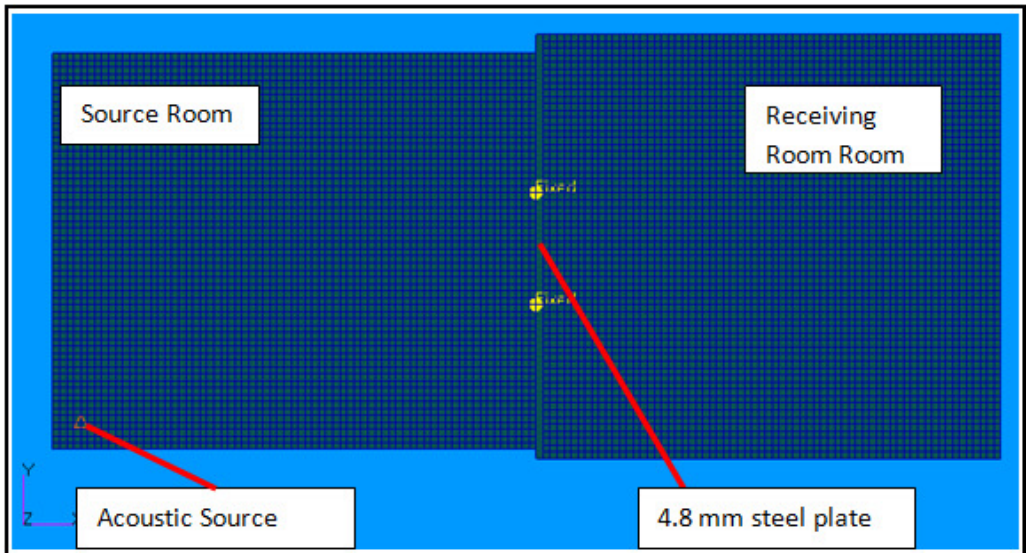

Figure 5.4 *2D finite element model of steel flat plate with 4.8 mm thickness*

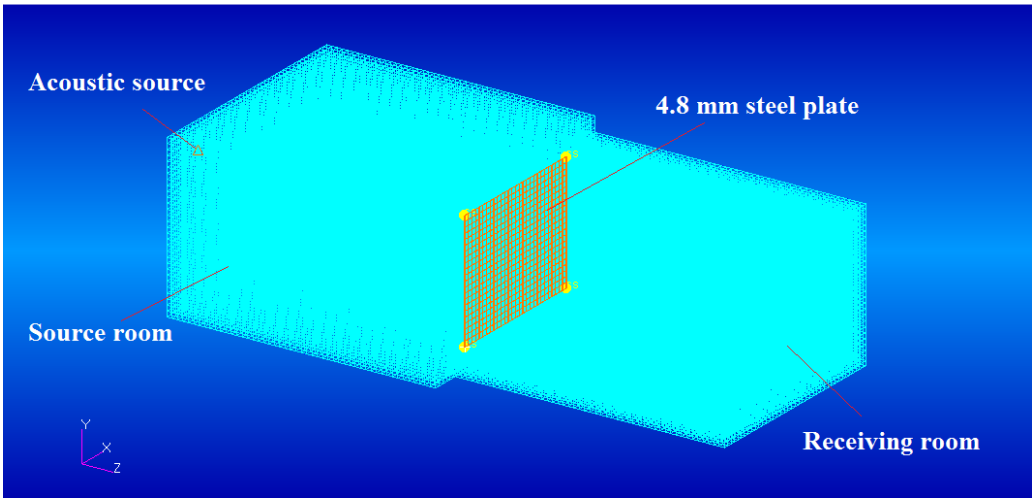

Figure 5.5 *3D finite element model of steel flat plate with 4.8 mm thickness*

The sound transmission loss plots of these analysis in octave band and 1/3 octave band are given in Figure 5.6 and 5.7.

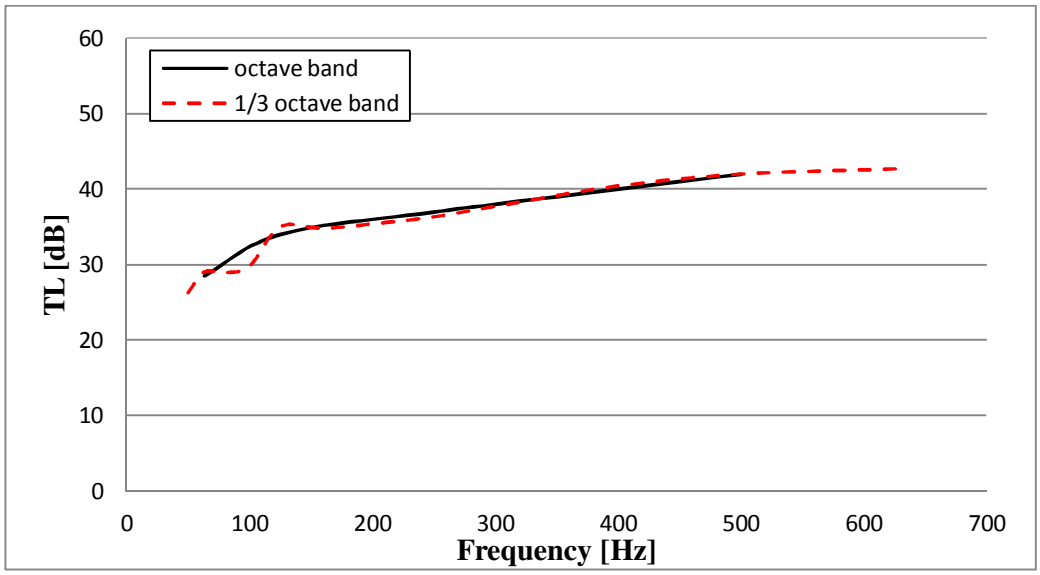

Figure 5.6 *The sound transmission loss of steel panel with 2D analysis*

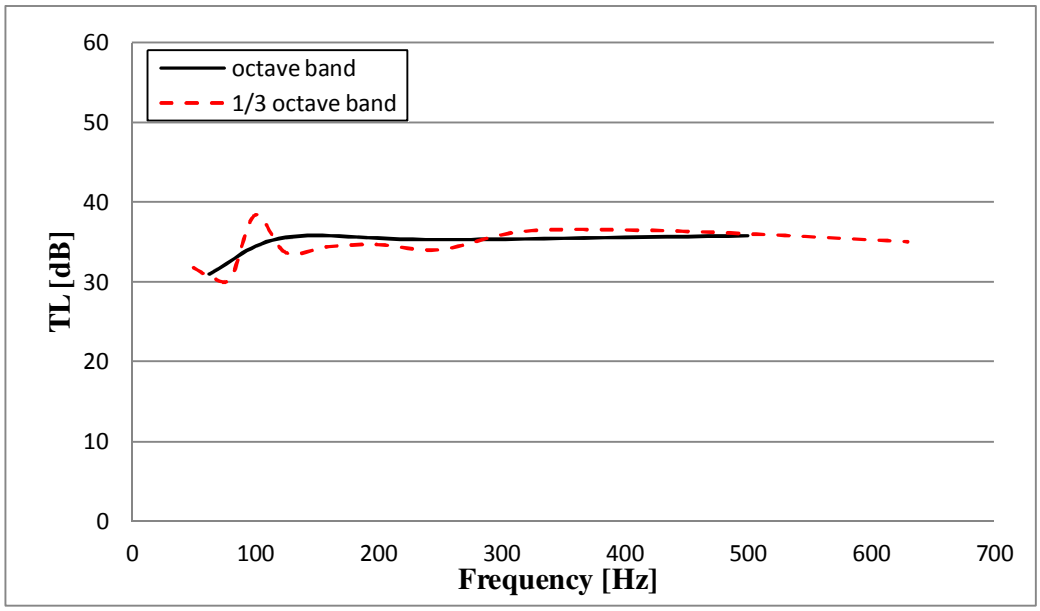

Figure 5.7 *The sound transmission loss of steel panel with 3D analysis*

The comparison of sound transmission loss plots of two and three dimensional analysis of steel plates and the analysis that Papadopoulos [33] has done is shown in Figure 5.8.

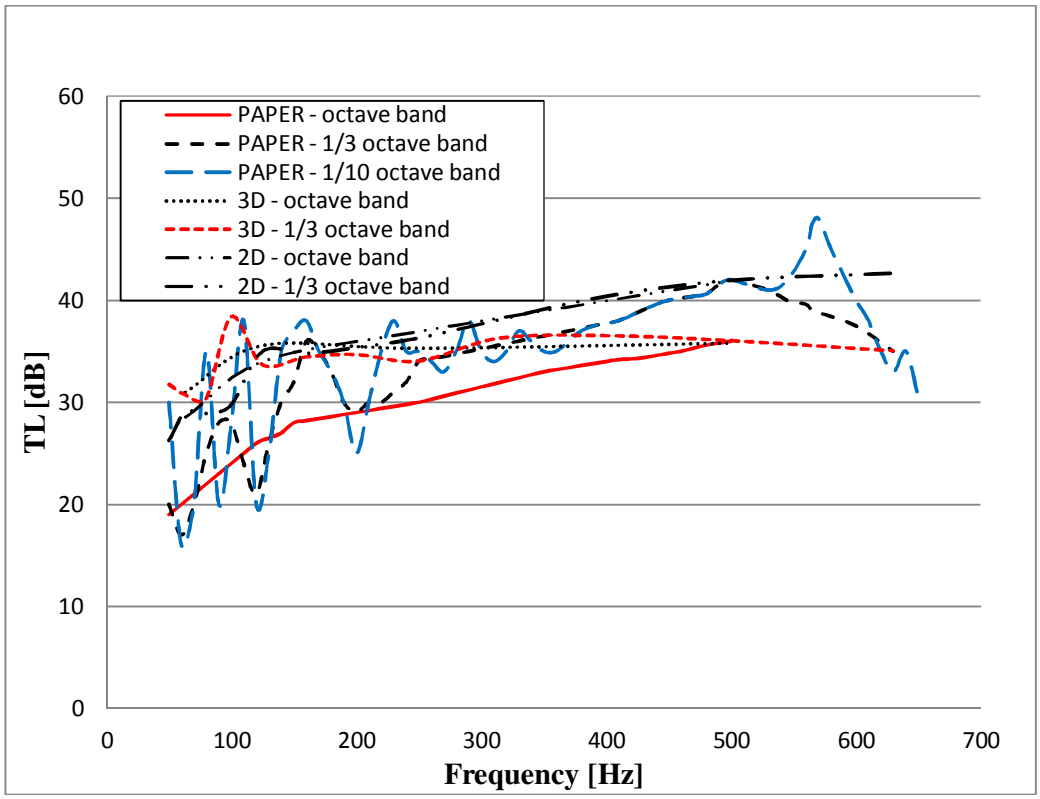

Figure 5.8 *Comparison of sound transmission loss plots of steel panel with 3D and 2D analyses and the study of Papadopoulos [33]*

It is seen that, two and three dimensional analyses have given close results and they both are consistent with the Papadopoulos's [33] analysis. It means that the sound transmission loss estimation prosedure by MSC.Actran is correct.

5.3 The Effect of Damping on Sound Transmission Loss of Panels

The effect of damping on sound transmission loss of panels can clearly be seen at the damping controlled region as shown in Figure 2.25. In other words, damping shows its effects at very high frequencies. The investigation of these effects are done with flat panel and curved panel representing a floor panel of a car in a large frequency range.

The investigation is done in a very broad frequency range which is obtained by combining three consecutive 2D analyses. The frequency ranges of these consecutive analyses are obtained with the considerations of computational time limits, computational capabilities of computers and reliable frequency regions. The amount of elements must not exceed 300000 in a two dimensional acoustical model if a Pentium Dual-Core CPU computer (2.20 GHz) with 2.00 GB RAM. For an example to computational time of an acoustical analysis, model with approximately 211000 elements and for 200 frequency values is analyzed within approximately 8 hours. Because of this restrictions, maximum of 6442.6 Hz can be reliably reached and the effect on sandwich structures in coincidence region, which is very important to be investigated, could not be reached.

As it is mentioned in Chapter 2, reliable frequency region depends on the mesh size and room dimensions. The lower frequency limit depends on the room dimensions. The sound wave must proceed at least two wavelength size to get a good diffuse field in acoustic rooms. Therefore the minimum edge of room dimensions must be larger then two times of wavelenght in the frequency which is the lower limit of frequency range. The upper frequency limit depends on element sizes.

There are two upper reliable frequency limits estimated under different considerations such as acoustics and vibration. These considerations depends on the standing and traveling waves. When an harmonic sound pressure is applied from a sound source, the sound waves travels until it encounters a boundary with another medium. Because of this traveling waves, the acoustical wavelength must be taken under consideration. For this purpose, it is suggested in Chapter 2 that the finite element model must have at least 5 finite element nodes in a wavelength thus in this study FE models have at least 10 elements.

When a harmonic force is applied on a structure, the both standing and traveling waves occur in structure and standing waves form the mode shapes at natural frequencies. Thus, standing waves and mode shapes can be taken under consideration. Once the mesh size according to acoustical consideration is chosen, the natural frequencies are estimated via normal mode analyses. Then, if the panel is flat, natural frequencies are also calculated and if the panel has a complex shape, natural frequencies are estimated via normal mode analyses with a very fine mesh size. The truncational error, between these natural frequencies increases with the mode number. The reliable frequency upper limit estimated by vibrational considerations is the natural frequency of which the truncational error is larger than %10. The reliable frequency upper limit is the smaller one of estimated by acoustical and vibrational considerations.

Curved panel is created as it represents the floor panel of FIAT Car model. The created panel, is the cross section (A-A) of floor panel as it is shown in Figure 5.9. It is shorter than its width because if it were longer, there would be also more elements thus it would be very hard to get a high reliable frequency upper limit. Curved panel is shown in Figure 5.10. The length of this curved panel is 1 m and has 1 mm thickness. The flat panel, also investigated in this study has the same dimensions. Both of the panels are supported simply and the way of application this boundary condition is discussed in previous section.

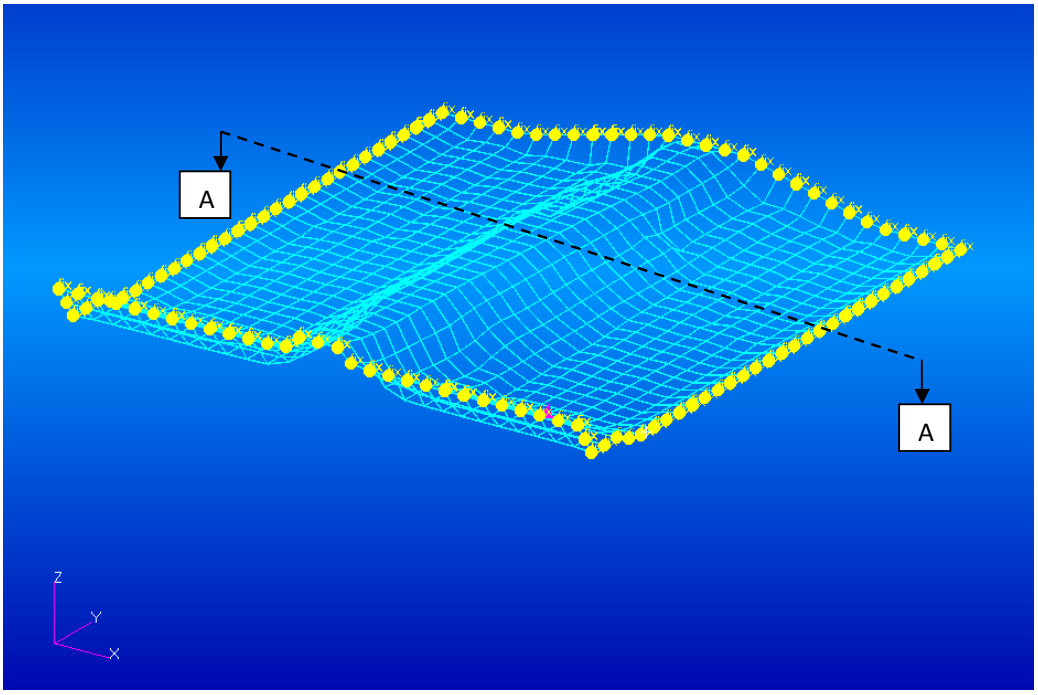

Figure 5.9 *The cross-section of floor panel of FIAT Car*

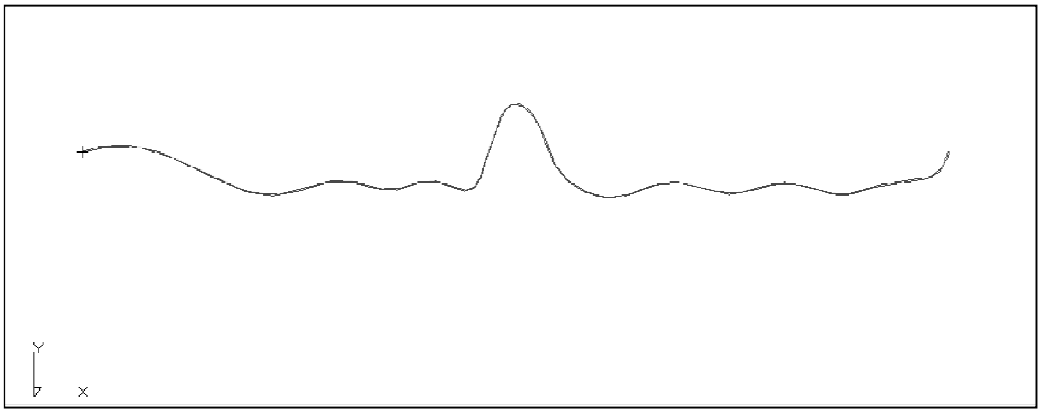

Figure 5.10 *Curved panel modeled for TL analyses*

Three consecutive 2D sound transmission loss analyses are performed and the results are combined in order to get results in a very large frequency range. The mesh size, room dimensions, analysis frequency range and upper and lower reliable frequency limits are shown in Table 5.2.

Table 5.2 *Features of 2D sound tranmission loss analyses*

	Configuration 1	**Configuration 2**	**Configuration 3**
Mesh size	0.015 m	0.0075 m	0.004 m
Upper reliable frequency limit (acoustical)	2286.6 Hz	4573.3 Hz	8575.0 Hz
Upper reliable frequency limit (vibrational)	656.8 Hz	1354.2 Hz	6442.6 Hz
Natural mode that upper reliable frequency limit (vibrational) is estimated	23.	33.	74.
Upper reliable frequency limit	656.8 Hz	1354.20 Hz	6442.6 Hz
Lower reliable frequency limit	200 Hz	400 Hz	650 Hz
Minimum room dimension	3.43 m	1.715 m	1.055 m
x dimension of source room	3.5 m	1.75 m	1.1 m
y dimension of source room	3.75 m	1.9 m	1.25 m
x dimension of receiving room	3.6 m	1.8 m	1.2 m
y dimension of receiving room	3.9 m	2 m	1.3 m
Approximate number of elements	128000	136000	211000
Analysis frequency range	180.5 – 710 Hz	362 – 1420 Hz	724 – 11360 Hz
Number of octave bands	2	2	4
CPU time	1 hours	2 hours	8 hours

In order to see the effect of damping, panel with four loss factor values such as 0, 0.1, 0.2 and 0.4 are analyzed for flat and curved panels separately and compared. The comparison of analyses on floor panel are shown in octave band, 1/3 octave band and 1/10 octave band in Figure 5.11, 5.12 and 5.13 relatively, whereas the comparison of analyses on flat panel are shown in Figure 5.14, 5.15 and 5.16.

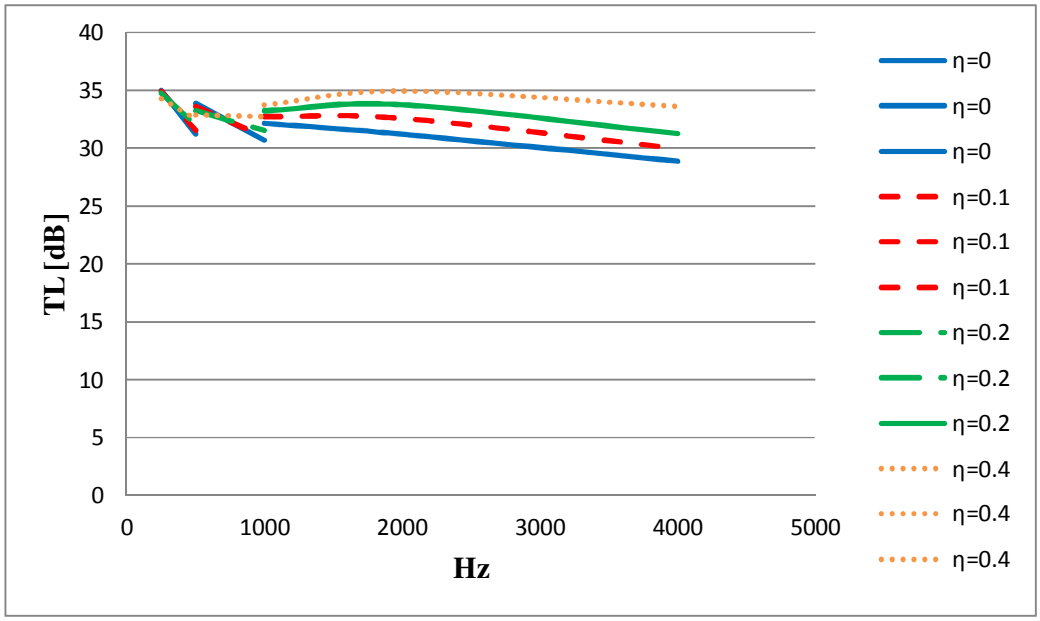

Figure 5.11 *The comparison of TL of curved panel with different loss factors in octave band*

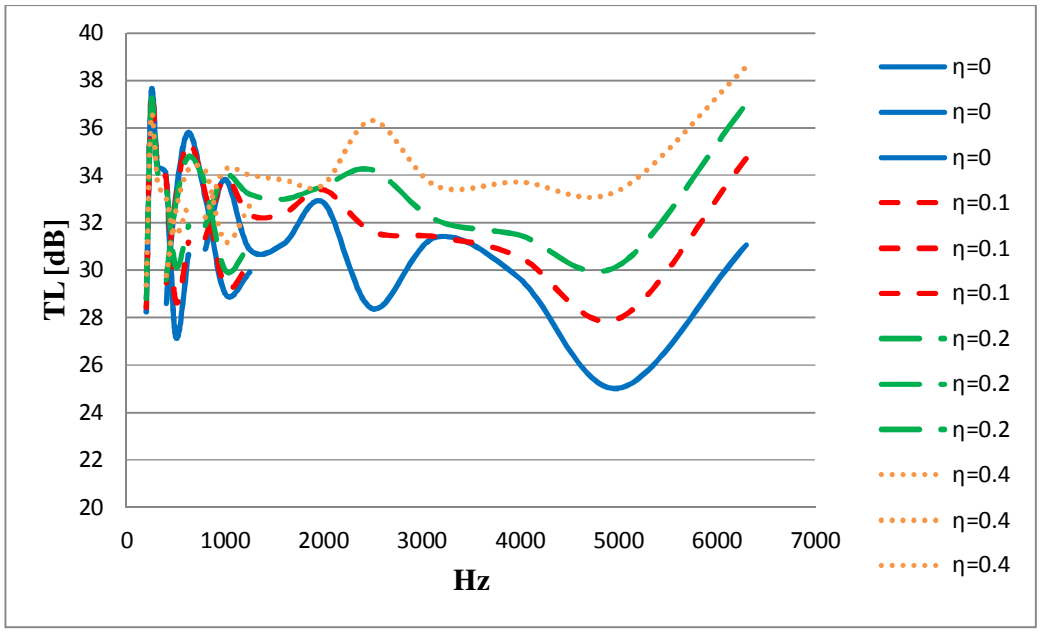

Figure 5.12 *The comparison of TL of curved panel with different loss factors in 1/3 octave band*

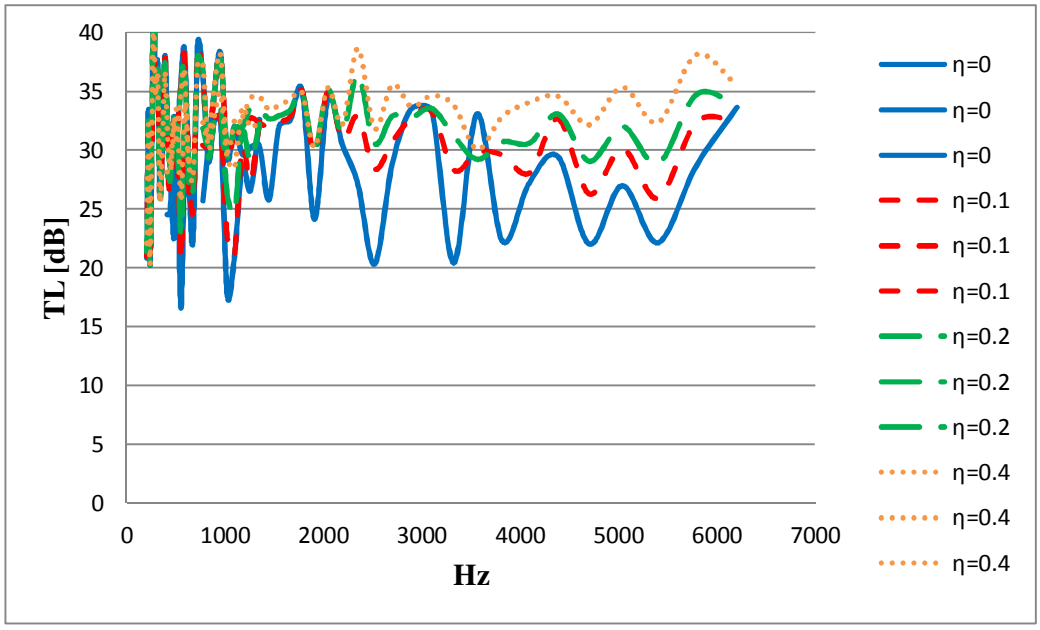

Figure 5.13 *The comparison of TL of curved panel with different loss factors in 1/10 octave band*

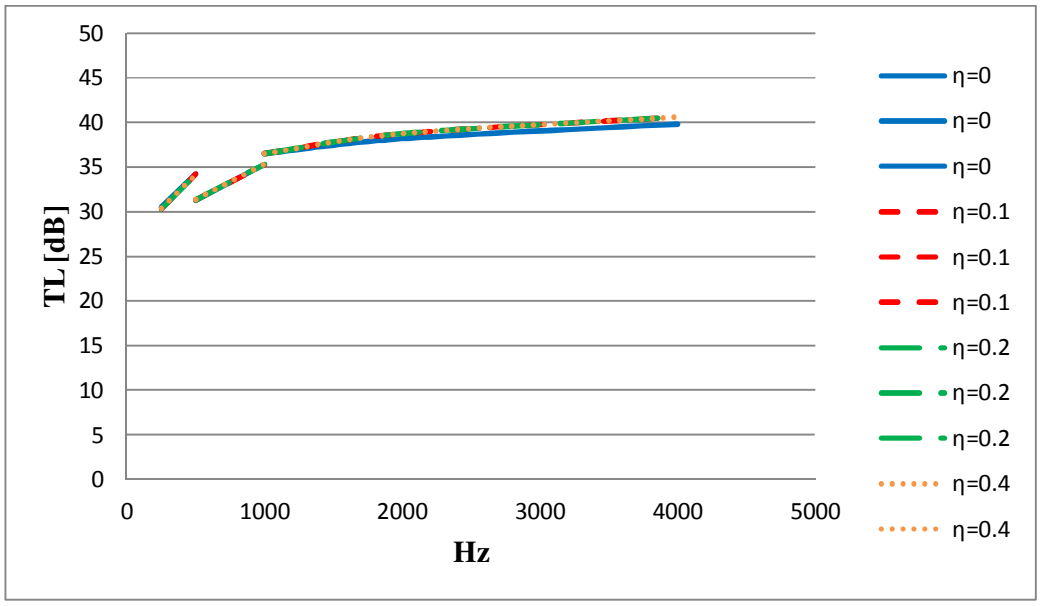

Figure 5.14 *The comparison of TL of flat panel with different loss factors in octave band*

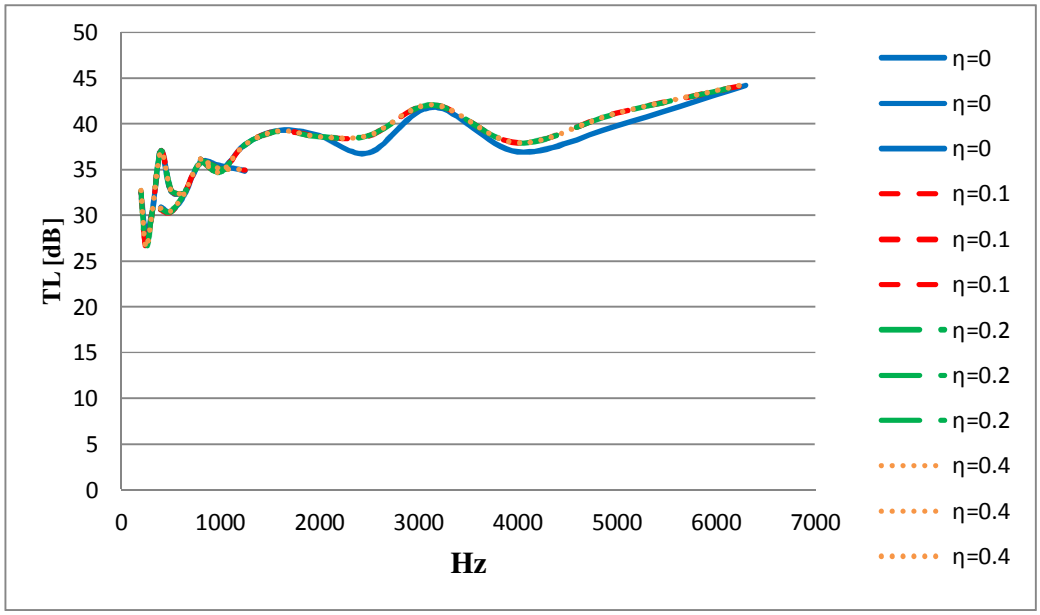

Figure 5.15 *The comparison of TL of flat panel with different loss factors in 1/3 octave band*

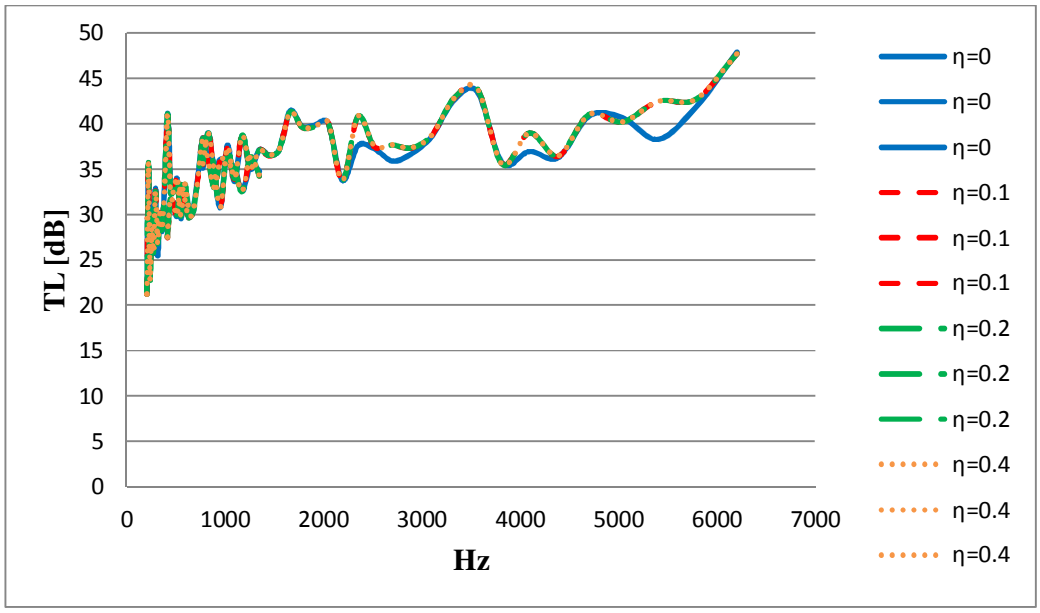

Figure 5.16 *The comparison of TL of flat panel with different loss factors in 1/10 octave band*

As it is mentioned at the beginning of this section, the damping has a very little effect on sound transmission loss of flat panels until it reaches the damping controlled region. In the damping region, sound transmission loss increases with loss factor. For curved panels, the increase of damping, causes sound transmission loss plots to be obviously more damped until it reaches damping controlled region, and in that region, sound transmission loss also increases and is more damped with loss factor.

The reason of the jumps between the consecutive analyses for curved panels could be the fact that verification of natural frequencies of MSC.Actran calculations with MSC.Nastran could not be done.

CHAPTER 6

DISCUSSIONS AND CONCLUSIONS

6.1 Summary and Conclusions

The static, vibrational and acoustic properties of sandwich structures are investigated within this thesis study. At the literature survey chapter, applications, advantages and disadvantages, manufacturing and modelling of sandwich structures are discussed and studies about static, vibrational and acoustic benefits and analyses of sandwich structures by several authors are presented.

In the third chapter, foam cored sandwich structures with clamped and simply supported boundary conditions are designed for body panels of FIAT Car with an optimization procedure. These structures show the same bending stiffness performance as the steel sheet metal panel with at least %50 less weight.

In the fourth chapter, the advantages of utilization of sandwich structures over free layer surface damping treatments is investigated for applications of passive vibration control methods in order to decrease the weight of FIAT Car's floor panel. This investigation contains a design prosedure which is firstly tested on flat beams because of its theoretical formulas are known. It has been seen that, the same damping performance (i.e. the average value of modal loss factor of 2nd, 3rd, 4th, 5th, 6th and 7th modes) for this study, of floor panel can be obtained using sandwich structures instead of free layer surface damping treatments with %68 less weight.

The structural damping of body panels can be increased by using sandwich structures especially with thin viscoelastic core whose damping is also very high. In the last chapter, the effects of damping on sound transmission loss of curved body panels are investigated. 2D flat and curved panel representing the floor panel of FIAT Car model are analysed in frequency range of 200 Hz – 6600 Hz. The sound transmission loss plots in a very wide frequency range is obtained by combining three consecutive analyses performed separately. Because of not relying on natural modes resulted in MSC.Actran calculation procedure, the TL calculations of curved panels are not fully reliable. Since, the damping effect of laminated steels are known, for simplicity instead of modelling of laminated steels are not through comparison of sound transmission losses of flat and curved sheet metal panels with different loss factors such as 0, 0.1, 0.2 and 0.4. It is seen that, until it reaches damping controlled region, damping has a very little effect on TL of flat panels but has an obvious damping effect on TL of curved panels. However in that region, damping has an increasing effect on TL of both flat and curved panels. But because of CPU restrictions, very high frequencies could not be reached and the effects of damping in coincidence region could not be investigated.

Considering the benefits of laminated metals, a special type of sandwich structure, with very thin viscoelastic core layers, they are very widely used in car body design. With this material, quieter designs can be made without adding additional sound-

absorbing materials. The core and face layers of laminated metals can both be assembled before and after the pressing of the panel. They can be welded or bended like a single layered plate on the chassis.

Other types as callular foamed, honemcomb cored and balsa wood cored sandwich panels are mostly used for lightweighting of the panels under physical loads such as bending, torsion and buckling etc. The attachment of core and face layers have to be before the joining process to chassis. The joining methods are discussed in Chaper 2.

Using sandwich structures instead of sheet metals the amount of emissions can be decreased because the power needs are reduced by weight reduction. With this study, it is understood that with using laminated metals effectively at high frequencies, the amount of acoustic barrier materials attached on body panels will be eliminated. In addition to these, the body panels with same weight and higher static, dynamic and acoustic performance can be obtained.

6.2 Future Studies

This thesis study can be expanded in many ways and the problems encountered during this study may be solved. First of all, problem of the inconsistency of natural frequencies between the results of the calculation of MSC.Nastran and MSC.Actran should be solved. As seen from the consecutive TL plots of both curved and flat panels, there are jumps occured at the ending of a plot and the beginning of the next one. These jumps can be caused by this problem and must be tried to be reduced. Furthermore, the TL analyses, can be verified with experiments.

In the previous section, it was said that, because of CPU restrictions, very high frequencies could not be reached. These very high frequencies can be reached by Statistical Energy Analysis method, and these method should be investigated for this purpose.

Furthermore, this thesis can be expanded by investigating the effect of foam cored sandwich panels on sound transmission loss analyses for both curved and flat panels.

REFERENCES

[1] Ozgen G. O., Finite Element Modeling and Analysis of a Passenger Car Body Structure, Orta Doğu Teknik Üniversitesi, 2001.

[2] Zenkert D., Handbook of Sandwich Materials, EMAS Publishing, 1997.

[3] Vinson J. R.. The Behaviour of Sandwich Structures of Isotropic and Composite Materials. Technomic Publishing Company. 1999.

[4] Mignery L. A., Quiet Steel® Body Panel Design with DAMP® - A Custom Preprocessor Utilizing MSC-PATRAN/NASTRAN, Material Sciences Corporation, Laminates and Composites.

[5] World War 2 Planes. World War 2 Aircraft pictures - RAF Mosquito. World War 2 Planes. http://www.world-war-2-planes.com/mosquito_full.html. 24.08.2011.

[6] Gurit Rail Business. Phenolic-Prepreg for Rail Applications Presentation. 2007.

[7] Sandwich Materials Hylite, Automotive Applications.

[8] Metawell GmbH., Material for Consequent Light Construction, 2005.

[9] ThyssenKrupp Steel AG. Bondal Steel Sandwich Material for Effective Reduction of Structure-borne Sound. Product Information Bondal, 2008.

[10] Roush, Laminated Steel – Dynalam Product Description.

[11] Gonzales M., Jordan R., Gerges S. Y. N., Modelling of Firewall Panel With Laminated Metal Using Experiment and Numerical Methods, 2008.

[12] I-Car Advantage Online, Technical Information For The Collision Industry, 6 March 2006.

[13] Source The Engineer, Manufacturing Talk, http://www.manufacturingtalk.com/news/mls/mls100.html, 10.11.2011

[14] Yu. Z., Static, Dynamic and Acoustical Properties of Sandwich Composite Materials, Auburn University, 2007.

[15] Zenkert D., An Introduction to Sandwich Construction. EMAS Publishing. 1997.

[16] Bitzer T., Honeycomb Technology – Materials, Design, Manufacturing, Applications and Testing, Chapman & Hall, First Edition, 1997.

[17] Actran 2007.1 User's Guide, Free Field Technologies, September 2007.

[18] Manet V., The Use of Ansys to Calculate the Behaiour of Sandwich Structures, Composites Science and Technology 58 (1998) 1899-1905.

[19] Balmet E., Bobillot A., Analysis and Design Tools for Structures Damped by Viscoelastic Materials.

[20] Farage M. C. R., Barbosa F. S., A finite element model for sandwich viscoelastic beams: Experimental and numerical assessment, Journal of Sound and Vibration 317 (2008) 91–111.

[21] Hazard L., Bouillard P., Structural dynamics of viscoelastic sandwich plates by the partition of unity finite element method, Comput. Methods Appl. Mech. Engrg. 196 (2007) 4101–4116.

[22] Wennhage P., Weight Minimization of Sandwich Panels with Acoustic and Mechanical Constraints, Journal of Sandwich Structures and Materials; 3; 22. SAGE 2001.

[23] Wennhage P., Weight Optimization of Large Scale Sandwich Structures with Acoustic and Mechanical Constraints, Journal of Sandwich Structures and Materials; 5; 253, SAGE, 2003.

[24] Wang S., Simulation of Beaded and Curved Panels with Multi-layer Damping Treatments.

[25] Möser M., Engineering Acoustics: An Introduction to Noise Control. Second Edition, Springer, 2009.

[26] Kuttruff H., Acoustics An Introduction, Taylor & Francis, 2006.

[27] Rossing T. D., Handbook of Acoustics, Springer, 2007.

[28] Bies D. A., Hansen C. H., Engineering Noise Control Theory and Practice, Fourth Edition, Spon Press, 2009.

[29] ISO 140-3 - Acoustics - Measurement of sound insulation in buildings and of building elements – Part 3: Laboratory measurements of airborne sound insulation of building elements, International Standard, ISO 140.3, Second Edition, 1995-05-15.

[30] Beranek L. L., Acoustics. Acoustical Society of America, 1996.

[31] Papadopoulos C.I., Redistribution of the low frequency acoustic modes of a room - a finite element-based optimisation method, Applied Acoustics 62 (2001) 1267–1285

[32] Papadopoulos C.I., Development of an optimised, standard-compliant procedure to calculate sound transmission loss: design of transmission rooms. Applied Acoustics 63 (2002) 1003–1029.

[33] Papadopoulos C.I., Development of an optimised, standard-compliant procedure to calculate sound transmission loss: numerical measurements, Applied Acoustics 64 (2003) 1069–1085.

[34] Xin F. X., Lu T. J., Analytical and experimental investigation on transmission loss of clamped double panels : implication of boundary effects, Acoustical Society of America, 2009, Pages: 1506–1517.

[35] Lee C. M., Xu Y., A modified transfer matrix method for prediction of transmission loss of multilayer acoustic materials, Journal of Sound and Vibration, 2009.

[36] Fredö C. R., Hedlund A., NVH optimization of truck cab floor panel embossing pattern, SAE International, 2004.

[37] Bregant L., Miccoli G., Seppi M., Construction Machinery Cab Vibro-Acoustic Analysis and Optimization.

[38] Zuo S., Yan J., Experimental Analysis for the Interior Noise Characteristics of the Fuel Cell Car.

[39] Liu Z. S., Lu C., Wang Y. Y., Lee H. P., Koh Y. K., Lee K. S., Prediction of noise inside tracked vehicles, Applied Acoustics 67 (2006) 74–91

[40] Young W.C., Budynas R.G., Roark's Formulas for Stress and Strain, 7th Edition, Mc Graw Hill, 2002.

[41] Plantema F. J., Sandwich Construction; The Bending and Buckling of Sandwich Beams, Plates, and Shells, New York Wiley, 1966.

[42] Structural Sandwich Composites, Military Handbook MIL-HDBK-23A. Department of Defense, Washington D.C., 20025.

[43] Jones D. I. J., Handbook of Viscoelastic Vibration Damping, John Wiley & Sons. LTD., 2001.

[44] Harrison M., Vehicle Refinement Controlling Noise and Vibration in Road Vehicles

[45] Özgen G. O., ME 708 Lecture Notes, Orta Doğu Teknik Üniversitesi, 2009.

APPENDIX A

OCTAVE BAND

Table A.1 *Octave band*

Frequency [Hz]		
Lower Limit	**Center Frequency**	**Upper Limit**
44	63	88
88	125	177
177	250	355
355	500	710
710	1000	1420
1420	2000	2840
2840	4000	5680
5680	8000	11360

APPENDIX B

THIRD-OCTAVE BAND

Table B.1 *Third-octave band*

Frequency [Hz]		
Lower Limit	**Center Frequency**	**Upper Limit**
44.7	50	56.2
56.2	63	70.8
70.8	80	89.1
89.1	100	112
112	125	141
141	160	178
178	200	224
224	250	282
282	315	355
355	400	447
447	500	562
562	630	708
708	800	891
891	1000	1122
1122	1250	1413
1413	1600	1778
1778	2000	2239
2239	2500	2818
2818	3150	3548
3548	4000	4467
4467	5000	5623
5623	6300	7079
7079	8000	8913
8913	10000	11220

APPENDIX C

TENTH-OCTAVE BAND

Table C.1 *Tenth-octave band*

Frequency [Hz]		
Lower Limit	**Center Frequency**	**Upper Limit**
43.7	45.3	46.9
46.9	48.5	50.2
50.2	52	53.8
53.8	55.7	57.7
57.7	59.7	61.8
61.8	64	66.3
66.3	68.6	71
71	73.5	76.1
76.1	78.8	81.6
81.6	84.4	87.4
87.4	90.5	93.7
93.7	97	100.4
100.4	104	107.6
107.6	111.4	115.4
115.4	119.4	123.6
123.6	128	132.5
132.5	137.2	142
142	147	152.2
152.2	157.6	163.1
163.1	168.9	174.9
174.9	181	187.4
187.4	194	200.9
200.9	207.9	215.3
215.3	222.9	230.7
230.7	238.9	247.3

247.3	256	265
265	274.4	284
284	294.1	304.4
304.4	315.2	326.3
326.3	337.8	349.7
349.7	362	374.8
374.8	388	401.7
401.7	415.9	430.5
430.5	445.7	461.4
461.4	477.7	494.6
494.6	512	530.1
530.1	548.7	568.1
568.1	588.1	608.9
608.9	630.3	652.6
652.6	675.6	699.4
699.4	724.1	749.6
749.6	776	803.4
803.4	831.7	861.1
861.1	891.4	922.9
922.9	955.4	989.1
989.1	1024	1060.1
1060.1	1097.5	1136.2
1136.2	1176.3	1217.7
1217.7	1260.7	1305.2
1305.2	1351.2	1398.8
1398.8	1448.2	1499.2
1499.2	1552.1	1606.8
1606.8	1663.5	1722.2
1722.2	1782.9	1845.8
1845.8	1910.9	1978.2
1978.2	2048	2120.2
2120.2	2195	2272.4
2272.4	2352.5	2435.5
2435.5	2521.4	2610.3
2610.3	2702.4	2797.7
2797.7	2896.3	2998.4
2998.4	3104.2	3213.7
3213.7	3327	3444.3
3444.3	3565.8	3691.5
3691.5	3821.7	3956.5
3956.5	4096	4240.4
4240.4	4390	4544.8
4544.8	4705.1	4871
4871	5042.8	5220.6
5220.6	5404.7	5595.3

5595.3	5792.6	5996.9
5996.9	6208.4	6427.3
6427.3	6654	6888.6
6888.6	7131.6	7383
7383	7643.4	7913
7913	8192	8480.9
8480.9	8780	9089.6
9089.6	9410.1	9742
9742	10085.5	10441.2
10441.2	10809.4	11190.6
11190.6	11585.2	11993.8

APPENDIX D

K_1 FOR DETERMINING MAXIMUM DEFLECTION

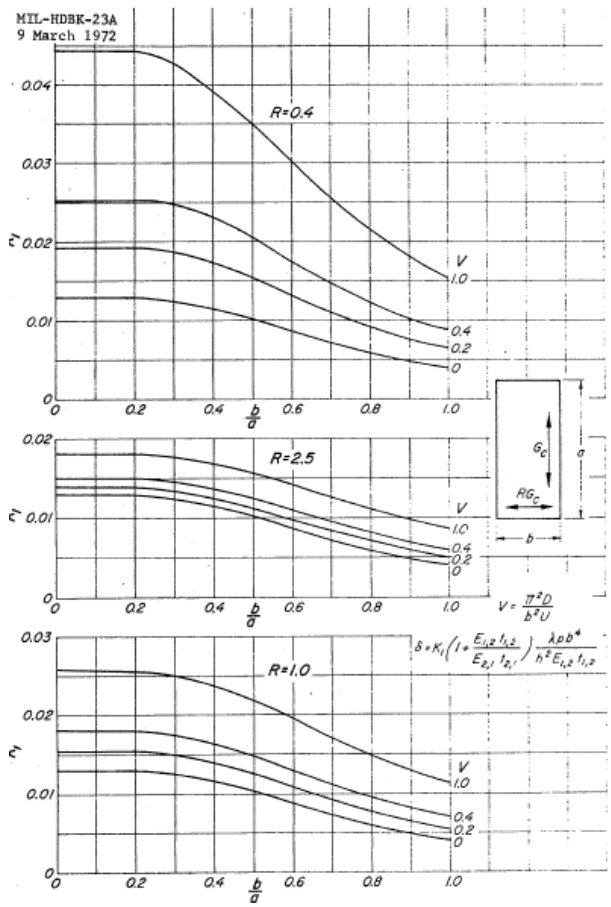

Figure D.1 *K_1 for determining maximum deflection*

APPENDIX E

K_2 FOR DETERMINING FACING STRESS

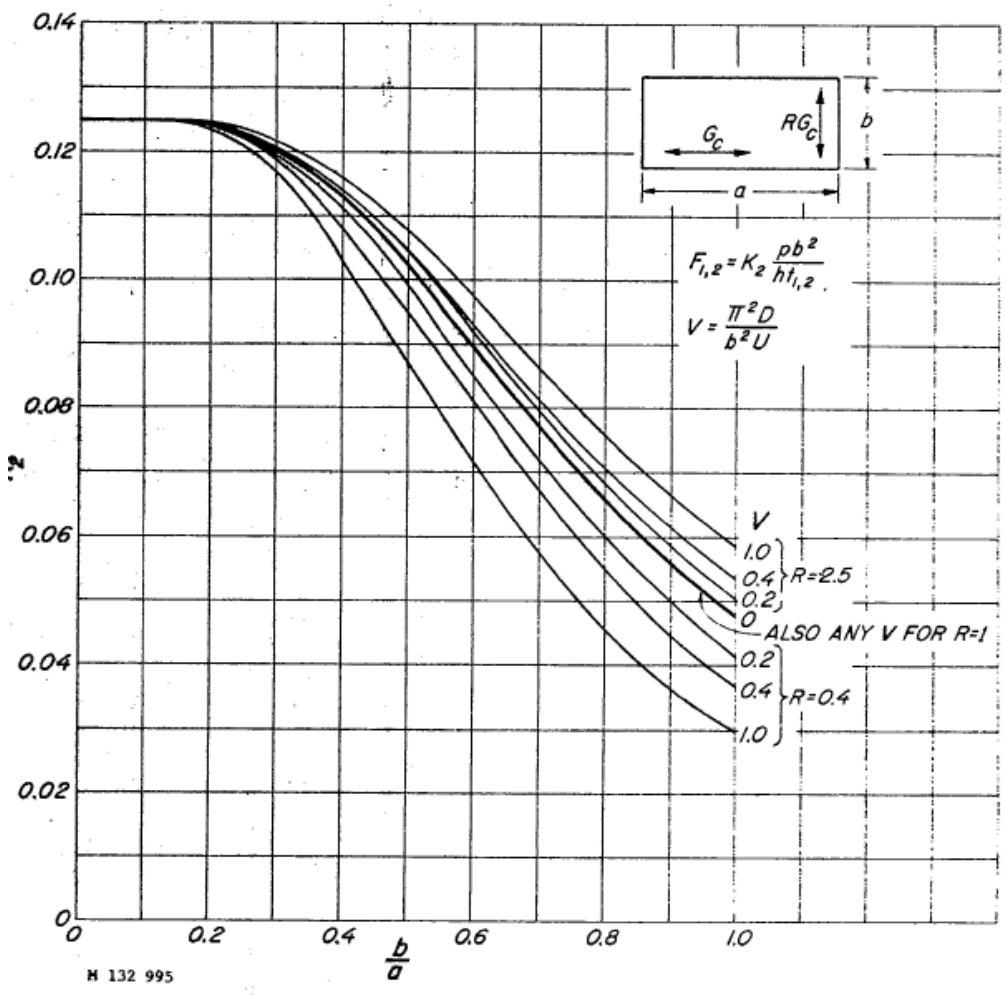

Figure E.1 *K_2 for determining facing stress*

APPENDIX F

K_3 FOR DETERMINING MAXIMUM CORE SHEAR STRESS

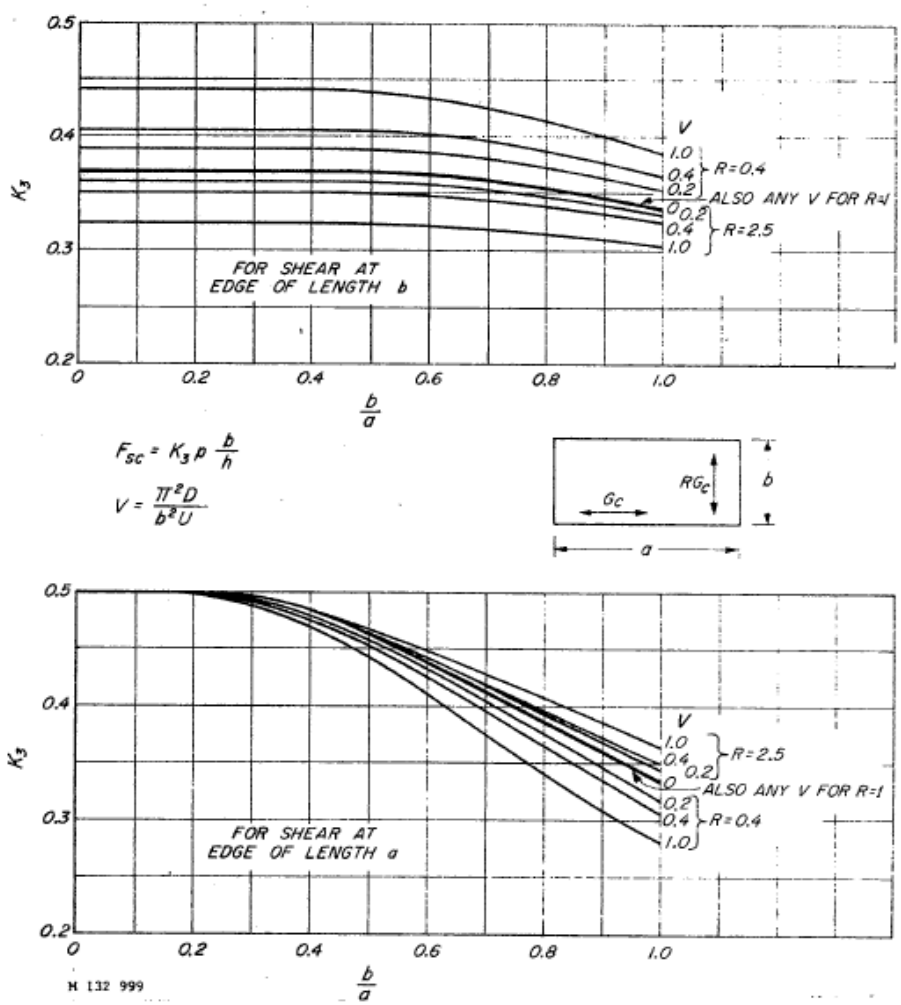

Figure F.1 *K_3 for determining maximum core shear stress*